ABSTRACT

MCFARLAND II, WILLIAM C. Analysis of Directed Fiber Placement using Air Laying Technique. (Under the direction of Professor Nancy Powell).

Weight reduction composites are of high interest in many fields, including the automotive industry. However, the high cost of composites constructed from woven preforms has diminished the interest in many cases. Nonwoven webs provide an attractive, low cost and high production volume alternative for preform fabrication. However, in order for nonwovens to provide the adequate strength required, fiber alignment must be achievable. Within the nonwoven industry, air laying techniques offer a versatile basis to investigate fiber alignment processes. Fiber alignment within an air laying system has been an area of very little research. Understanding the fiber and fluid interactions within these types of systems can provide the knowledge to create variables in order to control fiber orientation.

The primary objective of this research was to evaluate the feasibility of creating repeatable fiber alignment in a predetermined direction. Focus was placed on the perforated fiber collection surface. Custom fiber collection surfaces were designed and fabricated adjusting parameters such as aperture size, spacing and shape. Results showed that subtle fiber alignment was obtainable by aligning circular apertures. Oblong shaped apertures produced a higher precision of fiber alignment. Aligning the oblong apertures along their longest dimension produced the highest level of fiber alignment (20%) in a 10^{o} range. This technique could be integrated with current fiber alignment technologies to significantly increase fiber alignment. Doing so could present a high production volume, low cost process for creating high strength nonwoven composite performs.

Analysis of Directed Fiber Placement Using Air Laying Technique

by
William Clay McFarland II

A thesis submitted to the Graduate Faculty of
North Carolina State University
in partial fulfillment of the
requirements for the degree of
Master of Science

Textiles

Raleigh, North Carolina

2011

APPROVED BY:

Professor Nancy Powell Committee Chair	Dr. Pam Banks-Lee

Dr. Hoon Joo Lee

DEDICATION

This work is dedicated to my mother for her unconditional support and belief in me; to my father for his wisdom and encouragement; to my sister for teaching me humility; to Laurie for her love and unwavering patients; to all of my friends for their support and friendship; and to Lilly for always being the best listener.

BIOGRAPHY

William Clay McFarland II was born in Tampa, Florida on November 1st, 1985. He is the son of William and Karen McFarland and has one sister, Heather. William graduated from Clayton High School in May 2004. William attended North Carolina State University and in 2008 he received his B.S. degree in Textile Technology from the College of Textiles. In August of 2009, William began graduate studies at NCSU College of Textiles in Textile Technology and Management. His focus was in Automotive Textile-based Material Research, and he was awarded a graduate assistantship with Professor Nancy Powell, funded by the Office of the Provost, NCSU.

Research Blog: www.automotivecomposites.blogspot.com

ACKNOWLEDGMENTS

I would like to thank Professor Nancy Powell, Dr. Pam Banks-Lee and Dr. Hoon Joo Lee for their teaching through my years at North Carolina State University College of Textiles and their guidance on this project.

TABLE OF CONTENTS

LIST OF TABLES

LIST OF FIGURES

CHAPTER 1: INTRODUCTION

The types of textile materials or fabrics used for composite reinforcement applications can be sorted into several classifications. As a broad separation, these fibrous materials can be divided into "ordered" (woven and knitted fabrics) or "disordered" (nonwovens) orientations [1]. Both of these divisions of materials have their respective advantages and disadvantages. Typical textile-based composite preform construction has used "ordered" or aligned fibers, filaments or yarns in textile materials such as woven, multiaxial warp knit or stitch bonded fabrics [2]. The drawbacks of such materials include the formability limitations due to the fabric architecture along with the cost and time put into actual yarn and fabric construction prior to composite construction. However, research study will focus on the "disordered" or nonwoven classification of composite performs. This decision is due to the versatility, low cost benefits, high production rates and large area of potential research. The field of nonwovens (or disordered) fabrics can be broken down further into several types of fiber-based webs, which are determined by their unique web formation processes. Nonwoven web formation can be achieved in numerous ways including mechanically (carding), aerodynamically (air-laid), hydrodynamically (wet-laid), or by an electrostatic field (electrospinning); nonwoven webs can also be produced by a system pairing fiber fabrication and bonding in a single process (Spunbonding, Meltblown, etc.) [3]. A fundamental interest for this study is to focus on processes which will lower cost and increase product volume, while utilizing discontinuous fiber as the raw material. Compared to the other methods, air as a medium for fiber transport offers the most cost efficient path

with the greatest room for development. This is due to the deficiency of research or literature provided to further advance this processing method. Traditionally, air-laid nonwoven webs have been known for their loft, low mechanical strength and random fiber orientation distribution.

New developments in nonwoven technology have created production methods to align fibers in a specific or controlled orientation to fully extract their performance capabilities. These developments have been referred to as Direct Fiber Placement techniques. However, typically these processes posses slow production rates and very high cost [4]. Studies have shown that even partial alignment of fibers in the principal loading direction has been an effective way to increase tensile stiffness and strength by over 200% when compared to random orientation counterpart [5]. The main challenge in this technology is creating a process that is capable of high production speed with repeatability of fiber placement, which this study will investigate. Essentially, instead of focusing on creating a higher level of random fiber orientation, recent studies have begun investigating parameters to help orient the fibers (to a determined degree) in a desired orientation during a form of air laying. These studies focus on the use of these aligned fibrous mats to be used as performs in fiber reinforced composites. Conventional nonwovens have been known for their isotropic mechanical properties and have been stigmatized as being weak with minimal strength. If engineered correctly, these preforms could lead to low cost composites with high mechanical properties in desired directions. Compared to a woven preform, a nonwoven directed fiber placement preform would reduce the amount of fiber necessary in a component by ultimately using each fiber to its upmost potential within the system. Further developments in this area

could focus on entire unit weight reduction and parts consolidation for faster and more customized production.

Nonwoven fabrics are a growing field of textiles and have become of great interest to the automotive industry due to their low production and material cost and high process speeds. The automotive industry has always shown great interest in progress, made obvious by the average of between $16 to $18 billion spent each year by US automotive manufacturers on research and development [6]. Currently, key areas of interest include alternative fuels, fuel economy, sustainability, and end of life recyclability. In each of these categories new material development is a necessary component for its success. One of the requirements of the newly developed material in these situations is to provide weight reduction. Utilizing the weight reduction approach offers many advantages in the automotive industry which will be discussed further.

This study will concentrate on the factors within the air laying process which have the ability to be controlled in order to produce orientated nonwovens. The increasing interest in weight reducing and functional materials has created a demand for fiber such as carbon fiber, ultimately lowering the price of carbon fiber. As markets such as the automotive industry continue to an increased interest in high performance fibers, the cost will continue to decrease and the demand for efficient composite production will increase, making weight reducing composites a feasible material in the future [6,7,8].

1.1 Purpose of Study

The purpose of this investigation is to research fiber behavior in the air laid web formation process and determine parameters to control fiber resting orientation. More specifically, this investigation is to investigate the feasibility of producing a nonwoven preform with controlled fiber orientation for use in a composite preform. The aim of this research is to investigate methods of confidently controlling fiber orientation and orientation distribution in a preform strictly by aerodynamic means. These aerodynamic forces will be studied by altering the perforation design in the fiber collection surface. Furthermore, this investigation will research the rationale of fiber orientation and its importance in structural composite applications.

1.2 Research Objectives

1. Analyze discontinuous fiber behavior in an aerodynamically controlled process.
2. Evaluate effect of the apertures in a fiber collection surface on final fiber orientation.
3. Define controllable parameters in aperture geometry in order to produce desired fiber orientation.
4. Propose probable applications and benefits for researched process.

1.3 Significance of Study

Case studies of directed fiber placement processes show a significant improvement in the directional mechanical properties of an otherwise isotropic product, but are faced with speed and repeatability challenges [5,9]. Directed fiber preforming has been in commercial use for decades and has encountered a revival in recent years due to the potential for near net

shape preforming [10]. The use of directed fiber placement eliminates any intermediate mat or fabric construction, allowing the reinforcement fibers to be used in the cheapest form [10].

The goal of this study is analyze these processes in order to develop a low cost preform material possessing the necessary required strength. The following research focuses on a low cost web formation process using an air laying technique to investigate the feasibility of developing a method to direct discontinuous fibers in a desired manner to create engineered fiber orientations. This fiber orientation ultimately increases the nonwoven web strength in the direction of the fiber alignment. Furthermore, the intensions of the proposed web would be to additionally process by resin infusion in order to create a structural or semi-structural composite used in a transportation application. The development of engineered fiber placement in a nonwoven composite would allow automotive suppliers to create components with complex geometries, reducing the number of parts, ultimately resulting in overall vehicle weight reduction.

1.4 Benefits of Proposed Work

Successful completion of this research and experimental analysis will provide a novel system in which to further orient fibers in a nonwoven substrate. These nonwoven mats would be utilized as preforms for weight reducing composites. Aligning fibers in composite performs would increase the engineering capabilities of such composites and broaden the use of lost cost and high volume nonwovens as composite preforms. The interactions between air flow and associated fiber behavior could lead to new, efficient means to control the final fiber orientation in a fiber reinforced composite.

CHAPTER 2: LITERATURE REVIEW

The following sections present a culmination of reviewed literature pertaining to the topic of research. The first section will cover the air laying process as well as the behavior of discontinuous fibers through an air transportation chamber. The second section reviews the development of nonwoven composites along with the importance of fiber orientation in these materials. The final section explains composites which help with weight reduction in the automotive industry and the implementation of discussed nonwoven composites along with proposed applications and challenges.

2.1 Air Laying Process

The focus of this section is to analyze the aerodynamically formed web process, also known as pneumatic, or air laid web formation. Conventional systems utilize discontinuous (or staple) fibers which initially enter the process in a bale form, so opening of the fibers is the first step. The amount of opening depends on the entanglement of the fibers and if any blending is necessary [11,12]. The degree of opening also depends on the specific type of air laying equipment, but is much lower than a carding operation which is why cards are typically found as the first process [13]. Following the desired amount of opening and blending, carding would be required depending on if the fibers are from a bale, in order to create an amount of initial fiber orientation [11]. If the fibers are introduced as tow or filament form and cut prior to air laying, the before mentioned steps are not necessary. Conventional fiber collection systems are equipped with either a moving conveyor or rotating drum unit covered in a perforated screen which accumulates the fibers, creating the web and

transports it through the system [3]. However, developments have created techniques to form a net shape web via air laying over a three dimensional mold. This process is preformed in a batch-type of production and requires the collection grid to be stationary and typically created from perforated sheet metal stock [14]. There are many variations collection surfaces in the air laying process, however very little research has been performed on their effects.

The factor that each previously described system has in common is its use of directed airflow for fiber dispersion. In order to be efficiently controlled, the characteristics of airflow must be fully understood. According to Krcma [3], the orientation of fibers in an aerodynamically formed fiber web may be controlled either during the fiber transfer or during their deposition. The foundation of understanding an air laying system involves the understanding and control of airflow and the behavior of a fiber and fiber web in this flow. This section will provide a history of the air laying process and then will focus on the purpose and function of airflow and its influence on fibers through the air laying process.

2.1.1 History

The predecessor to air laying in nonwoven production was the carding process. However, carding creates highly machine direction oriented webs; hence, in efforts to increase random orientation and increase production rate, air manipulated dispersion technology was developed. An aerodynamically web forming system can be placed after carding during production in efforts to fully randomize the carded (highly oriented) fibers [15].

The first successful commercially produced air laying machine was the Rando-Webber created by Curalator (now Rando Machine Co.) in the 1940s [16]. The Rando-Webber created a consistent web formation system without the use of water as a transport medium and provided a solid foundation for air laying technology offering simple design and efficient functionality [17]. This system used a single card drum to dissipate the fibers into an air stream and collected the randomized fibers on a perforated drum. A major problem of the Rando-Webber was its line speed, being a single card system; there was a lag in production rate in order to produce the needed isotropic web [18]. To produce lofty webs, low line speed was necessary in order to build up the web on the collector to create a thick three dimensional isotropic web.

Figure 1 shows the Rando Webber single card mechanism and perforated drum collection system in a closed loop air circulation unit. The Rando Webber system was the pioneer for this area of simplistic web formation equipment, for example, using a single fan system for its closed airflow system. This closed loop generated pressure throughout the process, creating airflow at the card and suction at the drum. The closed loop air circulation units were very efficient when designed correctly. Other systems utilize partial vacuum (suction or sub pressure) flow and pressure (blowers or overpressure) flow, which will be discussed further in this review.

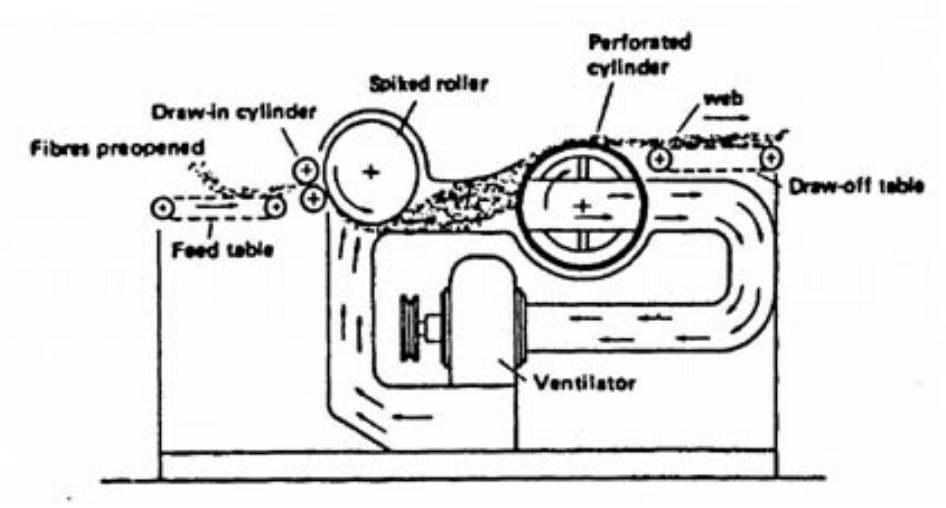

Figure 1. Rando-Webber Process [3; Krcma, 1971].

Furthering air laying development, companies such as Fehrer have used the Rando Webber design as groundwork to their innovative machinery. Prior to the Fehrer K-21, air laying was not designed to handle fine fiber (1.7-3.3 decitex) [18]. The Fehrer K-21 utilizes four sets of cards in series, to increase fiber blending through the process and to create a layering effect during web formation [18]. The innovative carding system in a series along with precise closed air loop circulation created a higher level of fiber control, making it possible to use finer fibers. In order to make that transition into finer fiber air laying, Fehrer had a strong understanding of the behavior and dynamics of a fiber within an air stream. Conventional air laid nonwoven webs have been characterized as being lofty (400-1500 g/m^2) and can be constructed with a wide range of fiber lengths and deniers [19]. Notable advantages of using air as a transport medium include its low cost, recyclability of air within the system and its ability to randomize and individualize fibers during transport [3].

2.1.2 Air Flow Behavior during Air Laying

The efficiency of these air laying machines is dependent upon the actions of the individual fiber through the system. These behaviors include how the fibers interact with fluids (air) and how the fluids influence the fibers. Understanding these parameters creates the ability to control the behavior.

Immense development has been invested into the creation of these aerodynamic systems; recent emerging computational and mathematically-based studies have made the true dynamics of these systems comprehensible [19]. The basic understanding of airflow through such systems begins with the essential knowledge of air pressure. The pressure of air can be controlled by either changing the temperature or amount of air in a system. Air pressure in a fiber air laying system is controlled by increasing or decreasing the air density of the system via fans or blowers [20]. There are two types of airflow in an air laying system, a push and a pull, the push is created by over pressure and the pull (suction) is created by sub pressure. The terms ‘suction’ or ‘airflow’ in a dynamic air system simply means the movement of a fluid from a state of higher pressure to lower pressure. Essentially, the airflow pushes the fibers from faster to slower moving air currents. Figure 2 shows a cross section of typical air transport chamber in an air laying process equipped with a conveyor belt. The fibers are fed through the air transport region from the top and are collected on the conveyor belt, accumulating to form a web.

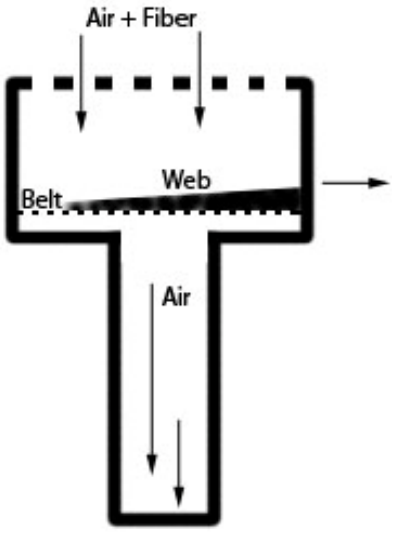

Figure 2. Cross Section of Transport Chamber.

Undisturbed air flow (meaning no fibers present) through this system should possess little to no turbulence. Turbulence is a disorderly flow composed of particles which follow an erratic path in three dimensions [21]. Very small turbulent flows frequently exist even in fluids which appear to have a smooth flow. Turbulence is created by continual variations of velocity, or pressure, in a flow [21]. In a system such as an air transport chamber, these changes in velocity are typically created due to the air flow coming in contact with large surfaces. When a fluid passes over an object, in this case, passes against the side walls of the transport chamber, boundary layers are formed around each solid surface.

When an object passes through a fluid or a fluid passes over a surface, the fluid molecules which come in direct contact with the object actually stick to the surface, due to the no slip condition (velocity is zero at the surface) [22]. These molecules which stick to the surface greatly reduce the flow of surrounding molecules, in turn slow down the adjacent

layers of molecules, creating a diminishing domino effect into the fluid. This area of molecular velocity reduction, as shown in Figure 3, is called the boundary layer. At lower air speeds (Reynolds number), the flow is typically linear, however at higher speeds, the boundary layer creates unsteady eddies, or turbulence [22]. This shows that the closer the walls are in the air transport chamber to the air flow, the higher amount of turbulence will be present. Essentially, walls or large surfaces in a chamber design are detrimental to controlling the air flow.

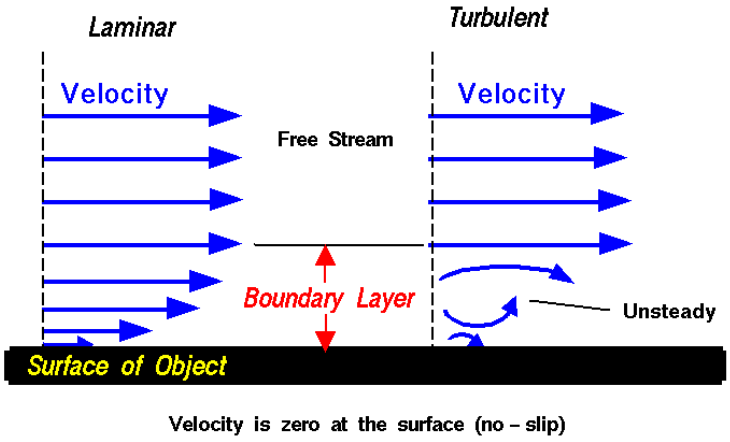

Figure 3. Boundary Layer [22; Benson, 2009].

Figure 4 shows the schematic of an air transport chamber used to study these boundary flows in air laying experiments conducted by Soltani and Ahmadi [23]. In their study, they were able to map the eddies created by the wall boundary layer, Figure 5 shows a velocity field across the chamber, as though you are looking in the direction of the flow [23].

The more concentrated the lines are in the field, the more turbulent the flows, almost creating a three dimensional visualization of the turbulent flows.

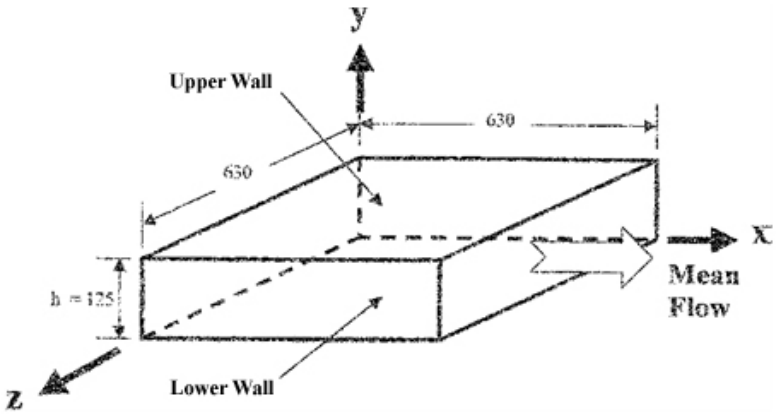

Figure 4. Schematic of Soltani and Ahmadi's air transport test chamber [23; Soltani &Ahmadi, 2000].

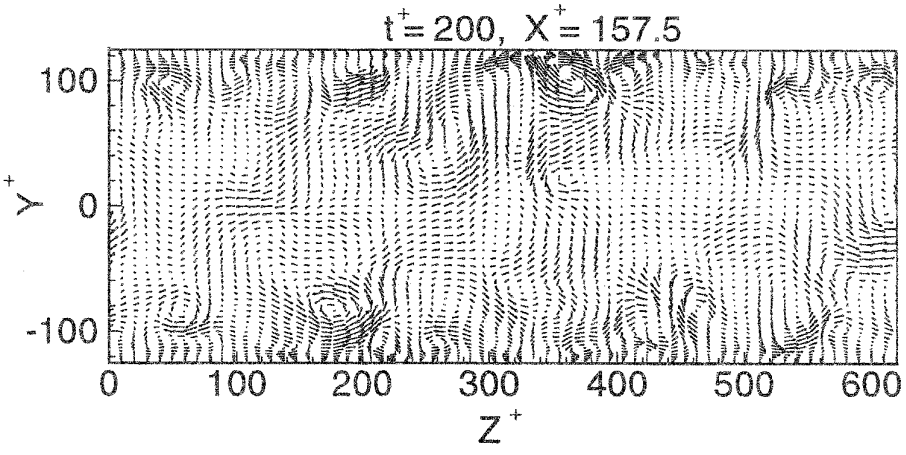

Figure 5. Eddies created by wall boundary layer [23; Soltani &Ahmadi, 2000].

These streams, shown around the edges of Figure 5, are relatively strong to a light weight fiber and have the ability to move fibers towards or away from the walls, ultimately affecting the fiber deposition process [23,24]. If turbulent air forces are present in the air transport chamber, the fibers will tend to follow the turbulent forces and ultimately unevenly accumulate. Figure 6a shows a vertical cross sectional airflow through an air transport chamber without any resistance (fibers or collection grid) with the input airflow at $u_i = 2$ m/s and $v_i = 2$ m/s (u_i = x direction, v_i = y direction) [19]. This visualization shows how the wall structures contour the air flow; however, the Reynolds number is too low in this case for any turbulence to be noticeable.

Figure 6(b) shows the air flow with resistance of a collection conveyor belt (no fibers), with the same input airflow at $u_i = 2$ m/s and $v_i = 2$ m/s (u_i = x direction, v_i = y direction) [19]. The presence of the collection grid shows how any resistance is capable of forming turbulence. Figures 6(a) and 6(b) are to demonstrate the significant change in airflow with the simple addition of a perforated collection belt. The images from Figure 6 were created in the study conducted by R. Bradean *et al* [19], in which the airflow was introduced at an angle (in the x and y directions) to create a longer curve in the air, which is shown by the loop on the left side of the chamber. This creates a longer air time for the fibers, allowing for higher levels of randomization and individualization of the fibers before accumulation [19].

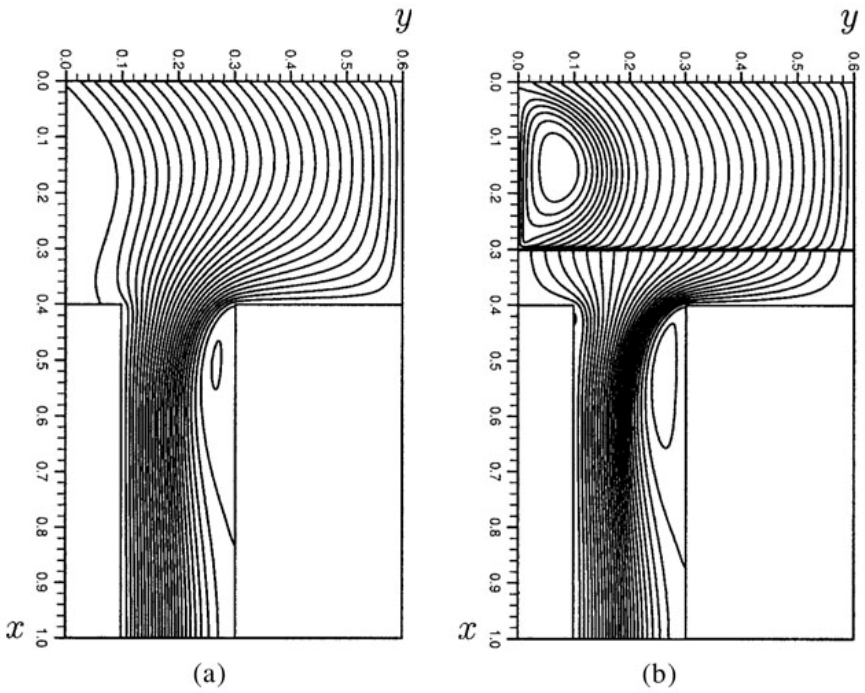

Figure 6. Computational Fluid Dynamic for no resistance (a) and belt resistance (b) [19; Bradean, 2001].

The review of literature pertaining to these air transport chambers shows the majority utilizes both over pressure and sub pressure. The over pressure is essential in randomizing the fibers and the sub pressure is to simply hold the web in place during processing or unbonded web transport. In systems with a high amount of over pressure, there are large boundary layers and ultimately high turbulence. Sub pressure systems, or systems only under partial vacuums, depend on gravitational forces more for fiber deposition. These forces will be discussed in the following sections. In processes such as aerodynamic fiber lay down where air is used to guide the process, the interaction of fiber and air flow is important.

Several studies have shown that the airflow movement has a direct effect on the fiber dynamics through an air transport chamber [23-26].

2.1.3 Individual Fiber Behavior in Airflow

This section will investigate the forces which influence the movement on a fiber through an air transport chamber. The interests of this study require the review of synthetic fibers, so the assumption will be made that fibers have a cylindrical shape. By understanding the influence of airflow on a fiber, parameters can be created to control the behavior of fiber. Prior to defining the acting forces on a fiber through air flow, it is important to understand that when studying these forces, air is a fluid and possesses characteristics, similar to those of water

Philip Jungbecker contested that the forces acting on a fiber can be divided into inner and external forces. The inner forces stem from the physical properties of the fiber itself, mainly the bending stiffness [25]. The external forces include hydrodynamic torque (twist), drag, lift and gravitational forces [26]. Figure 7 visualizes the external forces on an individual fiber. With an exception of the gravitational forces, there are two main contributing factors which create the hydrodynamic forces; air velocity and flow turbulence. In fact, when fibers are exposed to air velocities above approximately 20 m/s (depending on fiber diameter and length), individual fibers create their own boundary layers which have an influence in surrounding airflow turbulence [25].

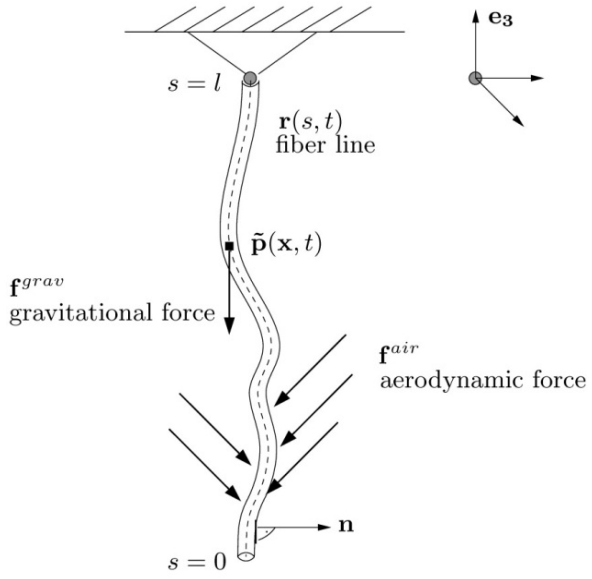

Figure 7. Forces acting upon individual fiber in transport chamber [27; Marheineke, 2006].

2.1.4 Air Velocity and Turbulence on Fibers

Air velocity, as mentioned earlier, is the speed of the movement of air across a surface (wall) or variance of velocity which creates turbulence. The energy spectrum of isotropic turbulence establishes that turbulence is driven by the larger eddies and is dissipated over time and space [27]. This determines that eddies will only become smaller over a given time and space. However, even the location of eddies not in contact with a surface have the ability to change over time as the air flow evolves [26].

Both air velocity and turbulence are present in the air flow chamber, however, the intensity of each force changes through the chamber. The use of over pressure and/or sub pressure determines the rate of both air velocity and turbulence in a system. This results in different fiber behavior at different distances from the collection grid in the chamber. For

example, Figure 8 shows a visualization of the velocity change ranging from greater than 0.45 m/s to less than 0.20 m/s across a plane set at 10 mm below the fiber input of the air transport chamber [28]. This turbulence is due to the accumulating web forming a gradient of air resistance in an over pressure system. This type of variation in velocity would create a high amount of turbulence for the individual fibers.

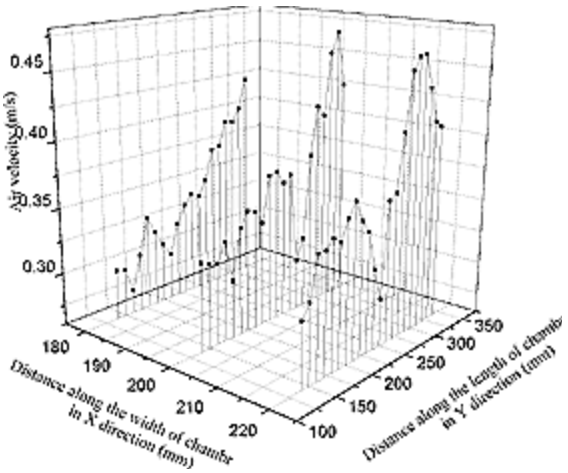

Figure 8. Air Velocity fluctuation at 10 mm below fiber input [28; Pourmohammadi & Russell, 2000].

As discussed in the Fluid Behavior in an Air Chamber section, boundary layers next to wall structures form high levels of turbulence. Research has shown that the eddies created at a surface typically stay in the same location, forming flow regions and have a tendency to push or pull the fibers towards or away from a surface and even make fibers accumulate on vertical surfaces[24].

The way that turbulence affects the movement of fibers is highly dependent on the configuration or angle of the fiber. Pourmohammadi and Russell showed that the configuration of the fiber entering the transport chamber is rarely influenced by the turbulent forces in the chamber [29]. Essentially, if a fiber enters the transport chamber with a radius curvature of θ, in the majority of cases, that fiber will land with the same θ configuration. This proves that fibers typically retain their initial curvature, however, the axis upon which that configuration lays changes due to the turbulence. Hydrodynamic torque affects fibers with higher degree of angle (or curvature) by rotating them around their z axis (running down the center of the fiber) faster and more often than straight fibers [23,25,26]. This also proves that fibers with low bending rigidity (which tend to naturally curve faster), potentially will rotate and twist more than more rigid fibers. Thinner fibers have lower bending stiffness than thicker fibers, hence, will be affected more by turbulence and may result in higher randomization.

Travelling from the top of the transport chamber down, the air flow tends to transition to a laminar flow, once the turbulent flows have dissipated. Figure 9 shows

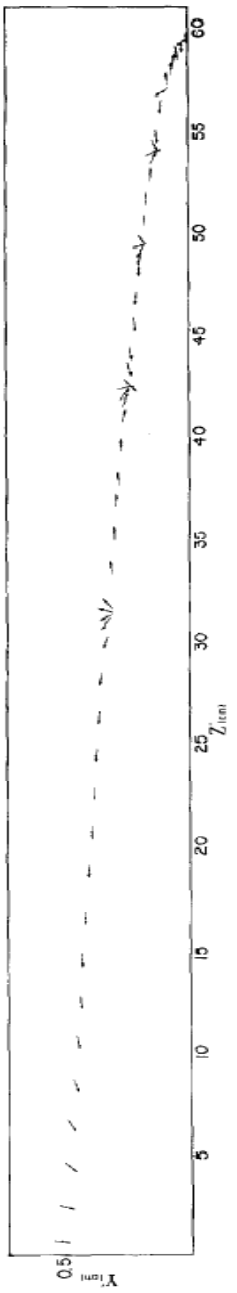

Figure 9. Fiber movement over time through an air transport chamber [30; Gallily, Eisner, 1978].

the movement over time of a fiber through an air transport chamber where the turbulent areas (towards the top, showing high rotation) fade to orderly laminar flow [30]. This study included the use of overpressure and sub pressure and Figure 9 shows that overpressure (introduced at the top of the chamber) induces a higher level of turbulent fiber behavior. Towards the bottom of the chamber, where the sub pressure is more established than the overpressure, the fiber begins to level out. The height at which the laminar sub pressure overtakes the overpressure depends on factors such as thickness and porosity of the accumulated web along with the air resistance of the collection grid [19]. The use of higher amounts of sub pressure will help create this transition at an earlier stage in the chamber. Since the aerodynamic forces on a fiber are dominant for their flight path, the use of sub pressure is beneficial in increasing fiber orientation because it helps straighten out the turbulent flows [25, 31]. By straightening out the flows, it essentially provides a path for the fibers to follow for deposition. In this region the velocity on the fiber increases, pulling the fiber down faster to ultimately land on the collection belt. The ratio of over pressure versus sub pressure has the ability to control the levels and intensity of velocity and turbulence. Higher amounts of over pressure yield greater turbulence, and more sub pressure provides oriented flow, leading to greater fiber orientation. Essentially, a system with greater sub pressure compared to over pressure should be more dependent on the collection board apertures. In a sub pressure system, the apertures act as air nozzles. Hence, by controlling the design of the apertures, the sub pressure system should yield high fiber orientation.

2.1.5 Types of Airflow and Their Effects on Fiber Accumulation

In aerodynamically controlled web formation systems, the characteristics of the web are highly dependent on the type of air system in the process. As mentioned earlier, the two types of air systems include over pressure (blowing) and sub pressure (suction). This section will review how each type of air system forms a fibrous web, the unique effects, their advantages and disadvantages.

The two types of air systems can be used individually or in combination, however when in combination, the ratio of over pressure and sub pressure can create different web characteristics [32]. Over pressure or compressed air creates a pushing effect on the fibers through the air chamber. As mentioned earlier, this type of pressure creates high amounts of turbulence and is advantageous for high randomized or high loft webs. However, over pressure can create unwanted fiber accumulation through the system (in turbulent flow fields) and can blow out fibers, creating unwanted voids in the accumulating web [24]. When used with a moving conveyor collection unit, the only orientation observed with over pressure is in the machine direction (MD) solely due to the movement of the accumulating web on the moving belt [33].

Sub pressure, on the other hand, creates a pulling effect on the fibers, providing more of a laminar path for the fibers. Air chambers with only sub pressure systems have produced results of higher fiber uniformity directly over the suction tube placement [33]. This proves that homogenously distributed sub pressure can provide high levels of fiber orientation in the

web. This idea has even led to patents being issued for machines which use adjustable aperture size to produce varying levels of fiber density throughout a single web [34].

A system which uses only sub pressure creates a fabric that possesses two distinct characteristics. Meaning the face of the fabric will be different than the back. This is due to the different levels of airflow the fibers undergo during the web accumulation. The initial fibers are pulled by the high suction force onto the collection belt, and then the following fibers are simply layered on top with less force and held into place by fiber adhesion and entanglement [33]. This creates a fabric with highly randomized base and a softer more machine oriented top. Figure 10 shows a cross section of fabric created by sub pressure, the left side is the bottom of the fabric that was subjected to a higher suction force than the lofty top (right side). From this analysis, it can be determined that in a system with only over pressure, the fabric would be of much higher loft.

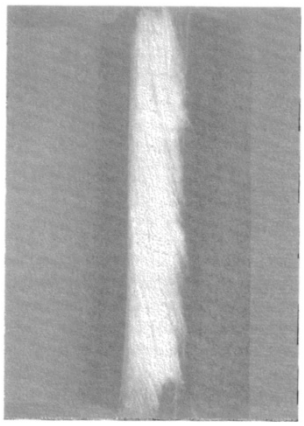

Figure 10. Web formed with sub pressure [33; Lin, 2001].

Web formation in a closed loop system utilizes both sub pressure and over pressure. The sub pressure is essential in order to initiate fiber accumulation and hold the base fibers onto the collection belt. Over pressure is desirable to create fiber individualization and randomization above the collection belt.

2.1.6 Effects of Fiber Accumulation on Airflow

These closed loop systems have been developed to help reduce the loss of steady airflow through the collection belt found in many air laying systems during formation. This loss of airflow is due to the increased thickness of the fibrous web and essentially, the increase of air resistance during web accumulation. The accumulation of fibers along the collection belt decreases the ability for the air to penetrate through, so it must find a path of least resistance, creating areas of high pressure. This area of high pressure is usually the entry point of the belt into the system because this is the area of least accumulation. As seen in Figure 11, in the transport chamber, the web is built in a progressive manner on the collection belt. The collection belt is moving from the left to right, accumulating fibers through the chamber. During web formation, fibers are moved by the stronger air pressure from the open area in the belt (left side), showing that the web thickness affects the intensity of the airflow [33]. This creates an unwanted horizontal airflow over the forming web from right to left which will be investigated further.

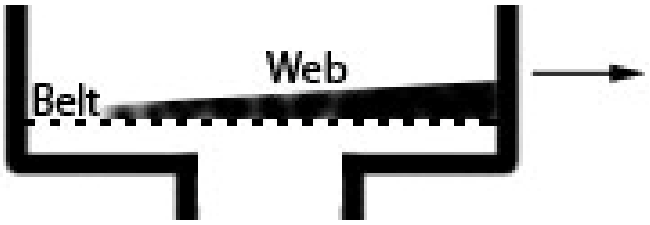

Figure 11. Fiber Accumulation on conveyor belt collection system.

To further prove the effect that web thickness has on the intensity of air flow, a study was conducted to plot the velocity of fibers passing through the transport chamber. Figure 12 shows the data from a Laser Doppler Velocimetry (LDV) analysis done on the velocity changes of fibers within a transport chamber set at a constant air velocity of 0.35 m/s [28]. Figure 12 shows a three dimensional layout across the chamber, the readings were taken at three locations across the width and length of the chamber all from 10mm below fiber insertion grid. The significant increase of velocity visualizes where the bare collection belt enters the chamber and where the fibers accumulate, decreasing velocity. This graph illustrates the fact that as the fiber web forms and becomes thicker, it allows less airflow to pass through. The airflow (both over pressure and sub pressure) are being diverted to the area of least resistance (bare collection belt).

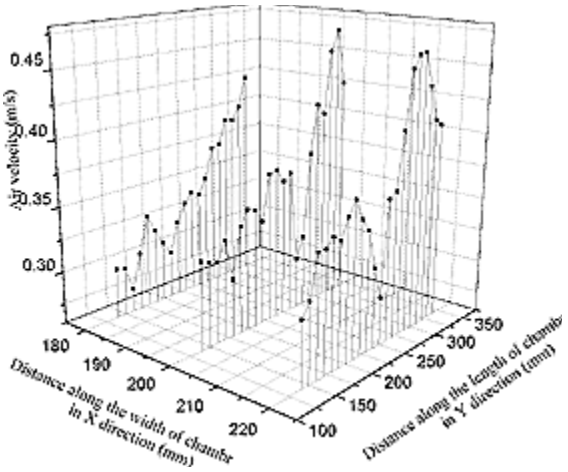

Figure 12. Fiber accumulation effecting the air velocity across the tranport chamber [28; Pourmohammadi &Russell, 2000].

The same study on fiber velocity by Pourmohammadi and Russell [28] shows that the closer the fiber moved towards the collection belt, the more uniform the velocity becomes. Figure 13 shows the velocity readings at 10 mm above the collection surface. This shows the uniform nature of the airflow associated with sub pressure even during fiber accumulation. This proves that the closer the fiber is to the collection belt, the more influence that laminar velocity (not turbulence) has on the fiber. As mentioned earlier, the sub pressure is the main source of laminar velocity. Since the source of laminar flow on individual fiber and web has been determined, the focus needs to be placed on how to control it. The collection surface itself has the potential to be engineered in a way to control flow.

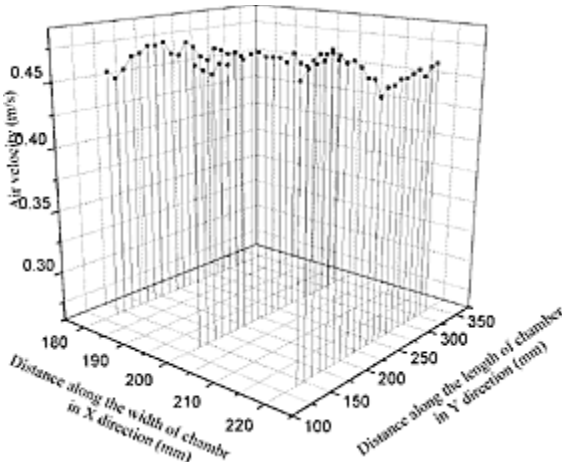

Figure 13. Velocity measurements 10mm above collection surface [28; Pourmohammadi & Russell, 2000].

2.1.7 Web Collection Surface

The medium used for web collection (also known as the collection grid) has evolved along with advancements in the processing techniques. The current nonwoven preform processing techniques are highlighted in section 2.2.1. Nonwovens as Composite Substrate. Conventional continuous air laying systems utilize a woven metal or polymer conveyor belt or perforated metal drum to accumulate the fibrous matt [1]. Figure 14 shows an example of a woven nylon conveyor belt. These types of belts would be used in order to mimic the belt's aesthetic effect onto the nonwoven fabric. Mesh belts are created with web aesthetics, durability and cost in mind; however fiber orientation is not a focus when developing these types of collection surfaces.

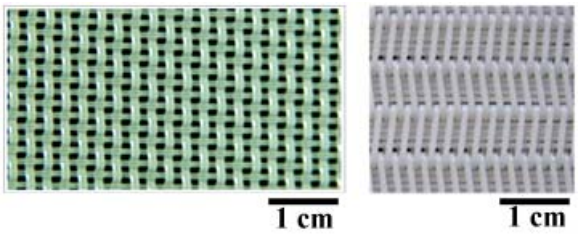

Figure 14. Conventional fiber collection conveyor belts [35; Retrieved from http://www.wiremeshdragon.cn/].

The perforated drums have proven to be more economical due to their smaller footprint and ease of maintenance. New developments in composite preform research have created processes which utilize an air laying technique creating three dimensional net shape forms for web production. Figure 15(a) shows a perforated sheet metal form used to create a cone shaped form utilizing an air laying technique. This metal form was used in a study which required the collection surface to remain stationary and the fiber deposition traversed above it [14]. Figure 15(b) shows the final component created from this three dimensional mold. This P-4 process focuses on developing three dimensional shapes with fiber alignment; however, there is no focus on the types and arrangement of collection surface apertures to aid in the desired fiber orientation.

a.

b.

Figure 15. Three Dimensional Nonwoven Preform Screens (a), fiber reinforced composite (b) [14; Cordell *et al.*, 2000].

2.1.7.1 Fiber Deposition Behavior

When a fiber comes to rest in the air laying process, there are two situations which can occur, the fiber can be deposited on a bare (empty) solid surface or come to rest atop already accumulated fibers. This section will discuss the different manners in which a fiber acts during these conditions.

A fiber which lands on a bare collection surface has the potential to go through one of six actions; hit-bounce, hit-fall, flat landing, penetration (into collection grid aperture), mid curve landing, or end curve landing [29]. According to Pourmohammadi and Russell, who analyzed 600 fiber landings, the most common was the hit-bounce, due to the high velocity the fiber is traveling prior to hitting the belt [29]. A hit-bounce is simply the act of a fiber landing on an end and due to its high rate of velocity, the fiber acts as a spring. The fiber initially bounces off the belt before the suction forces take hold to bring it to rest. In Figure 16, the horizontal line represents the collection surface, which in Pourmohammadi and Russell's study would be moving from left to right.

A large number of the observed fibers landed on an end or an angle relative to the belt, meaning that following initial impact, the fiber had to "fall" in order to come to rest on the collection surface. The understanding is that if a fiber lands on its end with an angle ranging from 10-90 degrees relative to the belt, it will more than likely endure a hit-bounce, and if it lands from 90-170 degrees, it will be a hit-fall [29]. Figure 16 shows the method of measuring fiber angle and an example of a fiber immediately prior to landing in relation to

the collection surface. This fiber in Figure 16 would more than likely undergo a hit fall due to its angle (~125^{o}).

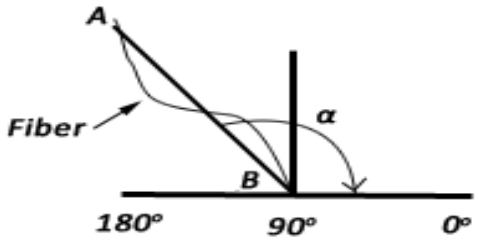

Figure 16. Fiber landing angle relative to the collection surface.

This data is from a study which utilized a conveyor belt collection system which may have affected the outcome of the data. However, the initial landing angles would not have been affected by such show a high landing orientation in the 100 to 140 degree orientation. This shows that fibers are moving toward 180^{o} orientation due to the increasing influence of the sub pressure. Figure 17 shows the distribution of fiber landing angles of the 600 recorded landings during Pourmohammadi and Russell's experiment. As seen, very few fibers landed completely flat (180^{o}) and the majority of fibers were angled between 110^{o} and 150^{o}, resulting in hit-falls being the most common action [29]. This outcome was highly influenced by the movement of the belt, causing the fibers to the left.

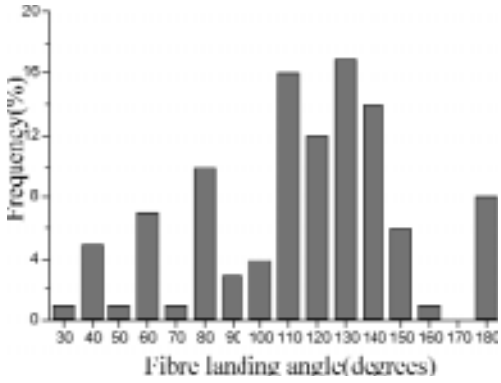

Figure 17. Fiber landing angle frequency relative to a bare collection belt [29; Pourmohammadi & Russell, 2000].

The other alternative in landing is for the fiber to find rest on a preexisting accumulation of fibers on the collection belt. During this occurrence, the fiber predominately keeps its existing configuration. The collection of fibers on the belt creates fiber adhesion, locking the residual fiber onto the web via entanglement and fiber-to-fiber adhesion.

2.1.8 Optimization to meet Research Objectives

This section will use the presented literature review to analyze factors which can be used to optimize an air laying technique to meet the research objectives. The objectives focus on understanding necessary variables which can be used to locally orientate fibers in a desired direction.

In the current study, optimization involves lowering the opportunity for turbulence and controlling laminar flow to provide greater orientation. As discussed in section 2.1.2. Fluid Behavior during Air Laying, turbulence is created from changes in air velocity and

from boundary layers created from solid objects. In order to control the changes in velocity, a system would benefit from a higher amount of sub pressure when compared to over pressure. This type of air stabilization via suction is known as laminar flow control, which reduces the boundary layer thickness and modifies the shape of the main velocity profile to improve stability [36]. Utilizing a laminar flow control method would reduce the randomization of the fibers in the chamber, allowing for greater orientation. The reduction of boundary layers will ultimately increase the stability of the velocity profile. Besides the individual fibers, there are three main factors that can produce boundary layers in the transport chamber; walls, accumulated web and collection surface [19].

First, the walls in such a system are designed to keep fibers from dispersing when using high levels of over pressure. However, in a system with larger amounts of sub pressure, walls would not be necessary if the ambient conditions are controlled.
Fabric specifications limit the amount of modification that can be done to the porosity of the accumulating web, so the two feasible areas of adjustment are the top input grid and the collection surface.

The top grid has the tasks to hold any clumps of fibers until the airflow has individualized them, the grid then helps direct airflow evenly across the chamber. Figure 18 illustrates the increase in airflow uniformity across the top grid when the air resistance of the top grid is increased from (a) 10^2 kg/(m^3s) to (b) 10^5 kg/(m^3s) [19].

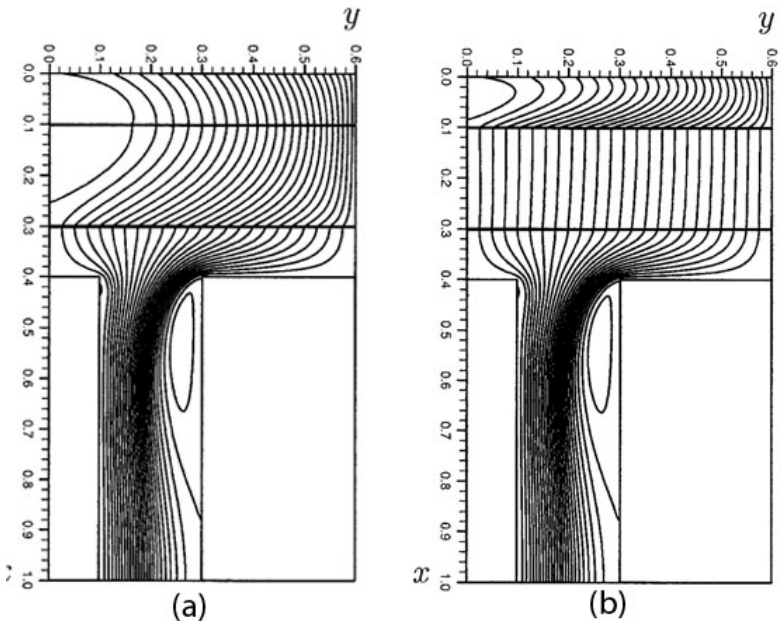

Figure 18. Airflow across grid, web and belt with different grid resistances [19; Bradean, 2001].

Figure 18(a) demonstrates the behavior of airflow across a top grid with the low air resistance, which resembles the flow curves with no resistance. Another desirable feature of increasing the grid resistance is the fact that any airflow parallel to the collection surface is reduced. As seen in Figure 18(b), increasing the grid resistance makes the holes in the grid act as nozzles, condensing the air to straight air tunnels. This can be advantageous, yielding a very uniform web across the surface area; however, with straighter air channels and low curvature, this leaves less time for the individual fibers to be exposed to the turbulent forces which influence higher randomization. Increasing the distance between the grid and collection surface can counter this effect, giving the fibers increased air time, allowing for extra time in the turbulence eddies.

The factor of increasing air resistance due to web accumulation must be kept in mind when analyzing the collection surface resistance. When the fiber web accumulates, the air resistance will not be the same across the collection surface due the web's progressive incline of buildup. By designing the collection surface to have a higher air resistance than the web, the uneven accumulating web will have less effect on the velocity. This will promote the transfer of air straight through the forming web rather than allowing the airflow to be influenced by an uneven air resistance. Higher level of airflow through the web results in a higher level of fiber packing. More efficient fiber packing allows for optimum airflow and reduces the risk of suction loss.

2.2 Fiber-Reinforced Composites

By industry standards, a composite is recognized as a material having two or more components in which one component stays in a solid state during manufacturing and neither is soluble by one another [37]. One of the constituents is referred to as the reinforcing element which is embedded or supported in the surrounding matrix [38]. In the realm of this study, these components will consist of a fibrous assembly embedded in a supporting polymer or plastic matrix.

Fiber-based composites offer high strength-to-weight and stiffness-to-weight ratios and have become strong alternatives to conventionally used materials including metals. The main benefit of a composite material is that, if well designed, they typically exhibit the best qualities of their components and often offer some qualities that neither component possesses [38]. From a practical viewpoint, the properties which govern the end use of any textile-

based composite are a function of the fiber properties, the characteristics of the fibrous assembly (web or fabric), the properties of the additives (web bonding, etc.) and the environmental conditions [39]. Due to the extensive range of raw materials used in textile production along with the versatility in fabrication of fibrous web structures, fiber based composites offer a seemingly endless spectrum of applications.

For example, advanced aerospace technologies, such as satellite development, demand the ability of a material to remain dimensionally stable during large temperature fluctuation ($-256^{o}F - 200^{o}F$) [38]. Due to thermal expansion, metals cannot meet these requirements, which leave composites composed of carbon and epoxy as the materials to successfully complete this application.

In highly competitive industries such as automotive or the airline market, properties such as overall weight reduction without sacrificing stiffness or strength are efficiently possible by replacing conventional metal alloys with composite materials [38]. However, one of the major drawbacks of composites is the high fabrication cost. For example, a part made from carbon/epoxy composite may cost up to 10 to 15 times the material costs, compared to conventional metals [38]. Even with possible falling raw material costs, process improvements must be done in order to bring the total cost down. In the modern markets it is vital to stay cost competitive by possessing the ability to lower cost while maintaining high production volume of a quality product. Improvements in processing and manufacturing techniques can greatly reduce costs and production rate.

Reinforcing fibers are available in a wide variety of performs, as shown in Figure 19.

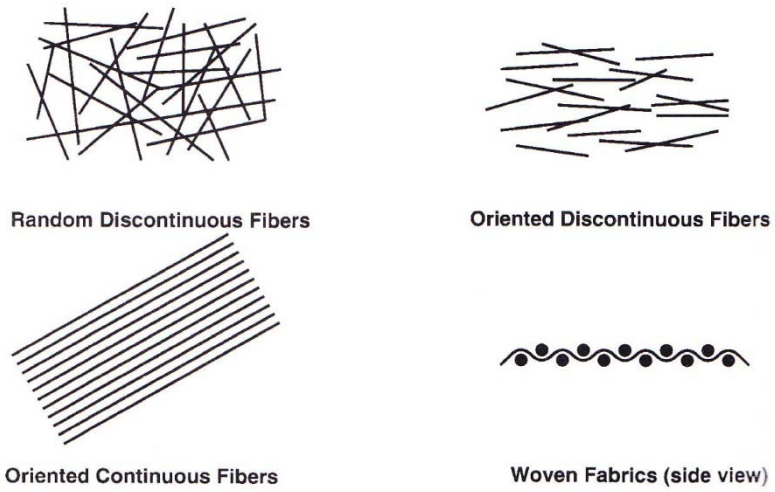

Figure 19. Types of fiber-reienforced composite preforms [40; Guell & Benard, 1997].

The most commonly used textile preform for composite applications are woven sheets. A simple woven sheet provides optimum strength in both the 0^o and 90^o orientations. This means that if a component requires strength in other directions (45^o for example), multiple layers must be constructed with the sheet orientation changing every layer. Figure 20 shows a visual of the type of layering required when using woven or unidirectional fibrous preforms.

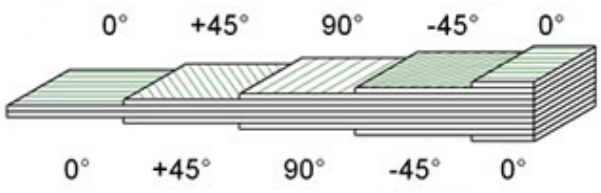

Figure 20. Layer stacking for fiber orientation [41; Retrieved from http://www.quartus.com/resources/whitepaper/composite/].

These layers must then be consolidated and subjected to a resin for hardening. The final applications of these composites are limited by thickness and geometry complexity amongst other parameters. Another drawback of layered sheet composites is delamination. Though these types of composites offer superior tensile strength in the fiber orientated direction, out-of-plane stresses may cause adjacent layers to separate or delaminate from one another [42]. If delamination occurs in an inner layer, it can be left unnoticed which could lead to a catastrophic failure.

An alternative to woven substrates is the lower cost, highly engineered nonwoven fabric. Nonwoven webs can be manufactured having three dimensional fiber placements, within a desired thickness, eliminating excessive composite thickness. Nonwovens preforms are constructed in a single layer, removing the chance of delamination. This study will focus on the use of nonwoven webs as a preform in composite manufacturing.

2.2.1 Nonwovens as Composite Preform

Due to their high production volume capabilities and low production cost, nonwovens are growing in interest as reinforcement elements in composite components. Compared to a woven or knitted substrate, nonwovens do not require a yarn production or separate fabric manufacturing process, ultimately consolidating the entire process.

Nonwovens are typically described as having isotropic characteristics, possessing the same properties in all directions, which is why manufacturers strive for complete fiber random orientation [2]. However, developments in manufacturing techniques allow designers to vary the amount of orientation in a component. By having the ability to change orientation

locally within a component, greater functionality can be created with a thinner cross-section. Compared to conventional woven preforms, nonwovens allow for such fiber reorientation within a design which can ultimately lead to optimized fiber usage and lower amounts of raw materials. Basically, nonwovens have the potential to eliminate fabric layering and produce desired fiber orientations in a single step.

A summary of commonly used manufacturing processes for nonwovens used as composite preforms is shown in Table 1. An open mould process means there is only one part of a mould used; the close mould refers to the act of having to close the fibrous preform between a dye and cavity [2].

Table 1. Commonly used nonwoven preform construction processes [2].

Manufacturing Route	**Outline of Fabrication and Processing Methods**
Open Mould Processes	
1. Hand Lay-Up	Chopped strand webs, woven, knitted or other fabrics are placed on the mould and impregnated with resin by painting or spraying. Layers are built up until desired thickness. Mould cures without heat or pressure.
2. Spray-Up	Chopped tow and resin are sprayed simultaneously into a mould and rolled to contour before the resin cures.
3. Vacuum bag, pressure bag, autoclave	Layers of fibers, typically woven sheets pre-impregnated with resin for a pre-preg. The pre-preg sheets are stacked on the mould in predetermined orientations, covered with a flexible bag and consolidated using a vacuum or pressure bag in an autoclave at a required curing temperature.
4. Filament Winding (three dimensional braiding)	Continuous filaments are fed through a bath of resin and then wound or braided onto a mandrel in a predetermined orientation and angles. The component is then removed from the mandrel for complete curing.
5. Centrifugal casting	Mixture of fibers and resin are introduced into a rotating mould and allowing the mixture to contour to the mould and cure *in situ.*

Table 1 Continued

Manufacturing Route	**Outline of Fabrication and Processing Methods**
Closed Mould Processes	
6. Hot press moulding, compression moulding	Sheet moulding compounds (SMC), fabric or pre-pregs are introduced into heated matched dies or tools and pressed into shape of the cavity and cured.
7. Injection moulding, transfer moulding	A mixture of molten polymer and short fibers is injected (at high pressure) into the cavity of a split mould and allowed to solidify or cure.
8. Pultrusion	A continuous feed of fibers in a predetermined orientation (typically unidirectional from a creel) is impregnated with resin and pulled through a heated die to give the shape of the final section. Curing occurs during the passage through the die.
9. Cold Press Moulding	A low pressure, low temperature process in which fibers are impregnated with resin and then pressed between matched dies. Heat is generated during curing.
10. Resin Injection	Fabric is placed in a mould and closed. The resin is injected at low pressure into the cavity and flows through the fibers to fill the mould space.
11. Reinforced reaction injection moulding (RRIM)	A rapid curing resing system involving two components which are mixed immediately before the injection process. Fibers are either placed in the closed mould before resin is injected or added as short chopped fibers to one of the resin components to for a slurry before injection.

2.2.2 Fiber Alignment in Nonwoven Preforms

Aligned fibers in a composite preform offer several benefits including higher strength and stiffness in the aligned direction [40]. Due to this strong advantage, several industries have become greatly interested in fiber alignment technologies. Aerospace technologies have developed automated fiber placement processes in order to consolidate parts, ultimately reducing the weight of the end unit. The rationale and developements will be discussed further. This section will investigate the interest in fiber alignment processes, the mechanical properties of the end product and the variables which determine those properties.

2.2.2.1 Continuous Fiber Placement

The instances when continuous fibers are used in a nonwoven process, the fiber architecture are typically one dimensional. The one-dimensional architecture describes the use of the continuous fibers in a single direction, giving the product very high strength in the orientated direction [2]. This one-directional technique can be used to create multi-directional architectures by layering the unidirectional layers and varying the angle of orientation on each layer [43]. When this method is preformed the fiber architecture resembles the layered woven fabric composite, without the process of interweaving the fibers. Although this eliminates the weaving process, as mentioned before, there is a drawback of the thickness being created when adding multiple layers.

Currently, this technique of direct fiber placement involves the use of a high precision robotic arm which lays continuous pre-impregnated tape into desired orientation or patterns on a preform [44]. The pre-impregnated tapes are unidirectional fibers infused with resin

typically in widths from 3 to 50 inches [38]. This particular process and the use of continuous fibers shows advantages such as parts consolidation and weight reduction in large cylindrical pressure vessels, i.e. airplane fuselages and pressurized tanks [4]. Although this type of process does greatly reduce the direct labor costs, the systems lack the ability to manufacture a wide range of three-dimensional structures, can only create a single orientation per pass and is very time consuming [44].

2.2.2.2 Discontinuous Fiber Placement

Studies by Dingle suggest that a composite preform made from perfectly aligned discontinuous fibers can, theoretically, be expected to utilize available fiber strength almost as efficiently as a unidirectional continuous fiber composite [40]. Although the tensile properties of discontinuous fiber composites have been found to be lower than continuous aligned fiber material, several industries (such as the automotive industry) rarely require completely unidirectional support and could benefit from the formability and flexibility of discontinuous fibers. However, discontinuous fiber reinforced composites are weaker than continuous fiber composites because of the stress concentrations located at the end of each fiber [40], this will be reviewed further in the following section.

Micromechanical analysis of discontinuous fiber composites shows that 95% efficiency of continuous fiber reinforcement can be achievable for fiber length (longer than the critical fiber length) with optimum aspect ratio for a given matrix and discontinuous fiber diameter [45]. Critical fiber length is the fiber length where the peak stress in the fiber

reaches the failure stress [40]. Essentially, it is the optimum length a specific fiber type must be in a composite to be used at its fullest potential before it fails.

This proves that along with an increase of the fiber volume fraction (from the current 10-30% in SMC), positively controlling the short fiber orientation can result in superior strength, stiffness and other in-plane mechanical properties in a desired direction [46]. The use of discontinuous fibers in the direct fiber placement process offers a higher versatility of possible product structures and mechanical properties.

State of the art versions of this technique use the stationary perforated mold, and filament tow is fed into a chopper gun, which is located atop a robotic arm in order to traverse the entire net shape [14]. Depending on the complexity of the preform, this discontinuous technique can facilitate cycle times around 5-10 minutes [14]. Also, depending on the complexity, this technique can achieve anywhere from 20% to 70 % alignment with poor repeatability [5]. Figure 21 shows the classifications of composite materials as discussed and highlights the area of interest in this study.

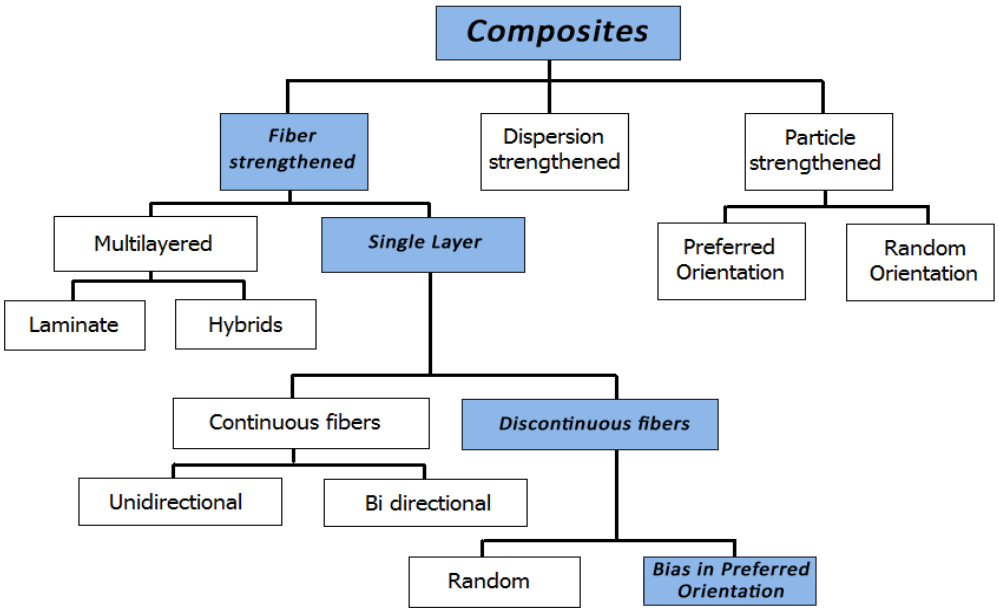

Figure 21. Classifications of fiber reinforced composites.

2.2.3 Mechanical Properties of Nonwoven Discontinuous Fiber Composites

This section will review the main mechanical properties that are of interest in nonwoven discontinuous fiber composites. Textile-based composite preforms have excellent properties within the plane of the component, in the fiber direction in tension; however, to a lesser extent, in compression [40]. As mentioned before, ultimately the fiber properties, the matrix properties, and fiber/matrix interface govern the final composite characteristics. Simply compared to more conventional materials, composites have the ability to allow the designer to tailor the desired mechanical properties by the selection of suitable resin and fiber type, fiber orientation and fiber volume fraction. By manipulating these variables, it is

possible to reduce in-plane anisotropy to produce a quasi-isotropic material and improve shear and transverse performance in predetermined direction [47]. As mentioned earlier, delamination is the most prevalent, life-limiting failure mechanisms for layered fiber-reinforced composites. Hence, utilizing short fiber orientations to reinforce in the z-direction would result in composites with dramatically improved delamination resistance.

2.2.3.1 Strength Due to Fiber Alignment

It has been shown that just a small fiber alignment bias is sufficient to significantly improve the properties of an otherwise isotropic part [2]. Figure 22 shows a fiber in a matrix which is crossing a cracked plane with applied load (F). When load is applied in Figure 22(a), the interfacial shear stress between the matrix and fiber will remain constant through the loading phase. However, Figure 22(b) shows a fiber at angle (θ), creating flexural stresses to the fiber during loading, which causes a loss of fiber strength and ultimately reduces the fracture strength of the composite [48]. This experiment found that the tensile strength of the fibers decreased with the increase of inclination angle [48]. When the angle of the fiber increases, the stress distribution across the fiber becomes more uneven, creating larger areas of stress.

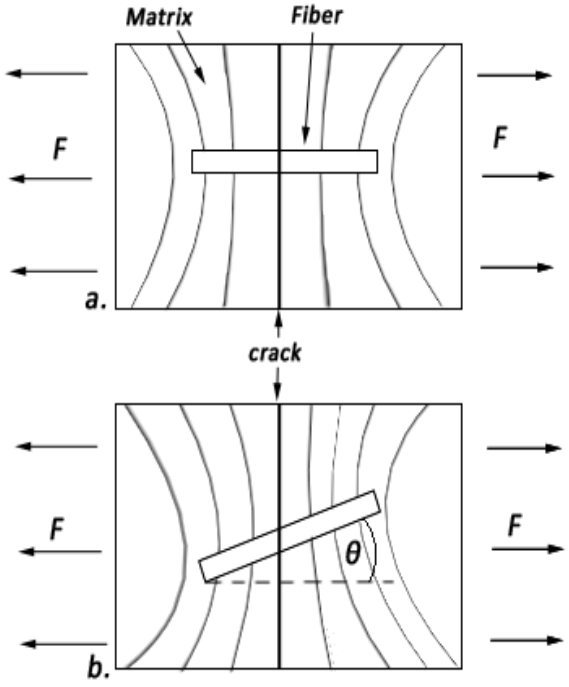

Figure 22. Schematic drawing of forces acting on a fiber across a crack (a) parallel to the crack (b) fiber crossing at an angle.

Research has found that even partial fiber alignment in nonwoven preform webs has the ability to increase the overall stiffness and strength by over 200% [5]. Fiber alignment in the load direction also increases the fiber efficiency factor for the strength of the composite meaning that the more orientated the fibers are in the load direction, the fibers are being used to a greater potential [48].

The opportunity of these fibers to align in a desired direction in specified local areas of a component could produce a truly engineered, tailored preform. Such research has opened the door to directed fiber alignment technology, producing nonwoven composites with highly accurate fiber direction. The challenge with this type of technology is the repeatability and

cost of creating a process that will produce the same results in a production setting. The strength of a fiber-reinforced composite can best be put into perspective by working backwards and studying how and why it fails.

2.2.3.2 Failure Mechanisms

How a composite fails helps identify and analyze what type of load it is capable of withstanding and to what degree. There have been many studies conducted on the behavior of composite failure and within the realm of nonwoven substrates, fiber volume fraction, fiber type and fiber orientation have been found as key properties when determining the failure strength [49,50-54] . Giurgiutiu [49] analyzed the behavior of composite failure and was able to separate them into three categories: progressive ductile, progressive brittle and sudden brittle failures.

- Progressive ductile failure is described as after a laminate reaches its yield point, it still possesses residual strength, allowing the composite to gradually fail. This type of failure is common in composites which have strong fiber to matrix cohesion.
- Progressive brittle failure is defined by when a laminate in a composite fails; it loses its entire load carrying capabilities. This type of behavior is conducive to a composite with a weak matrix/fiber interface, which makes fiber pull out after the yield point more common.
- Sudden brittle failure is when the weakest lamina fails; the failure propagates through the composite, meaning the entire composite fails after the weakest segment fails. This behavior is mostly seen in systems with weak matrix components.

The before mentioned studies have shown that no matter which failure mechanism a composite experiences, the strength of the nonwoven composite is partially dependent on the amount of orientation in the direction of the load. This study will focus on the importance of this orientation, an efficient process in which to obtain orientation and possible applications. Giurgiutiu studied each of the before mentioned three types of failures in relation to three different fiber orientations: random, slight fiber biased towards the 0^o, and strongly biased (2% of fibers) in the 0^o [49]. Each of these fiber orientations was placed through each of the before mentioned failure behaviors, and the results proved to be the same every time. The random web composite has the lowest tensile strength, and the strongly biased webs have the highest amount of strength. Figure 23 shows three stress strain curves; (a) progressive brittle failure, (b) progressive ductile failure and (c) sudden brittle failure. In each of these graphs, W represents the strongly biased web, KR is the slightly biased web and H is the random [49]. An important note of this study is the fact that even though the highly biased web is the strongest of the three, it is only the strongest by a minimal amount (~9% higher strength) [49]. This proves through any type of failure, even a slight orientation in a nonwoven composite greatly increases its yield strength.

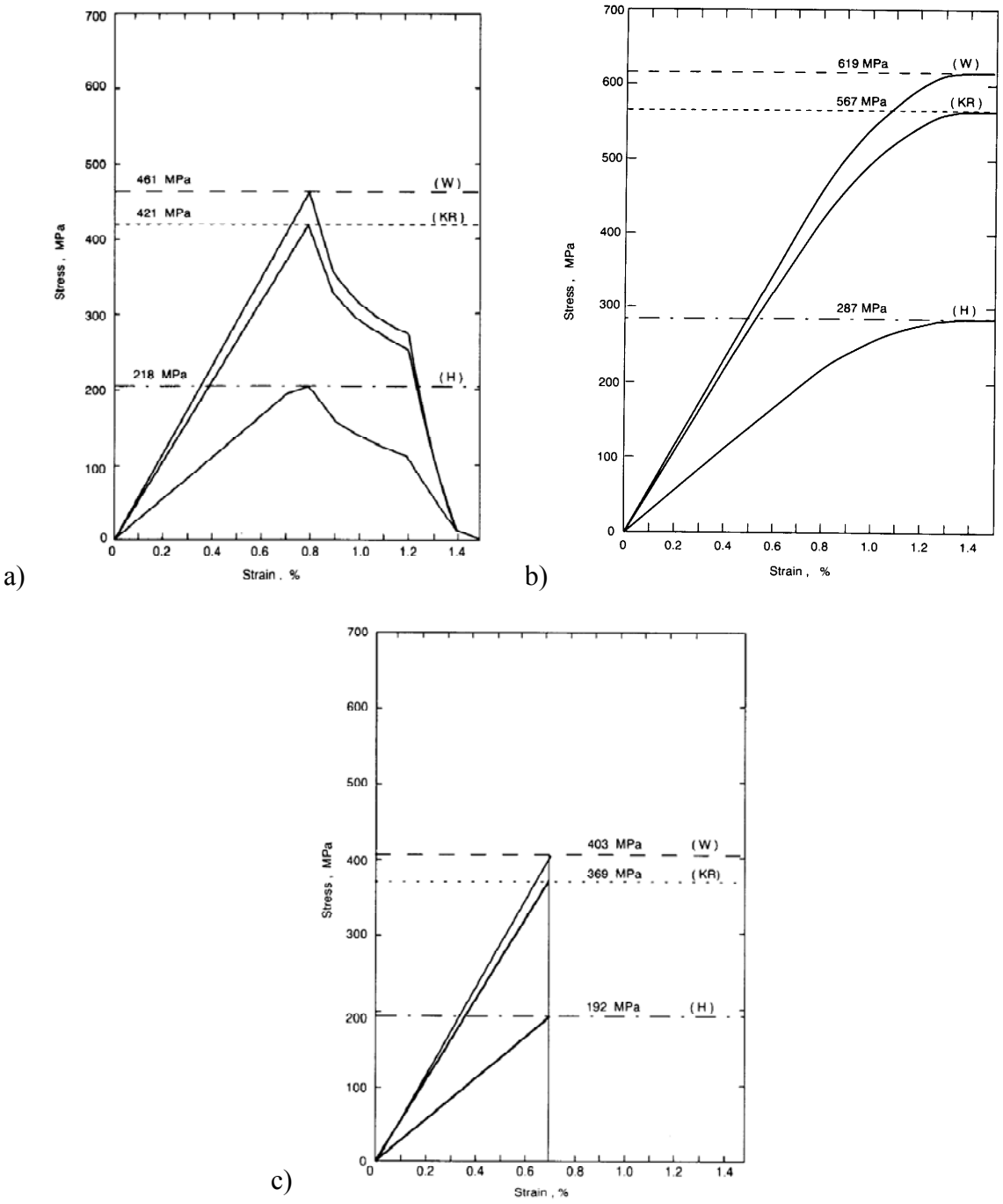

Figure 23. Progressive brittle composite failure (a), Progressive ductile composite failure (b) and sudden brittle composite failure (c) [49; Giurgiutiu & Reifsnider, 1994]

Studies have even taken into account normalizing the volume fraction, which produce the same results [5]. This establishes that in any standard process, selective fiber alignment can be seen as a valuable asset by significantly increasing mechanical properties in a particular direction. An important focus is being able to engineer a process to create this fiber alignment either locally or globally within a component.

2.2.4 Use in Complex Geometries

Many industries which have very high production volumes are interested in fiber reinforced composites due to their ability to be molded into complex geometries during manufacturing. From an engineering aspect, this means the advantage of utilizing fewer parts and a lower weight for the end unit.

Currently, when a nonwoven is used for a preform in a composite application, a sheet molded compound (SMC) or a continuous filament random mat (CFRM) is used [10]. These are flat nonwoven mats infused with resin which are cut to shape and stamped or stretched across a mold to form a component. Pre-constructed webs are useful for flat components or parts with very little degrees of draw [10]. Figure 24 shows a simple example of how these sheets are molded.

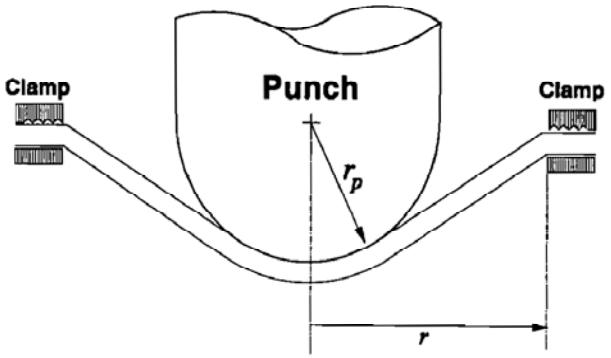

Figure 24. Simple example of sheet molded compound stamping [10; Rudd *et al.*, 1995].

However, these sheet molded compounds are limited by their two dimensional fabric architecture and encounter problems with deep draws and complex geometries [10]. Deep draws can result in fabric shear or fiber stretching which can produce weak spots in the preform which will be reviewed in the following section. This is the reason why spray-up style nonwoven preform processes have become of high interest in complex preform construction.

By allowing the fiber to contour to the mold instead of stretching it over a mold allows the fiber to retain its initial strength. Figure 25 shows an example of an air laid style of preform construction over a marine motor cover with deep draw geometry. The type of preform shown in Figure 25 could not be made from SMC without severely damaging the mat. The idea is to create the fibrous preform around the mold instead of molding a fibrous sheet, eliminating the fibrous mat construction.

Figure 25. Marine motor cover constructed by nonwoven spray up fiber deposition [55; Brandt & Reeve, 2001].

2.2.4.1 Challenges

During a production process that involves a human operator, there is always a higher cost for operation, and room for human error will always exist. This is the reason why companies try to automate as much of their production as possible. Hand laying composite performs is not only time consuming, but expensive and leaves room for human error. However, even automated procedures include areas for error.

When a two dimensional mat (woven, knitted or nonwoven) is converted to a three dimensional preform (ex. compression molding, hand laying, etc.) there are four behaviors which could occur; stretching of individual fibers, fabric shear, inter-fiber slip and inter-ply slip [10]. Each of these has the ability to change the property of the fabric, ultimately

changing the structural performance of the composite, making accurate material properties difficult to predict.

During molding for complex geometries, nonwoven SMC mats undergo varying levels of deformation, which changes the mechanical behavior of the preform and can be characterized by; elastic modulus along fiber axis, elastic modulus and shear modulus in the plane of the cross section, shear modulus and Poisson's ratio in the axial planes [39]. Each of these changes can go unnoticed and create a unpredicted failure.

Any of these highly stressed areas in a preform can create a void space in the fibrous web. When resin infused, these void spaces generate resin rich areas, creating a higher opportunity for brittle failure due to matrix damage [1].

One of the largest challenges with preform construction is the repeatability [9]. As previously mentioned, nonwovens are of high interest because of their high production volume potential. However, if the process is not repeatable within a certain range, it becomes useless to a high volume production industry. In large industries such as aerospace and the automotive industry, it usually takes years of research and development to eliminate any production problems. Nonwovens provide an excellent foundation for improvement and further development into structural components.

2.3 Model of the Automotive Industry

The development of the automobile signified one of history's greatest advances, providing a means for people and their ideas to travel faster and further than ever before. Contributions from early industry pioneers such as Dr. Ferdinand Porsche, Ransom Olds and Henry Ford changed the perception of automobiles as being unattainable by making them affordable to the majority of the population. A larger market base meant more options and diversity in automobile design. Customer demands caused the automotive industry to mature and learn how to adapt to an outside variable. However, by making automobiles more attainable and readily available, the number of vehicles on the roads grew exponentially. Other factors, such as oil prices, war, environmental and safety standards started to affect the design and production of the automobile.

In 1941, World War II caused a depletion in the steel supply for the automotive industry so Henry Ford introduced a light weight composite-bodied vehicle made with soybean fibers in a phenolic resin [56]. The idea of weight reduction in automobiles has always been alive in the racing industry, however, with innovative ideas such as this, manufacturers began looking into ways to introduce weight reduction into production models. A LIFE magazine article in 1952 covered a small company by the name of Glasspar who created a fiberglass automobile body which was more than half the weight of the current steel body [57]. This development inspired the idea of the fiberglass-bodied Chevrolet Corvette, which was released in 1953.

However, at this time, the price was too high for light weight composites to fully be adopted for the full production level and no manufacturers could find legitimate reasoning for the investment in such technology. Into the 1960's, car designs progressively grew in size and weight, ultimately lowering their fuel efficiency. The oil crisis which began in 1973 enlightened customers on the influence of petroleum on the automotive industry and finally provided a reason to think more efficiently (fuel and production efficiency). As the first congressional mandate on the automotive industry, Congress enacted the Energy Conservation and Policy Act of 1975, which included Title V, "Improving Automotive Efficiency", establishing fuel economy standards [58]. The result of this act was the push for smaller, lighter and more fuel efficient vehicles, forcing manufacturers and suppliers to begin investing in lighter material options.

Figure 26 shows the price of petroleum, the increase in the late 1970's and the most recent increase beginning in 2000. The United States average automotive production from 2000-2008 was over 16.7 million units a year, but due to the oil prices, has decreased to just over 10.5 million in 2009 [59]. This shows that customers are being affected by the oil prices and may choose to keep their vehicles longer than they have in the past. The current oil issues have caused many manufacturers to look towards other means of fuel or power train sources.

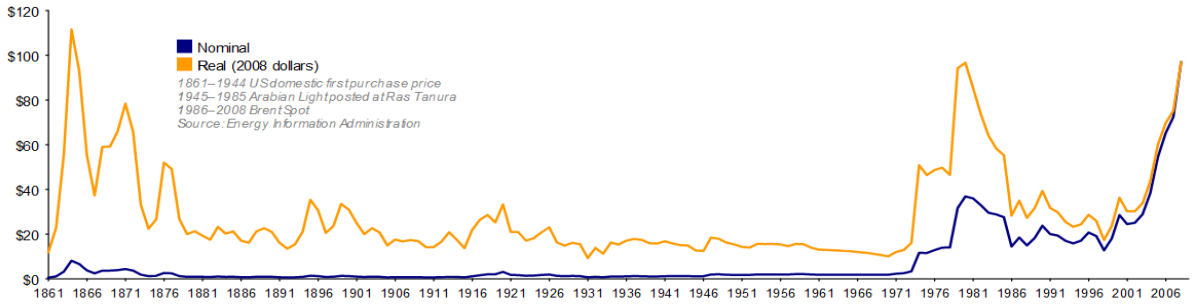

Figure 26. Oil prices from 1901-2009 [Wards.com].

Environmental effects such as global warming and pollution have laid groundwork for the "green" revolution. Customers have turned to making decisions based on the products environmental impact or sustainable qualities of a product. In the automotive market, this means there is a higher demand for cleaner and more fuel efficient vehicles. This however, creates the major challenge of balancing environmentally friendly engineering and production while maintaining (or exceeding) their standards for comfort, safety, price and reliability established by each brand. Manufacturers have the ability to handle the environmental stance from different angles, since vehicles affect the environment in different ways through their life cycle. These affects include the consumption of energy (fuel economy) and resources (materials), waste generation, greenhouse gases, hazardous substance emissions and the waste created at the end of the vehicle life. Manufacturers along with designers are aiming to maintain this balance by investing in lightweight materials for lean weight and sustainable designs.

Out of the total energy consumed over the life cycle of an automobile, approximately 94% is consumed during the usage phase, 4% in the production of the materials, 1% in the

manufacturing of the vehicle and 1% in the disposal of the vehicle [60]. This indicates that the focus should be placed on making the use of the automobile more efficient rather than the production or deposal. In efforts to regulate this, in 2009, the United States government put into place the first ever greenhouse gas pollution standard for automobiles, requiring a 5% annual increase of fuel efficiency from 2012-2016, ultimately resulting in automotive manufacturers providing a line of vehicles with an average of 35.5 miles per gallon[61].

The idea of weight reduction not only offers the benefit of better fuel economy which ultimately lowers emissions for gasoline vehicles, but overall energy efficiency for any type of drive train. Textile-based composites offer several benefits when being used in automotive applications. Fiber-based composites have a lower density than metal alternatives, are more versatile and can be produced to offer recyclable and biodegradable components. Mixing and matching specific fibers and processes can yield a tailored performance profile. Currently carbon fiber composites and sheet molded composites (SMC) are of main interest for production. Carbon fiber woven composites are of interest due to their high strength, low weight and resistance to UV degradation. Random fiber SMC's, on the other hand, offer high volume production, low cost, but lack in the strength when compared to woven composites. In order to establish a probable material, it would need the production ability of SMC with the strength comparable to woven composite.

2.3.1 Energy Efficiency

In the United States, fuel economy is regulated by the government mandated Corporate Average Fuel Economy (CAFE) standards. These standards regulate the miles per

gallon of vehicle manufacturer's fleets for passenger and light trucks [62]. The initial standard in 1978 was 18 mpg, currently in 2010 it has risen to 27.5 mpg and it is destined to increase to 35 mpg in 2020 [63].

The continuing efficiency of a vehicle can be directly related to the sustainability of an energy source. Providing an energy efficient vehicle also secures environmental sustainability. The idea of sustainability is the act of looking into future implications of current actions and decisions. Essentially, it is the ability to foresee a crisis and act accordingly which may require the use of more common sense rather than economics during design and engineering [64]. Manufacturers and suppliers are found backed into a corner with an economy on the rocks and sources of petroleum drying up; the need for efficiency, in every aspect, is higher than ever. But, just as the automobile is a complex integration of a number of subsystems, efficiency will not be reached by a single solution. For example, the future for alternative fuels appears very bright due to the great emphasis in research and development, however, mainstream implementation is still very far off. Increasing fuel efficiency appears to be the most viable direction for manufacturers to take. An important platform used to help improve vehicle efficiency and thus fuel economy is weight reduction.

For every 10% reduction of mass in a vehicle, the fuel economy is increased by 6-7% [63]. For a mid-sized family vehicle weighing 3,200 lbs, it takes a 100 lbs. mass reduction to achieve 0.6 miles per gallon improvement in fuel economy [65]. In terms of emissions, reducing a vehicle's weight by 220 lbs. results in CO_2 reduction up to 20.1g/mile [65]. Figure 27 shows a comparison of vehicle weights to their fuel economy over 100 miles, with a line at the average family-size car at 3,000 pounds [62]. This graph shows that fuel

consumption is roughly proportional to the weight of the vehicle. Figure 27 proves that energy efficiency is proportional to the energy efficiency of the vehicle, showing the need for weight reduction in automobiles.

The textile field has been of increasing interest to automotive suppliers as a source of reducing weight in vehicle components. Modern technology and refined processing have produced textile-based composites with significantly better mechanical properties and more versatility for functional applications when compared to conventional materials.

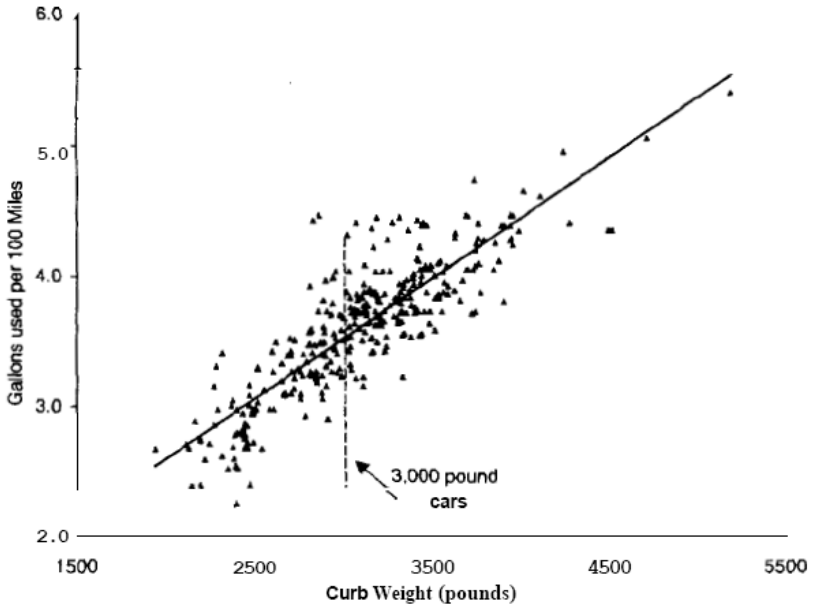

Figure 27. Relationship between vehicle weight and fuel consumption [62; U.S. National Research Council, 2002].

2.3.2 Weight Reduction

As a result of the CAFE regulations, US automotive manufacturers turned to weight reduction and smaller engines to achieve better fuel economy. The average vehicle weight decreased 4050 lbs in 1976 to 3050 lbs in 1986 [66]. However, the average vehicle weight has started to creep back up from the mid 1990s due to new safety equipment, emission controls and entertainment systems. Due to the requirement of the safety equipment and emission controls, other means of weight reduction are necessary to lower the vehicle weight.

The weight, or mass, of a vehicle has two primary effects on the force needed to move the vehicle – first, to overcome the rolling resistance to maintain a constant speed, and secondly, to provide acceleration [65]. Since most passenger vehicle driving involves a considerable amount of both types of actions, the mass of the vehicle proves to be an important factor in overall fuel economy. The implementation of weight reduction design methods do provide improved fuel economy, which in turn yields lower emissions. Automotive manufacturers making efforts to utilize weight reduction design methods typically follow three basic approaches [65]:

- Material substitution; utilizing alternative lighter weight and/or stronger materials more broadly.
- Advanced CAD vehicle design and manufacturing techniques; to optimize load distribution and reduce the use of redundant materials.
- Efficient vehicle design; optimize cargo and passenger space to manage a more overall compact body design.

One added benefit of weight reduction is that is creates the ability to lower the vehicles center of gravity and equalize the mass vehicle mass distribution which improve the vehicle handling [66]. In terms of production, weight reduction can be used to lower the number of parts necessary for a component. A lower number of parts have the ability to provide higher production volumes, which would help justify the tooling costs. Weight reduction is important in all forms of transportation, commercial or private and establishes advantages in both markets.

In Europe, the car industry is responsible for 12% of the carbon dioxide emissions [65]. In order to contribute to the international fight on global warming, the European Union (EU) passed mandates to the automotive manufacturers. These types of government enforced regulations have been a main driving force behind the market growth of the composite market in Europe.

Another factor is the actual size of the vehicle. Many consumers feel that larger vehicles are safer and might be reluctant to support weight reduction in fears of only being offered small cars. Physics dictates that an occupant in a heavier vehicle will be safer in the event of an accident. However, studies show that in two-vehicle crashes, an increase in mass of vehicle A exposes the occupants of the vehicle B to increased risk [67]. This study also shows that increasing the size of a vehicle (without increasing the mass) reduces the risk to the driver and also reduces risks to the other car occupants [67]. Larger vehicles by volume offer increased occupant and cargo room which, in the event of an accident is valuable crash protection. This proves that light weight vehicles can be large in dimensions and be safe.

Placing importance on highly engineered parts is the key to successfully reducing weight and retaining safety.

2.3.3 End of Life Recyclability

An increased concern focuses on the environmental impact of vehicles and has led automakers to improve the recyclability of newly manufactured vehicles. This direction leads to ideas of not only creating automobiles which are easy to assemble (i.e. part consolidation) but which are easy to disassemble for ease of recycling. The European Union has mandated that all vehicles must be 85% recyclable and up to 95% by 2015 [68]. There are no such requirements in the United States as of yet, however, if any automaker exports cars to the European Union, they will have to comply with these regulations. These types of regulations have led vehicle manufacturers to begin designing vehicles with new criteria including [69]:

- Engineering environmentally friendly aspects and recycling into products right from the concept phase.
- Reducing complexity by using fewer material types.
- Avoiding mixed materials and marking components with recycling codes where possible.
- Use of materials that can be easily recycled and use of materials containing recyclate where available.
- Design for easy separation.

Each vehicle manufactured requires around 45 lbs. of textile products, in which nonwovens accounts for around 11%, making the yearly demand for nonwovens in 1999 for

the automotive market around 120,000 tons [70]. The continuously increasing demand for these weight reducing materials is reflecting on the types of raw materials used. Synthetic fibers have a finite source so focus needs to be placed on using natural fibers in automobiles. Placing the emphasis on the importance of functional design, typically lower strength natural or biodegradable raw materials could have the capability to be used in fiber-based composites.

Another concept which may begin to gather interest in the automotive industry is the use of closed loop recycling. The theoretical closed loop recycling requires no new raw materials and exists from re-used and recycled secondary materials [60]. Automotive waste would be used to specifically produce new vehicles. The main drawback from implementing this type of system would be the degradation of materials over time and repeat use. Further research in recycled material rejuvenation would need to be performed.

Instead of focusing on the recyclability of a vehicle, some automotive sustainable models are focusing more on the longevity of the vehicle. All aluminum bodies and the use of composites provide Mercedes the ability to guarantee its cars against corrosion for 30 years [68]. By increasing the life cycle of a vehicle from 10 to 20 years, the number of times a car has to be produced and dismantled could be reduced by half [60].

2.3.4 Automotive Applications for Fiber Orientated Nonwoven Composites

As mentioned earlier, when dealing with fiber reinforced composites, the properties of the final composite are highly dependent on the fiber properties, the matrix properties and the fiber-matrix interaction.

The mechanical properties of polymer-based composites are sometimes highly influenced by the environment. For example, polypropylene exhibits up to 200% elongation-at-break at 23^{o}C, but as the temperature is reduced to 0^{o}C or lower, it turns brittle and the elongation-at-break is reduced to only 1-2% [66]. Because of this behavior, the optimum applications would be interior structures. Due to the tensile modulus, tensile strength and impact strength of composites utilizing fibers from 5-25 mm, applications can range from seating structures (frame covers), door modules, dashboards, front end modules, bumper beams and spare-wheel wells [66].

Random oriented fiber performs with engineered bias can be combined with woven or stitched fabrics in a composite for applications requiring higher stiffness, high creep resistance, high fatigue resistance and high crash resistance [66, 71]. These combined composites could be used as semi-structural components such as body panel supports, fenders and even roof panel inserts as highlighted in Figure 28.

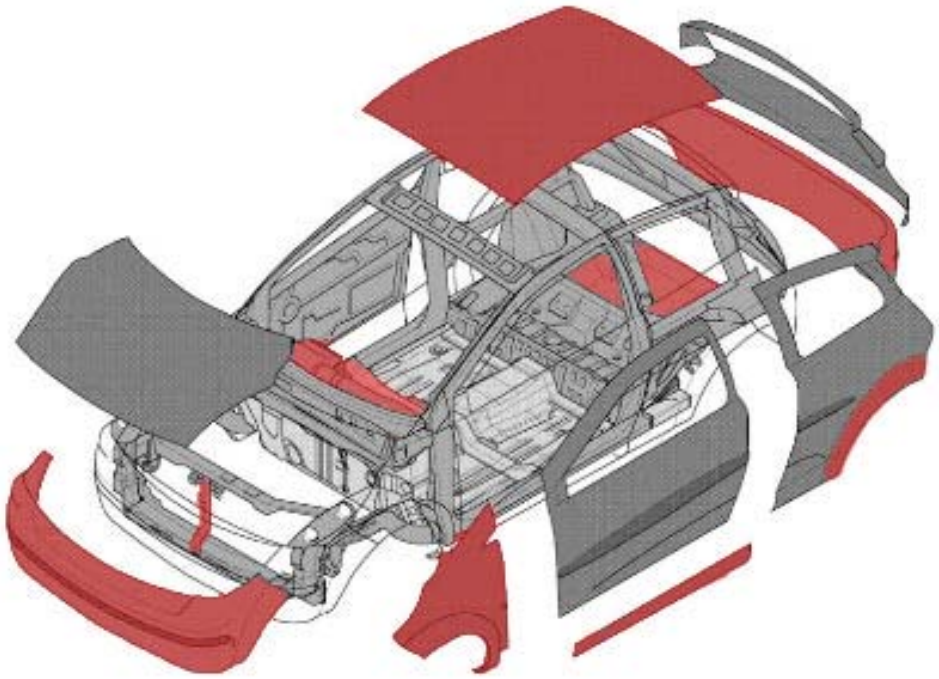

Figure 28. Automotive components with potential to be produced from aligned nonwoven composites.

CHAPTER 3: METHODOLOGY

The purpose of these experiments is to examine the fiber orientation in the air laying process, creating a relationship between fiber behavior and collection surface aperture geometry. There have been no previous studies focusing solely on the aperture effects on fiber orientation. Hence, following experiments follow minimal previously established standards. Also, due to the original perspective of this project, many procedures and components are unique and required custom design and fabrication. Ultimately, the following experimentations are to fulfill the research objectives.

3.1 Research Objectives

The research objectives are as follows:

1. Analyze discontinuous fiber behavior in an aerodynamically controlled process.
2. Evaluate effect of apertures in a fiber collection surface on final fiber orientation.
3. Define controllable parameters in aperture geometry in order to produce desired fiber orientation.
4. Investigate probable applications and benefits for researched process.

3.2 Design of Experiments

The following experiments have been designed to properly determine a relationship between aperture geometry and fiber behavior in an air laying system. Custom collection surfaces were designed and fabricated in order to measure the resting orientation of fibers in an air transport system. The measurements would determine the effect, if any, of the aperture

geometry and resulting fiber orientation. The following section describes these experiments in full.

3.3 Establishing Methodology

In order to develop custom made aperture geometries in a timely fashion, a rapid prototyping three dimensional printing system provided the flexibility and speed necessary to complete this research. SolidWorks® CAD software provided the necessary three dimensional rendering interfaces for design and fabrication would be performed using a newly acquired ZCorp® three dimensional printer [72]. These collection surfaces required the construction of thousands of precision fabricated apertures (4080 to be exact). So, prior to the design and fabrication of the surfaces or boards, testing was required to determine the design tolerance capabilities of the ZCorp® three dimensional printer. This consisted of a hole test using the ZCorp® three dimensional printer to establish the smallest possible hole size which could be successfully printed. Following printing, each component must then be exposed to a viscous resin for final hardening. This preliminary test also investigated which hole sizes would remain open after resin hardening.

3.3.1 Fabrication using Three Dimensional Printing

The ZCorporation® printers can utilize several three dimensional CAD file formats including Stereolithography (STL), which is supported by SolidWorks®. SolidWorks® was used for all of the three dimensional design prior to any fabrication [72].

The three dimensional printing or building process requires three main steps: printing, depowdering and resin setting. The printing process is very similar to a standard desktop

printer, however, instead of only printing in a X and Y direction, this type of three dimensional printer adds a Z direction (height). Successive layers are added to one another to create a three dimensional part. Figure 29 shows the ZPrinter® 450, the build chamber, build bed and depowdering chamber.

Figure 29. ZPrinter® 450 [73; Retrieved from http://www.zcorp.com/en/Products/3D-Printers/ZPrinter-450/spage.aspx].

Prior to the printing process, the printer takes the given file and digitally slices the image into the appropriate number of layers in order to print. Printing is the process of actually building the design, the printer spreads a thin layer (0.089-0.102 mm) of powder,

then prints an adhesive (and color if necessary) in the necessary design for that designated layer [73]. This process is visualized in Figure 30, the orange represents the adhesive and the blue is the powder layers.

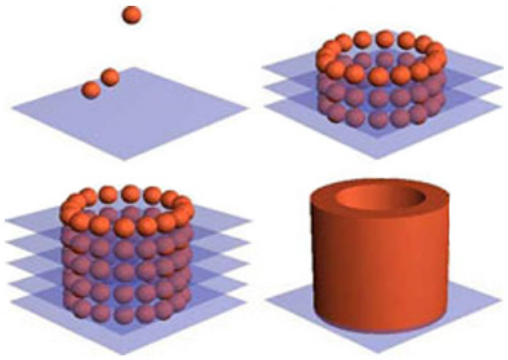

Figure 30. Three dimensional printing process starting at top left, top right, bottom left then bottom right [74; Ligget, 2010].

Due to the accumulation of powder, at the end of printing, the entire build bed is full of powder which is used to support the fragile part. The part is required to cure in the supporting powder for 90 minutes. After the required 90 minutes, the printer removes the surrounding powder by vacuum under the build bed, this process is known as clearing the build bed. Figure 31 shows three time lapsed pictures of a model after printing when the support powder is being removed after curing.

Figure 31. Depowdering process in ZCorp ZPrinter® 450 Three Dimensional Printer [73; Retrieved from http://www.zcorp.com/en/Products/3D-Printers/ZPrinter-450/spage.aspx].

Following the removal of the part from the supporting powder, the adhesive is typically firm enough for the model to be transported to the depowdering chamber. The depowdering is shown in Figure 31 and is placed under a vacuum to clear out any extra powder. The depowdering chamber is also equipped with an air blower hand tool, as seen in Figure 31, to help with detailed powder removal. Complete powder removal is necessary to allow for all design details to be visible and for optimum resin contact. The final step is to resin set the model, hardening the build and increasing durability. This step requires the part to either be submerged, or coated with the resin and allowed to dry for one hour. This step can be tedious and the viscous resin has a tendency to fill in and settle in minute details. Table 2 shows the specifications of the ZCorp® used in the testing.

Figure 32. Manual powder removal [73; Retrieved from http://www.zcorp.com/en/Products/3D-Printers/ZPrinter-450/spage.aspx].

Table 2. ZCorp ZPrinter® 450 Specifications [73]

Color Capabilities	180,000 Multicolor (2 print heads)
Resolution	300 x 450 dpi
Vertical Build Speed	0.9 inches/hour (23 mm/hour)
Build Size	8 x 10 x 8 inches (203 x 254 x 203 mm)
Layer Thickness	0.0035 - 0.004 inches (0.089 – 0.102 mm)
Number of Jets	604

3.3.2 Three Dimensional Printed Hole Test

The air laying industry uses a range of aperture sizes in for collection surfaces with no published evident standard. Choices of sizes depend on the size of the fibers used and desired web properties. For the scope of this study, in order to concentrate on specific range of aperture sizes, the capabilities of the three dimensional printer must first be determined.

The purpose of this initial test was to establish feasible hole size on the three dimensional printer. Also, this test was to determine what sized holes can be successfully printed without being clogged by powder and which of those holes can successfully be resin hardened without being blocked by the viscous resin. Figure 33 shows the SolidWork® file from which the test block was created. The circular hole sizes (a) (running vertical) range from 0.2 mm (bottom) to 2 mm (top), progressively increasing by increments of 0.2 mm. The four shapes located horizontally across the top are long holes (oblong) ranging from 0.2 mm in width to 0.4 mm (b). The measurements on the left of the circular holes (c) indicate the hole diameters, and the measurements on the right (d) show the distance the holes are from one another.

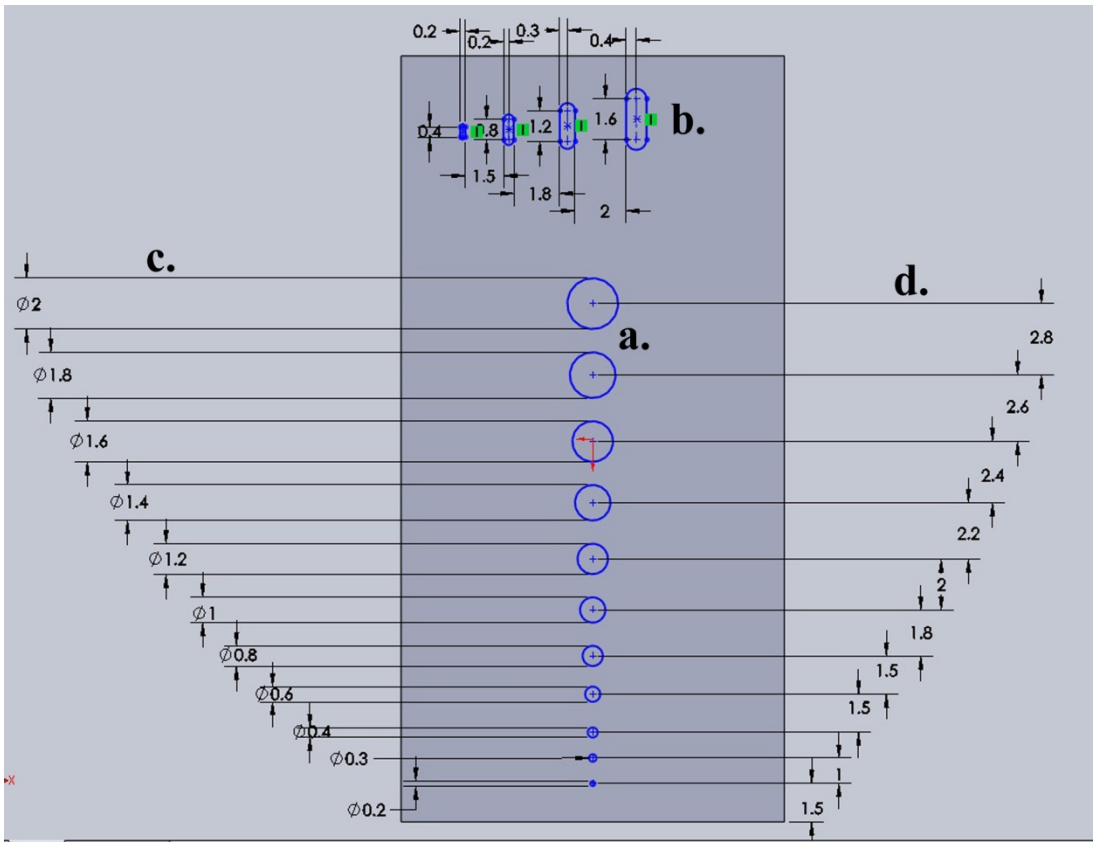

Figure 33. SolidWorks® image of Hole Test design [72; SolidWorks].

The results of the preliminary hole test showed that only the 2 mm hole was able to be printed without superfluous clearing of the aperture. Additional cleaning allowed for the 1.8 mm and 1.6 mm holes to be cleared. However, following resin hardening and due to the viscous nature of the resin, only the 2 mm hole remained open. Figure 34 shows a picture of the three dimensional print out from the test and the visible open 2 mm hole. These results create design boundaries necessary for the experimental tests in this study.

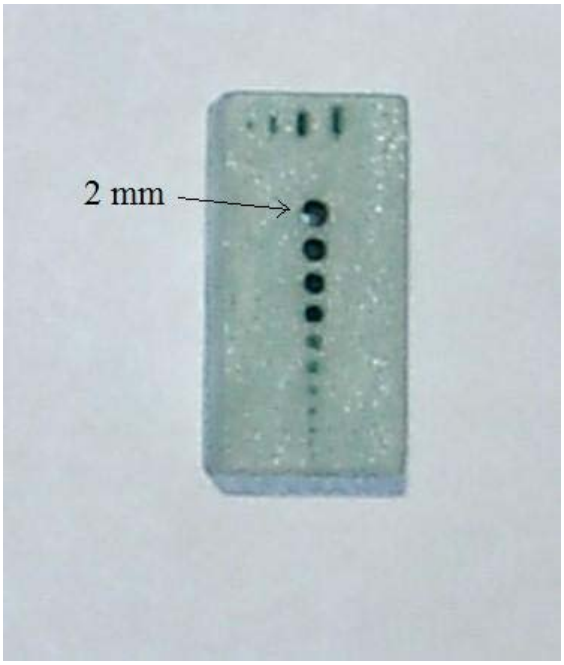

Figure 34. Hole test after resin hardening.

3.4 Testing Equipment

3.4.1 Fiber Collection Boards

In order to test variants of aperture sizes and geometries, eight perforated boards, each possessing its different aperture density, size and/or angle and shape were designed. These boards were designed using SolidWorks® and fabricated in the Z Printer® 450. The previous test determined that the smallest hole size capable to be printed is 2 mm in diameter. Five of these boards utilize circular apertures, two of them use oblong hole shapes and one was designed with triangular apertures. The triangular apertures were unable to successfully be printed, so the remaining seven boards will be analyzed.

3.4.1.1 Fiber Collection Board Design

Each fiber collection board was created using three steps within SolidWorks® computer aided design software. The first step was to create dimensions for the apertures. A single aperture was created in two dimensions to the required size and spacing from the edge. Step two was to create a pattern layout in which to repeat the designed aperture. The offset pattern angle along with aperture spacing was determined during this step. Finally, the two dimensional pattern was extruded into a three dimensional aperture through the board

Each of the seven perforated surfaces used in the series of experiments measures 89 mm x 89 mm square (total area of 7921mm^2). The aperture geometry dimensions of each board were set by the following variables:

Table 3. Fiber Collection Board Dimensions and Characteristics

Description	**Board 1**	**Board 2**	**Board 3**	**Board 4**	**Board 5**	**Board 6**	**Board 7**
Aperture Shape	 circular	 circular	 circular	 oblong	 circular	 circular	 oblong
Aperture Dimensions	2 mm diameter	2.5 mm diameter	2 mm diameter	4.25 mm (length) 1.75 mm (width)	2.5 mm diameter	4 mm diameter	4.25 mm (length) 1.75 mm (width)
Offset Pattern Angle 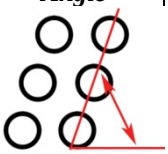	45°	45°	45°	Aperture shape set at 135°, Pattern is set at 62°	45°	45°	Aperture shape set at 135°, Pattern is set at 45°
Aperture Spacing 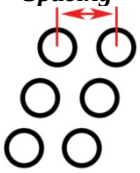	3.25 mm	3.75 mm	2.5 mm	5 mm	3.25 mm	5.25 mm	5 mm
Board Surface Area (mm^2)	5769	5407.7	3994	5412	5769	4590.9	5798.8
Board Void Space(mm^2)	2152	2513.3	3927	2509	2152	3330.1	2122.2
% Void Space	27.16%	31.7%	49.6%	31.68%	27.16%	42%	26.79%
Further Comments					Aperture cross section: 		

All measurements were gathered using the Measurement feature in SolidWorks® [72]. Figure 23 shows the Measurement Tool being used to find the surface area of Board 7. Detailed board schematics and step by step screen shots of the design process from each board can be found in Appendix A.

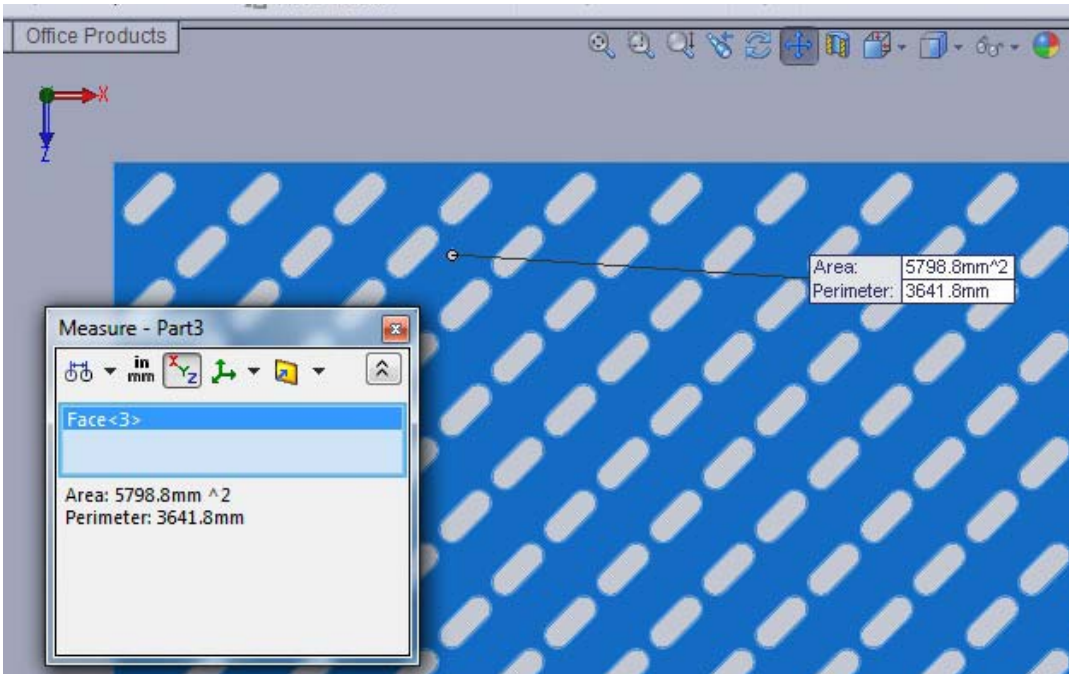

Figure 35. Surface area using Measurement Tool in SolidWorks® [72; SolidWorks].

3.4.1.2 Board Fabrication

Three dimensional printing on the ZPrinter® 450 has the potential to take up to several hours and depending on the detail of the part, depowdering can require several hours as well. In order to save time, resources and cost, the individual board designs were

consolidated into two larger complete boards. The three dimensional printer limited the size of the printed components to fit within a 203.2 mm (8 inches) square build area. Due to this, the complete boards measure 190.5 mm x 190.5 mm and are 7 mm thick. Figure 36 shows a three dimensional rendering of one of the complete boards prior to printing.

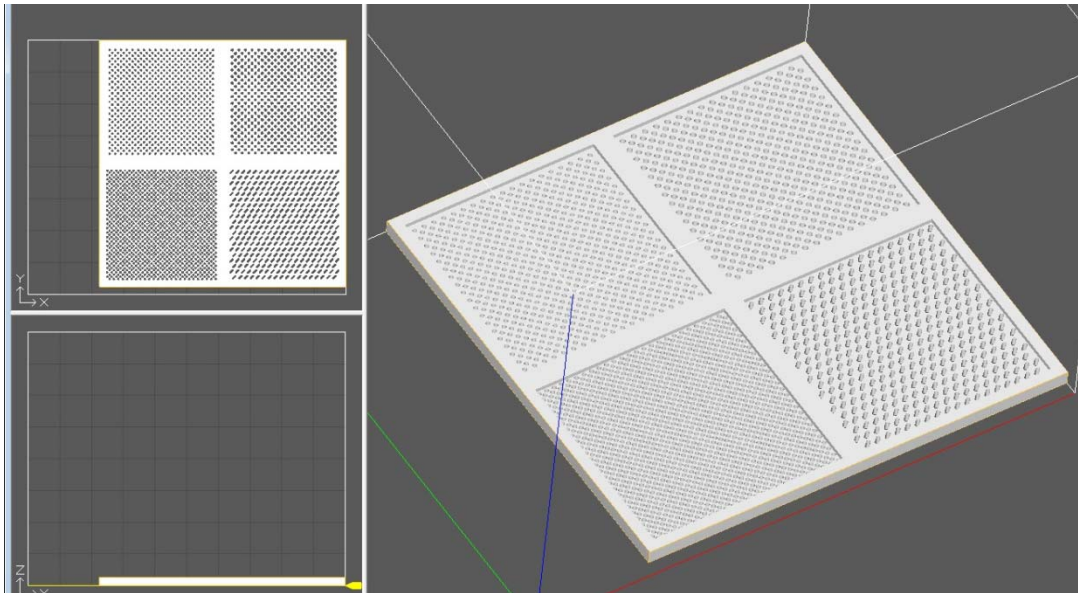

Figure 36. Three dimensional rendering of complete board prior to printing.

Each of the two printed complete boards required 1 hour and 45 minute print time, 90 minute cure time, required depowdering, and resin hardening. As mentioned earlier, the only complication encountered was the inability to print out the triangular apertures. The holes remained clogged after printing, so that board design was not used in the experiments.

3.4.2 Air Chamber Design

In order to conduct this research, it was necessary to design and build a customized air transport testing apparatus. This piece of equipment would have to provide a standardized setting in order to effectively evaluate the effects from the collection boards on the final fiber orientation. A vacuum system would be necessary to provide the pressure difference through a designed suction box. A suction box would need to be designed to hold the collection boards and provide the least amount of flow obstructions for optimum air flow. Figure 37 shows a schematic of the suction box design.

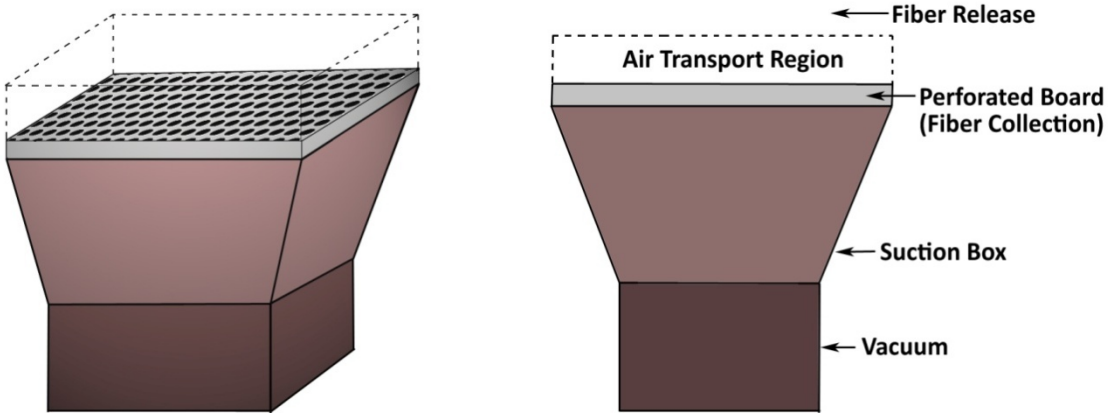

Figure 37. Air transport chamber rendering.

Above the fiber collection board would be an air transport region, constructed of open mesh screen in order to eliminate any boundary layers which may cause turbulence. This

piece of equipment will only utilize subpressure, or suction, to eliminate any chance of fiber blowout caused by overpressure.

A motor and housing unit from a small vacuum system was utilized as the vacuum source. The suction box was created with foam core board and papier-mâché in order to create an airtight structure with a smooth transition to accommodate both the square collection boards and the round vacuum inlet. Papier-mâché was utilized for its ease of moldability into the desired shape. Powdered resin glue was used in the papier-mâché recipe in order to increase the bonding strength of the pulp and create an airtight structure.

After the papier-mâché cured and was fitted to the vacuum, the entire apparatus was then sealed using caulk to form a complete airtight flow in order to use the vacuum to its fullest potential. Figure 38a shows an up close picture of the caulk sealing around the openings and Figure 38b shows the final air transport region, fiber collection board, suction box and vacuum setup.

In order to maintain a consistent height of the air transport region a screen box was created to surround the board as seen in Figure 38b. Mesh screen was used in order to create a visible boundary but to eliminate the potential of turbulence caused by solid surfaces and to allow ample light through to the board surface for photographs.

(a)

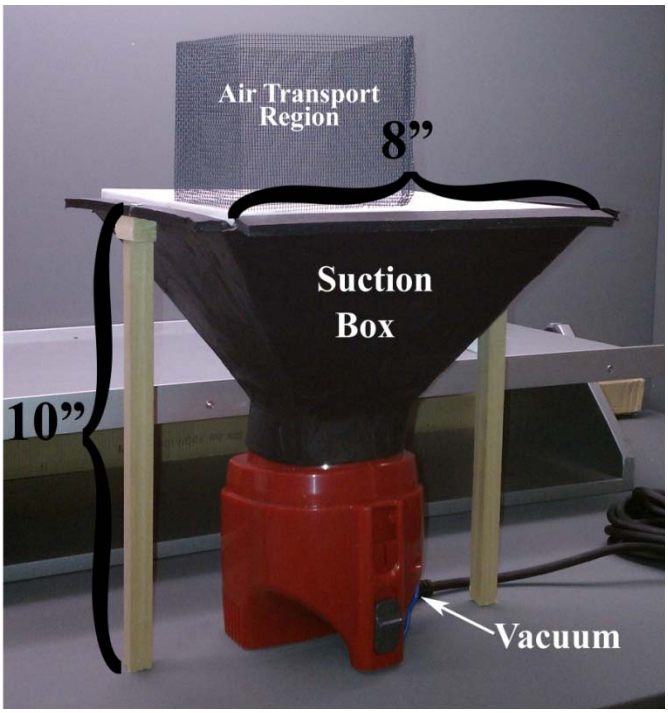

(b)

Figure 38. (a) Airtight seals around suction box and (b) final air transport chamber.

3.4.3 Camera and Lighting

Conventional fiber orientation measurements for nonwovens are acquired by using a backlit system [74-76]. However, in order for backlight to be used, the fibers or web need to be moved, which is not an option in this experiment. This experiment requires the measurement to be taken when the fiber comes to rest without obstruction. A lighting system needed to be implemented that did not require any movement of the fiber and provided ample contrast between the fiber and the collection board. Photographs of the fibers needed to be taken immediately after settling on the board, so a camera stand along with proper lighting was necessary.

A Beseler CS-14 copy stand provided standardized and controlled lighting and camera positioning for all of the photographs. Figure 39 shows the initial set up of the copy stand with camera positioned above the collection surface. The final set up consisted of two 100 watt light bulbs and the camera positioned 15 cm above the collection surface. A Canon PowerShot® S3 digital camera was used for the photographs, utilizing 6.0 mega pixels along with the Macro setting to further enhance small details.

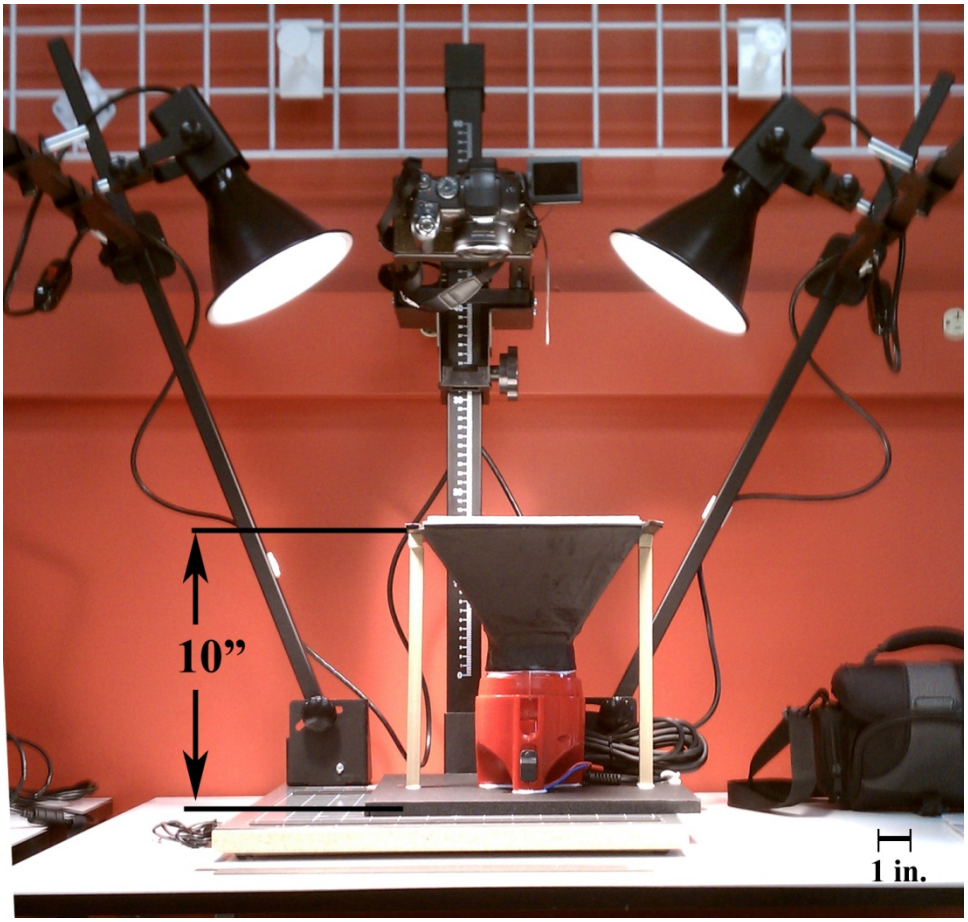

Figure 39. Final camera and lighting setup.

3.5 Materials

The fibers used in these experiments were chosen to simulate the most commonly used in the current air laying industry. Since the objective of this research is to provide a fibrous preform which can be thermally bonded and resin infused, the fibers used needed to possess these capabilities as well.

The fibers used were supplied by Stein Fibers, Ltd. out of Charlotte, North Carolina. Table 4 shows the fiber characteristics.

Table 4. Fiber Properties

Material	Low Melt PET
Construction	Bicomponent (sheath/core)
Size	6 denier
Color	Black
Length	~30mm (relaxed); 39mm (stretched)
Crimp	~20%

According to Stein Fiber's Engineering Sales and Marketing Personnel, Daniel Almirall, the current nonwovens industry utilizes fibers in the 30-40mm range for their ease of processing [personal communication, July 14,2010]. Crimped fibers are also commonly used to provide inter fiber friction and cohesion in an unbounded web. Black fibers were chosen to provide a visible contrast to background of the white boards in the photographs. Only the fibers which possessed the highest linearity were used in the experiments. Figure 40a shows an example of the linear fibers which could be used compared to unacceptable fibers for this experiment shown in Figure 40b.

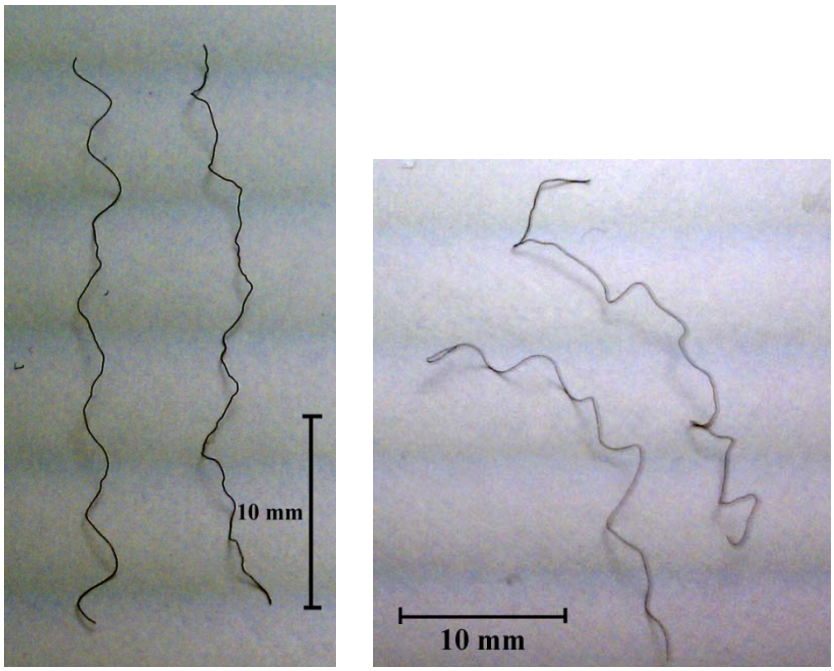

(a) (b)

Figure 40. Examples of acceptable linear fibers (a) and unacceptable fibers (b).

3.6 Experimentation

This section will describe the fiber collection board and sample preparations. The following procedures were carried out for each sample in order to provide consistent measures resulting in as accurate data as possible.

3.6.1 Board Preparation

The following procedures were followed for each of the 7 boards prior to air laying:

Due to the fact that each complete board is composed of 4 individual sections, 3 of the boards in each analysis were not used. Since the suction box fits to the entire board, the 3 unused boards produce unnecessary air flow. In order to contain the airflow to the board

under analysis, the 3 boards not to be analyzed were sealed with masking tape. Figure 41a shows the masking tape sealing the bottom of the boards not to be analyzed and 41b shows the masking tape around the edges of the complete board atop the suction box, to create an optimal air seal.

The square mesh screen was then placed around the board to be analyzed to create a consistent fiber release height and keep fibers from travelling outside of the air transport region.

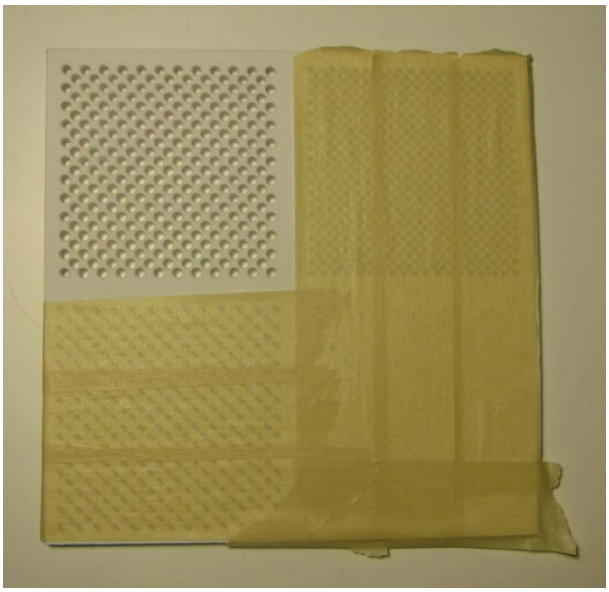

(a)

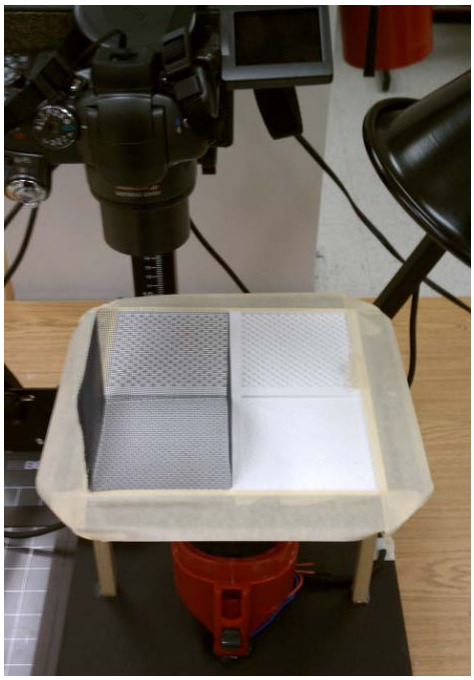

(b)

Figure 41. (a) Masking tape to seal the surrounding apertures and (b) masking tape to seal the edges of entire board.

3.6.2 Air Laying Steps

Given that there were no established test standards or procedures for the experiments and due to the fact that the range of results was unknown, there were no initially set sample size. The sample size began as 50 pictures of fiber orientations per board, but the data was not indicative of a definite variation. On those grounds, the sample size was increased to 100 pictures per board, and then the proposal for investigating repeatability was established. These were the deciding factors by which the 200 pictures per board came into place.

Once the board to be analyzed was fitted to the suction box and the system was sealed, the vacuum was turned on and the following procedures were followed for each of the 200 photographs per board (1400 photographs total):

Handheld forceps were used to hold an individual fiber at a 90^{o} orientation relative to the board, as shown by the white line in Figure 42. Figure 42 is a photograph before cropping to show the entire field of view from the cameras setting. When orientated, the fiber was released and allowed to flow to the collection board.

Subsequent to the landing, the fiber would undergo a visual inspection which included the following check points:

- The fiber is flat on the collection board.
- The fiber is not lodged in any apertures or the screen boundary.
- The fiber possesses the same linear orientation as prior to release (is not extensively curved).

If the dropped fiber possesses each of these parameters, the digital camera was used to capture a photograph of the entire board to crop and analyze further. Figure 43 shows an example of a photograph taken of a board immediately after a fiber settled.

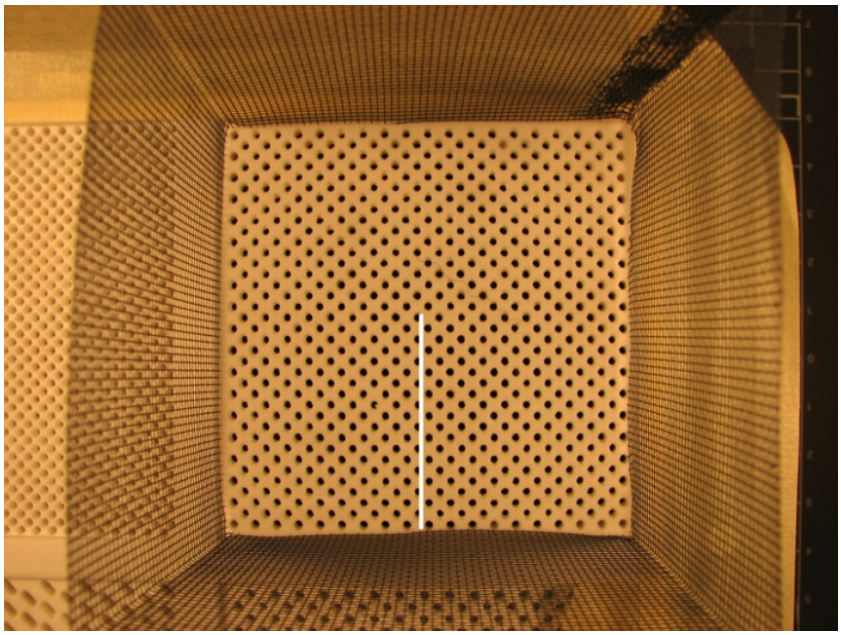

Figure 42. Fiber orientation prior to release.

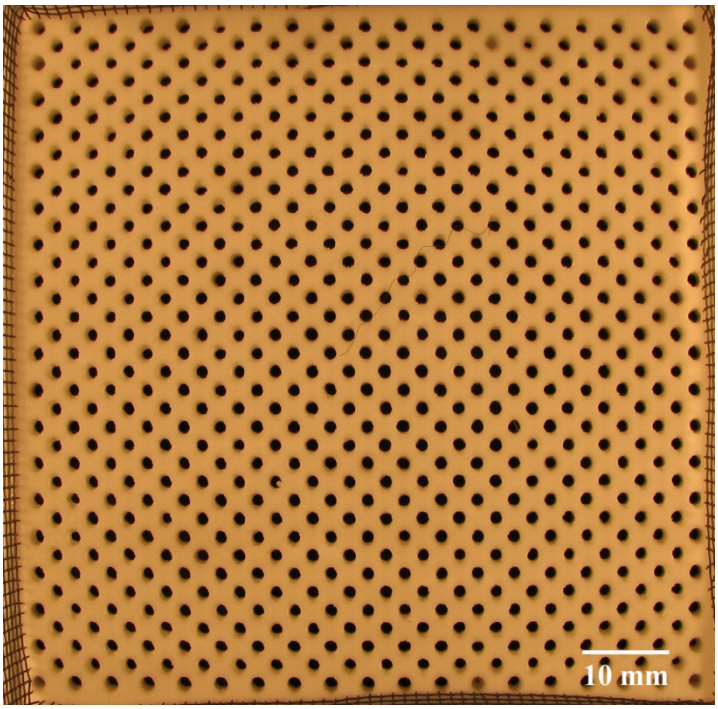

Figure 43. Actual view of fiber settled on board.

3.6.3 Fiber Orientation Measurement: Direct Tracking

In order to provide the most accurate measurements, each fiber will be manually tracked using a direct tracking method. The first step in establishing a direct tracking method is to determine the variables which may affect the final measurements and create limits accordingly [74-76].

As mentioned in Table 4, the fibers used in this experiment contain around 20% crimp, which is an important factor to account for before direct tracking. The purpose is not to model or measure the crimp, but set limits to prevent the crimp from affecting the final measurement. In order to negate the crimp in the final measurements, the correct chord

length must be chosen. The chord length is a predetermined length by which a straight line can be drawn and measured to determine an angular measurement [75]. As a fiber is tracked, its orientation is measured by combining all of the end-to-end chord segments along the fiber [75]. This is why that if an incorrect chord length is chosen for a crimped fiber, the final data could be skewed. For example, if a fiber is long and contains crimp, a small chord length will create tracking across the entire fiber, factoring in every curved feature [75]. To obtain reasonable estimates of the entire fiber orientation when dealing with crimp, the chord length should reach from tip to tip[75]. This means that in this study, the chord length will be the full length of the fiber.

In order to create a common visual, it must be assumed that a sine wave is sufficient for describing the crimp [74]. Through the sine wave, a best fit line must be drawn the span of the chord length. The best fit line is then the factor to be measured for angular calculation. Figure 44 shows the sine wave as a crimped fiber, the best fit line and the angle (α) for orientation measurement.

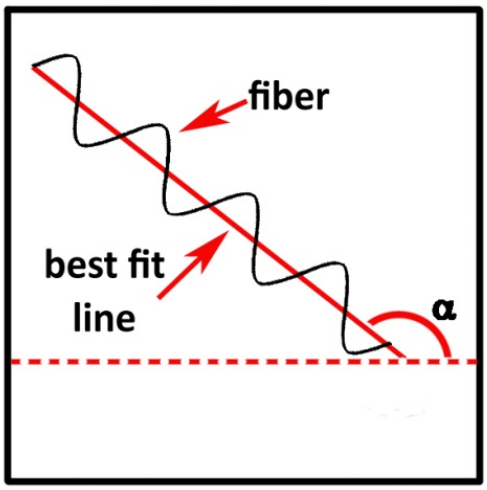

Figure 44. Sine wave as fiber, best fit line and orientation angle.

3.6.4 Fiber Orientation Analysis Procedures

The following procedure was followed for each of the total 1,400 photographs taken of each fiber's orientation:

Adobe Photoshop CS3® was used to open and analyze each photograph [77]. Prior to each stage of photograph analysis, the fiber collection board was verified to be squared with respect to the camera in order to have a common reference point for each photograph. When the photograph was opened in the software, the fiber would be located, centered and zoomed in to accurately determine fiber placement, as seen in Figure 45.

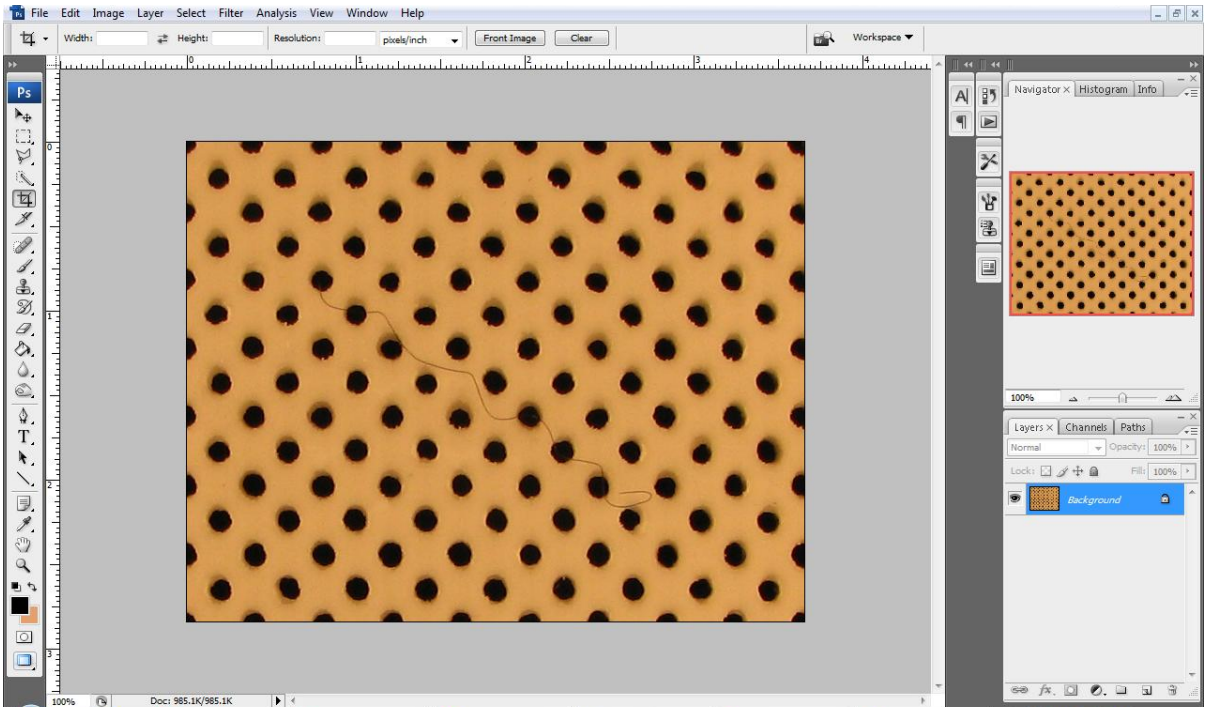

Figure 45. Step one of photograph analysis, zoom into and center fiber [77; Photoshop].

The Ruler Tool was used to determine the fiber angle by placing the first end on the lowest end of the fiber and following the best fit line through the fiber to the opposite end. The Ruler Tool and Angle measurement can both be seen in Figure 46 [77]. Each angle measurement was rounded to the closest whole number and recorded in a spreadsheet, which was used to create histograms of each board relating the fiber orientation (0^o-180^o) to the frequency of occurrences. Each histogram was then split into 18 bins of 10 degrees to represent the data in an optimum visual graph.

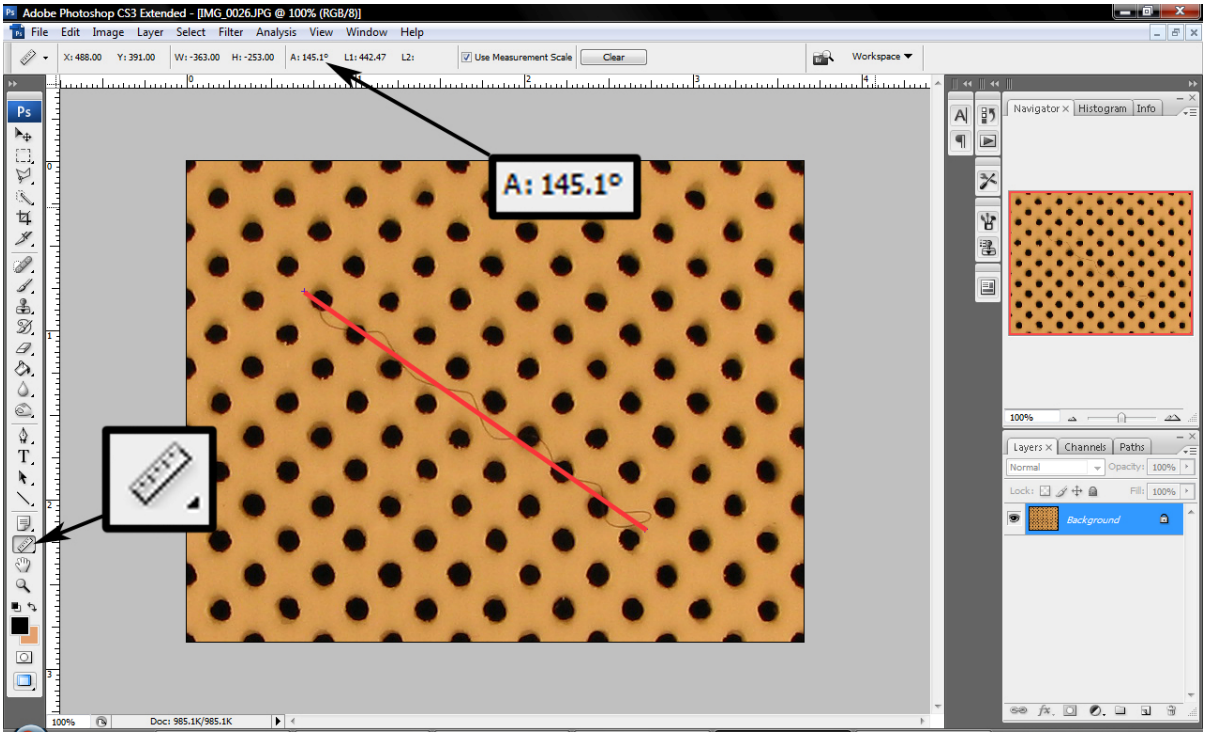

Figure 46. Measuring fiber orientation via Ruler Tool in Photoshop® [77; Photoshop].

CHAPTER 4: RESULTS AND DISCUSSION

The main objective of this research is to investigate the influence of aperture geometry in fiber collection boards found in air laying systems. This investigation can determine parameters to further increase fiber orientation which would be useful to increase strength in nonwoven composite performs. Utilizing the materials, methods and experimental design covered in Chapter 3, a systematic study of 7 different fiber collection boards was conducted to analyze the different fiber collection board aperture geometry's ability to orient the fibers in a predetermined direction.

4.1 Orientation Data Accumulation

The collection of photographs and angle measurements occurred in two stages for each board; each stage consisted of 100 photographs. By doing so, the repeatability of any orientation occurrence could be evaluated. Following the collection of all of the angle measurements from each board, the data was entered into an Excel spreadsheet and analyzed. The dark blue portion of each graph represents the first 100 photographs taken and the light blue is the second 100 photographs. Each histogram was set to graph both stages and represent the cumulative frequency.

For each board, the raw data was sorted into 18 bins, each having a 10 degree range. This proved to visualize the data range in the optimum settings for the histograms. Figures 47-53 show the acquired histograms, each with a photograph of the board in order to relate any data driven assumptions to the design of the board. All of the graphs were normalized, making each graph relative to one another. Figure 54 shows a histogram focused on the tall

peak from Figure 53, which breaks the 10 degree range peak from Figure 53 into individual angles. The rationale behind each histogram will then be discussed in further detail.

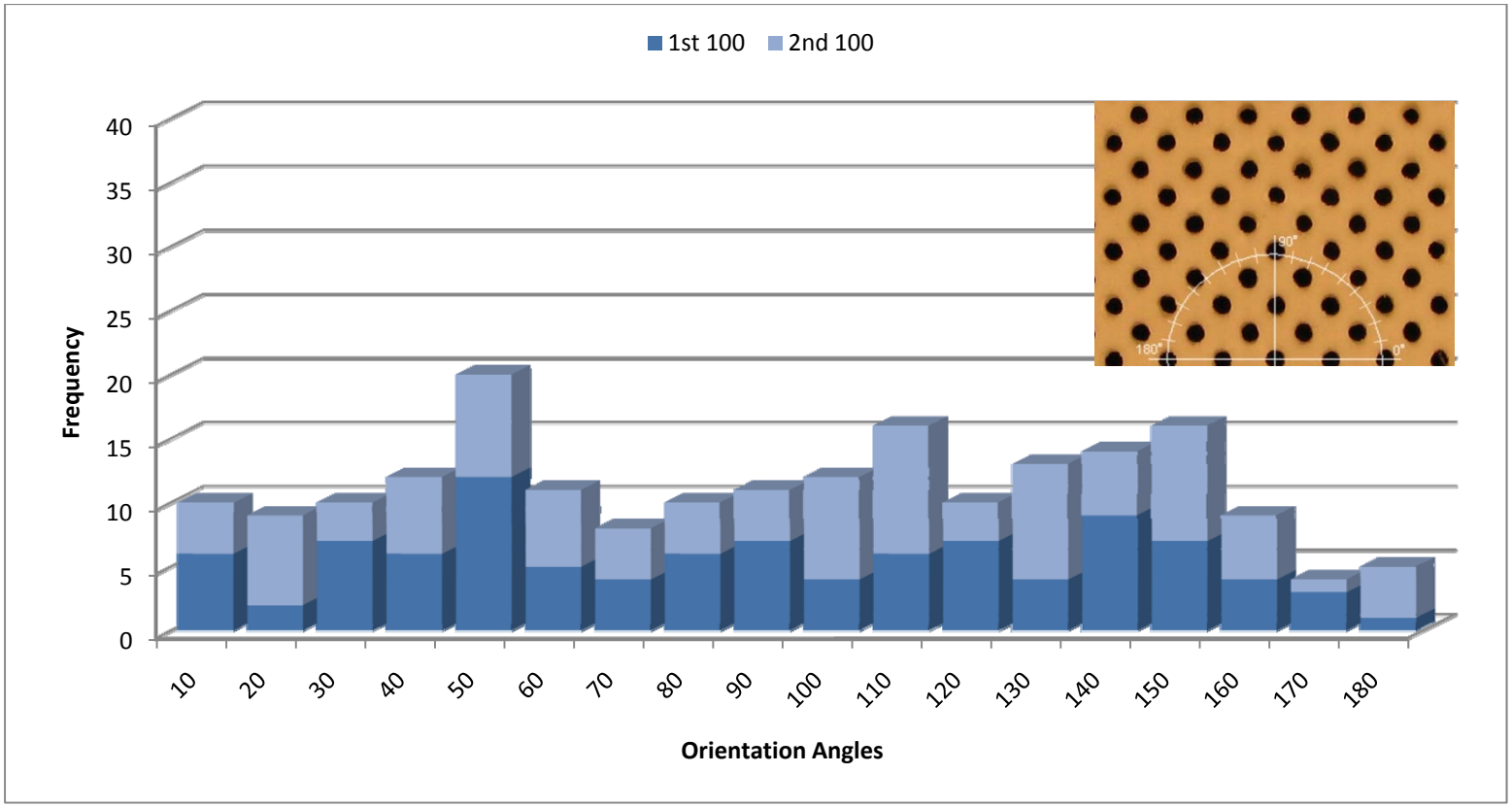

Figure 47. Frequency of orientation angles from Fiber Collection Board #1.

2mm circular apertures set at 45^{o} offset pattern with 3.25 mm spacing.

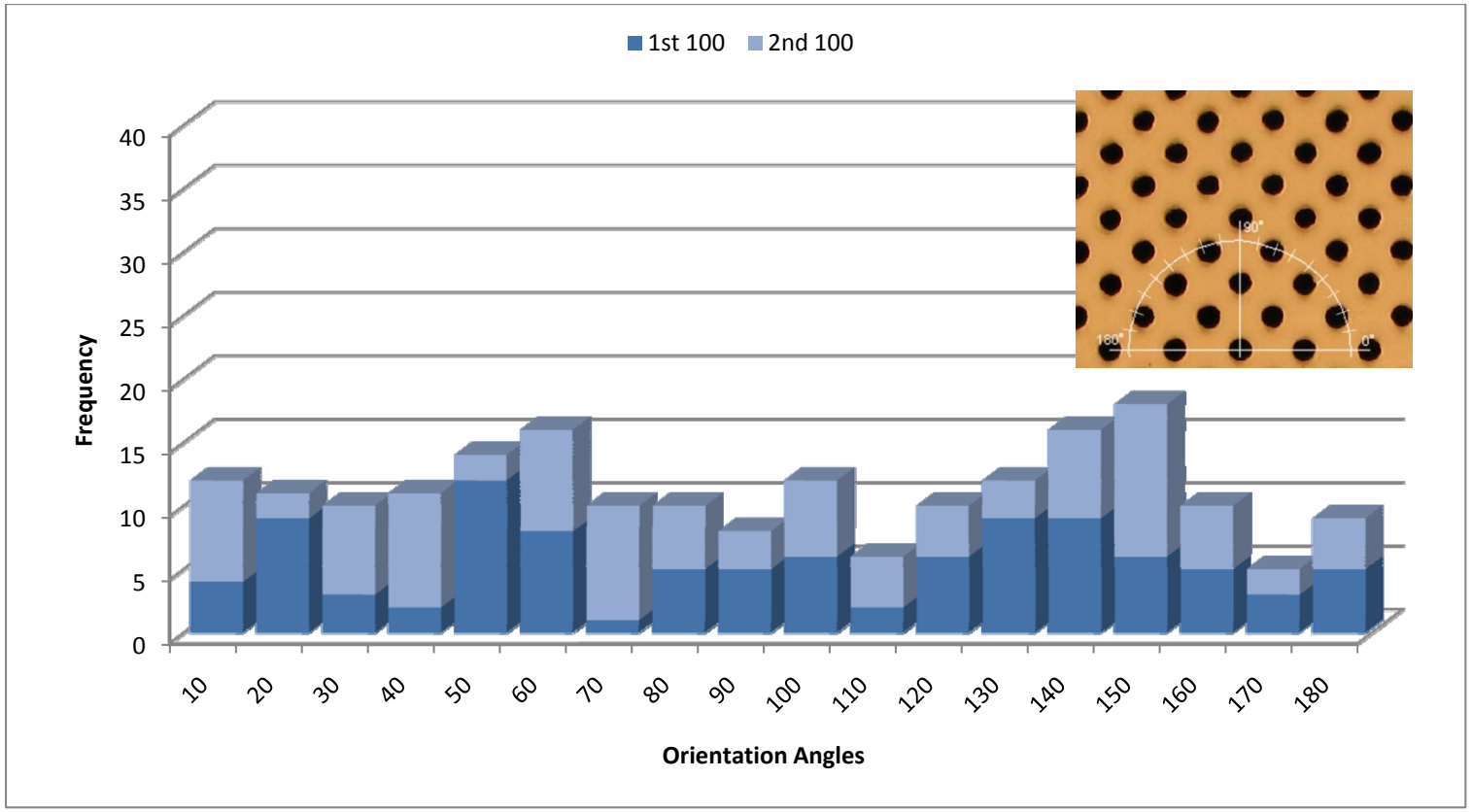

Figure 48. Frequency of orientation angles from Fiber Collection Board #2.

2.5 mm circular apertures set at 45^{o} offset pattern with 3.75 mm spacing.

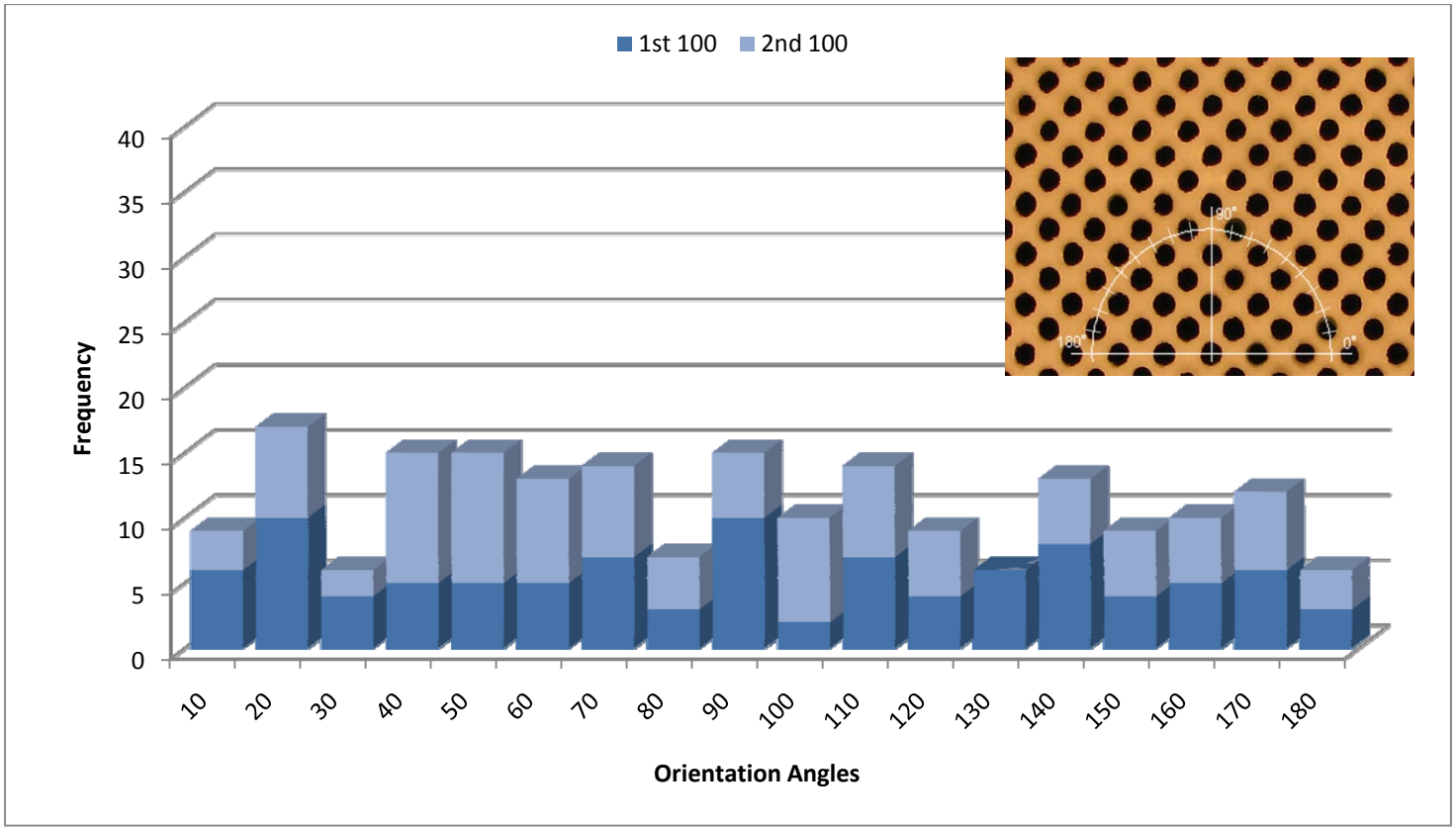

Figure 49. Frequency of orientation angles from Fiber Collection Board #3.

2 mm circular apertures set at 45^{o} offset pattern with 2.5 mm spacing.

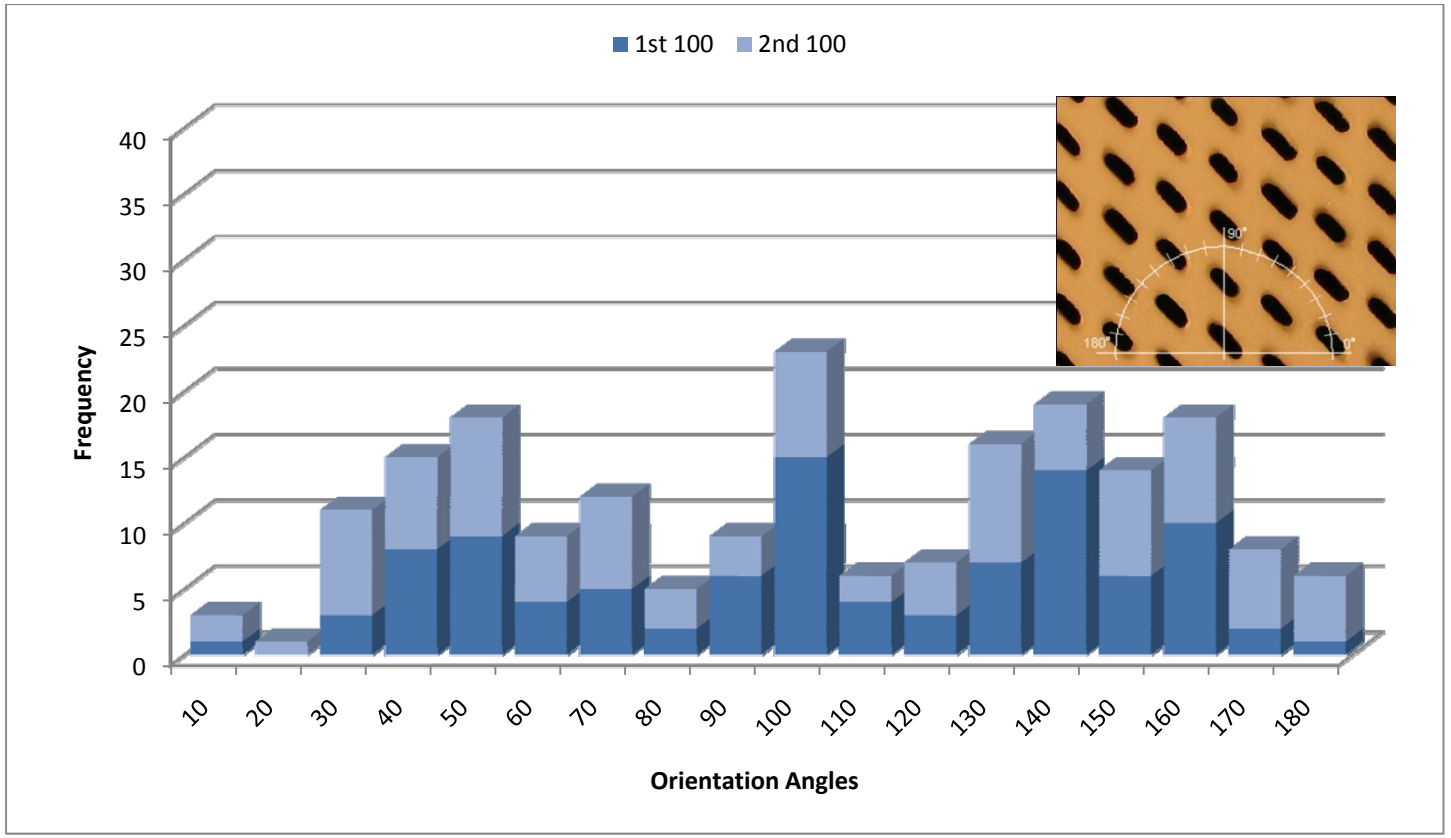

Figure 50. Frequency of orientation angles from Fiber Collection Board #4.

135° oblong apertures set at 62° offset pattern with 5 mm spacing.

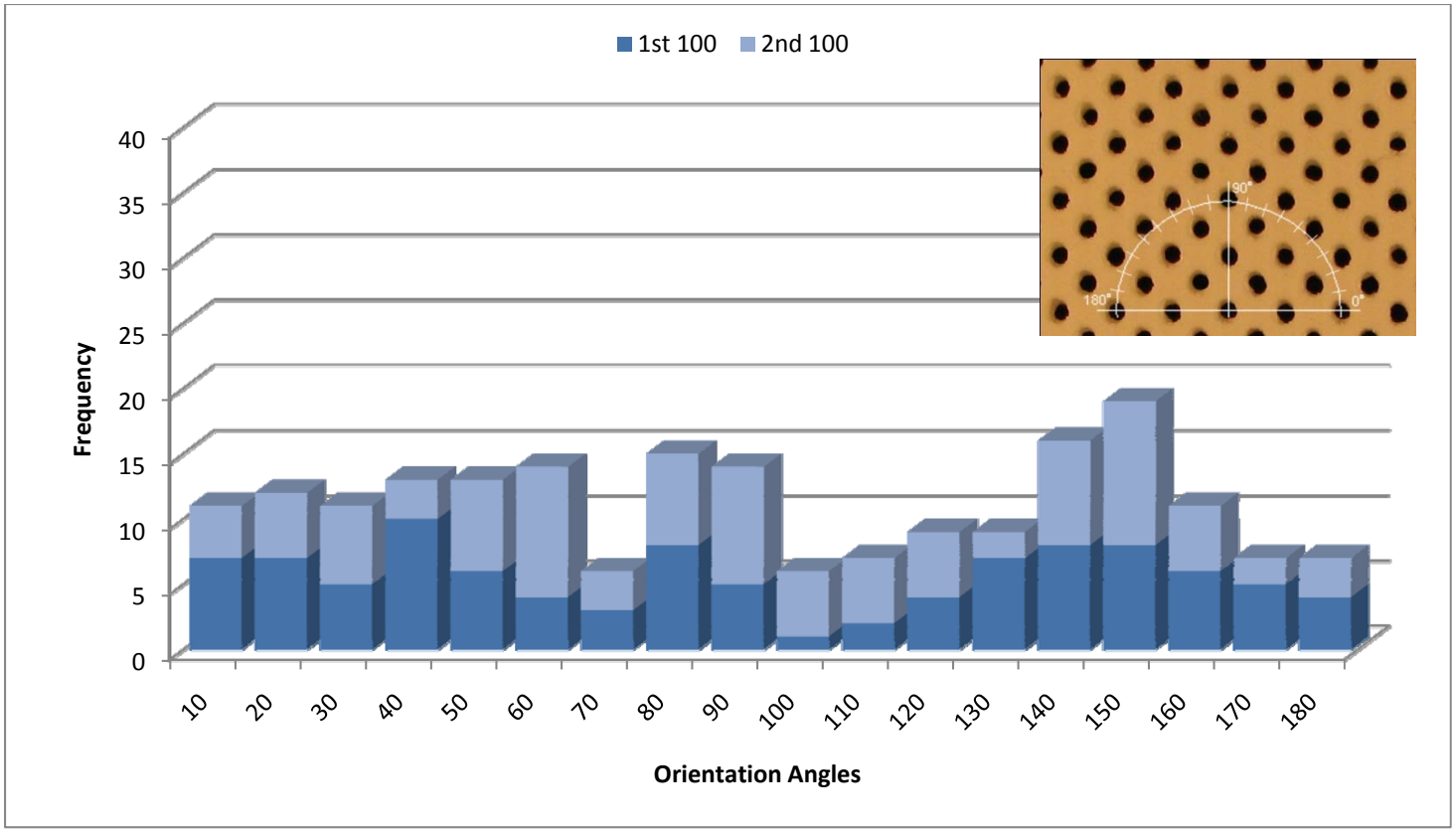

Figure 51. Frequency of orientation angles from Fiber Collection Board #5.

2.5 mm apertures with countersunk cross section set at 45^{o} offset pattern with 3.25 mm spacing.

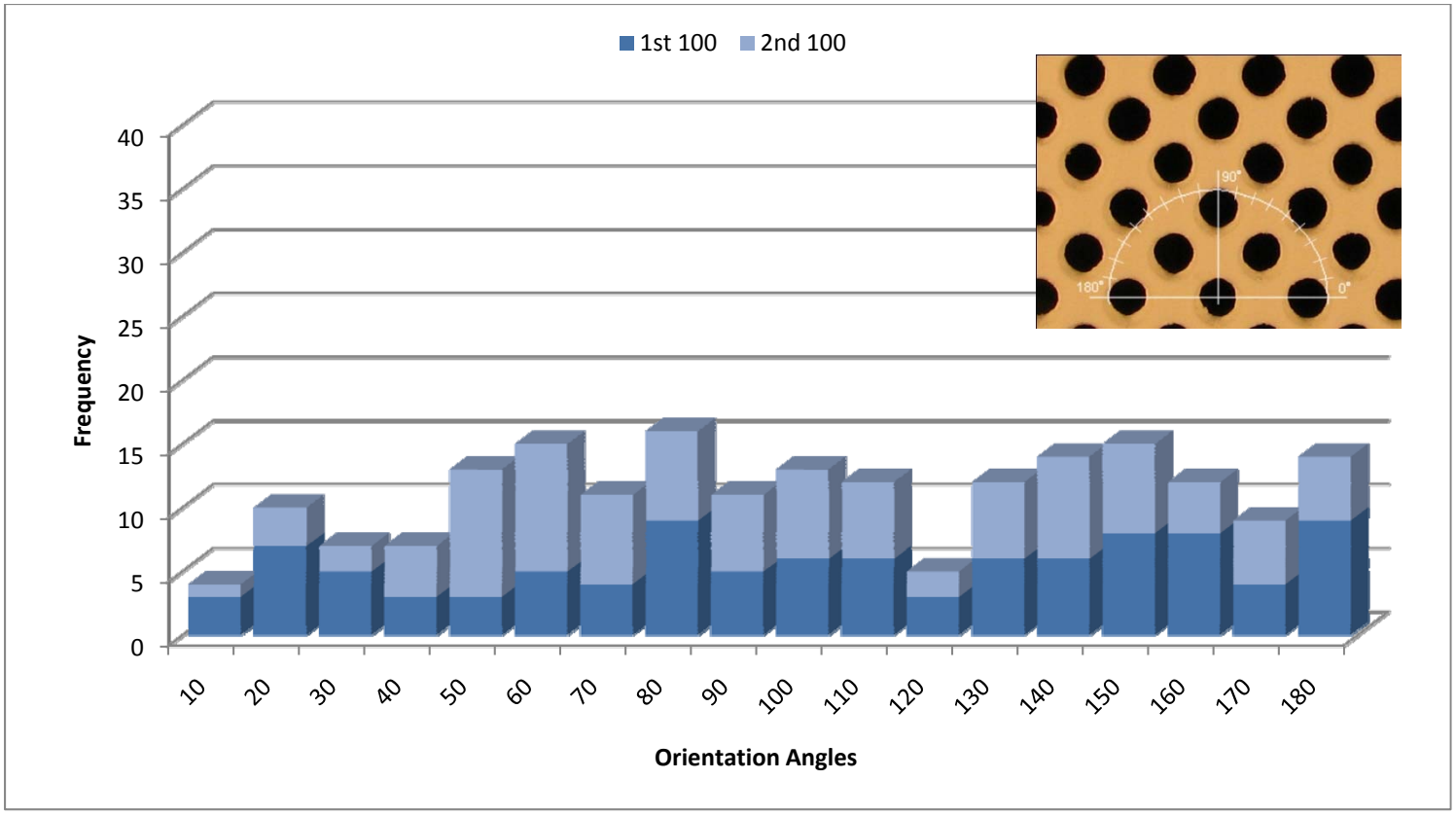

Figure 52. Frequency of orientation angles from Fiber Collection Board #6.

4 mm circular apertures set at 45° offset pattern with 5.25 mm spacing.

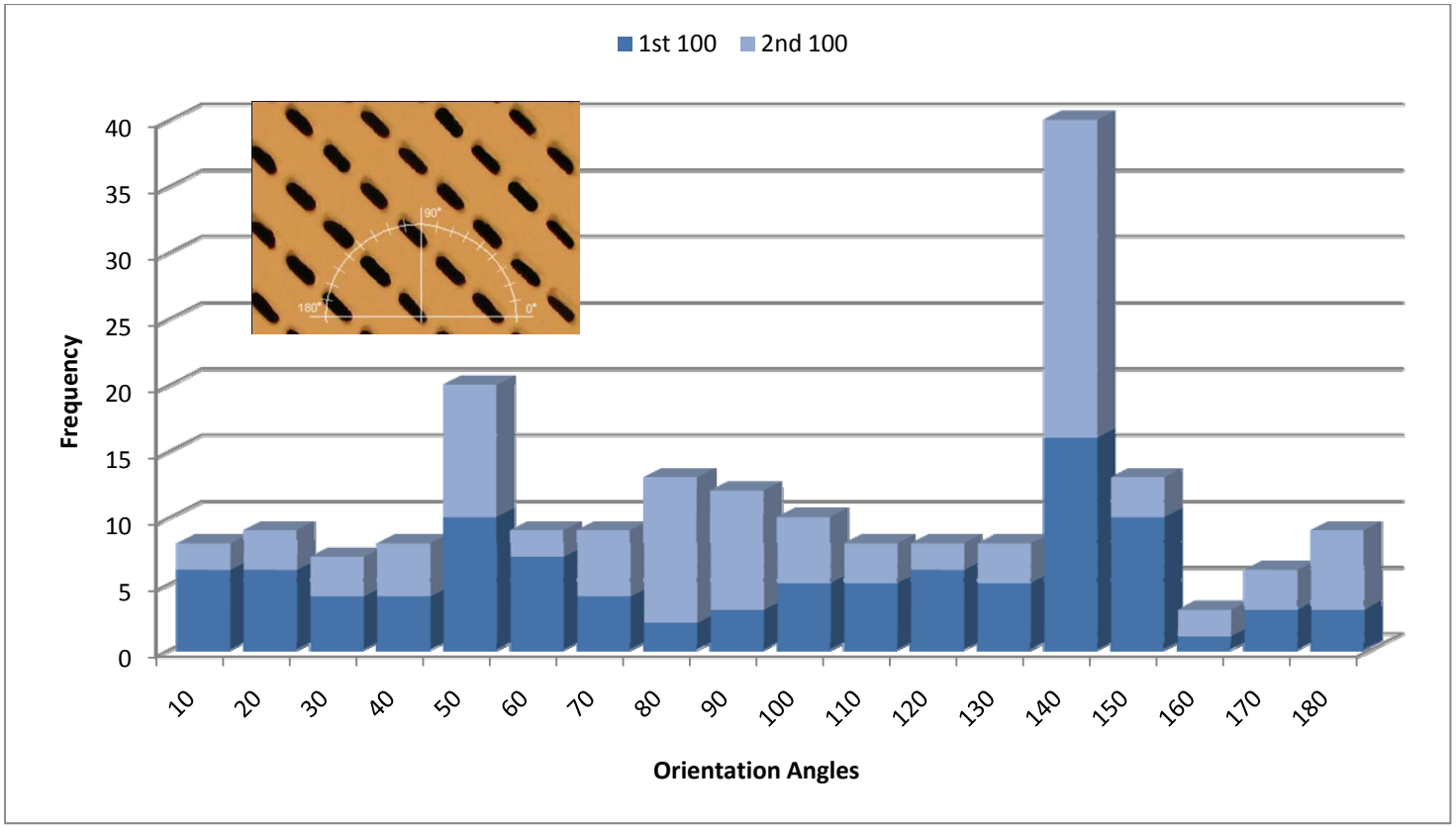

Figure 53. Frequency of orientation angles from Fiber Collection Board #7.

135° oblong apertures set at 45° offset pattern with 5 mm spacing.

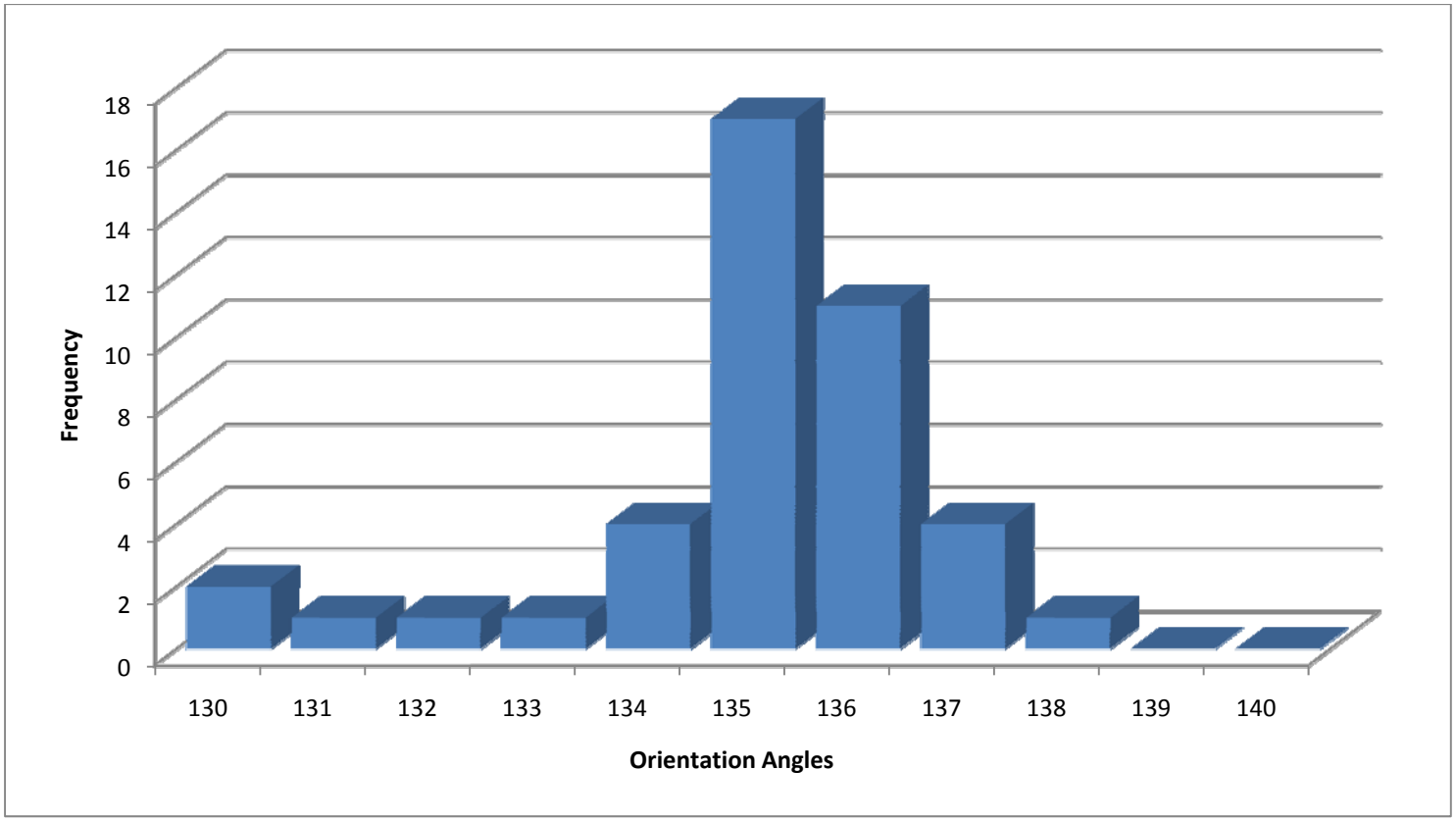

Figure 54. Individualized degree histogram from peak produced on Fiber Collection Board #7.

4.2 Circular Aperture Results

Each of the fiber collection boards that utilized circular apertures was designed having a pattern layout at an angle of 45^{o} as seen in Figures 47, 48, 49, 51 and 52. This created three definite linear arrangements in the pattern layout as shown as red lines in Figure 55. These linear arrangements are found at 45^{o}, 90^{o} and 135^{o}.

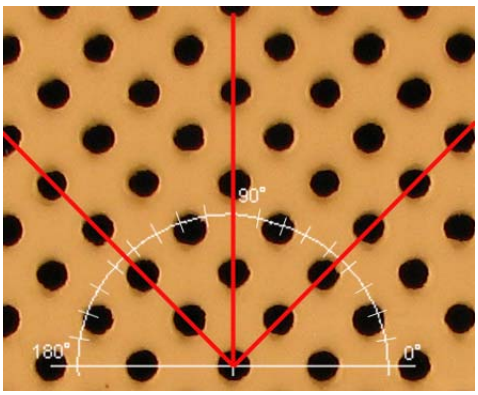

Figure 55. Linear patterns within layout.

When these fiber collection boards fitted with these linear arrangements are placed between a pressure difference (under suction), the linear arrangements orientation has the ability to act as a wall of moving fluid. This behavior is visible in the data from fiber collection board #1, visualized in Figure 47. There are three distinct peaks which gradually increase from lower angle measurements. Each peak is located in close proximity to one of these mentioned linear arrangements, showing the influence of the aperture pattern on the fiber orientation. However, there is a gradual increasing distribution leading up to each peak,

determining that the linear arrangements in fiber collection board #1 have a wide tolerance and their influence is not finite.

The same type of behavior can be seen in fiber collection Board #2, Figure 48. There are still three distinct peaks; however the 45^{o} and 135^{o} arrangements provide a more evident influence. The apertures in fiber collection Board #2 are 0.5 mm larger than in fiber collection board #1, resulting in a further spacing between holes. This influences the distance between the holes in the 90^{o} linear arrangement greater than the 45^{o} or 135^{o}. On these grounds, it is noticeable that the increased distance between the holes in the 90^{o} orientation decreased the 90^{o} linear arrangement's influence on the fiber orientation. Essentially, the increased distance separated the holes to an extent that the fluid flow could not form a strong enough wall effect and was over powered by the 45^{o} and 135^{o} linear arrangements. Other factors to observe in the data from fiber collection Board #2 are the lower peak heights and wider distributions when compared to fiber collection Board #1. The justification behind this behavior can be found in the larger aperture size found in fiber collection Board #2. This provides higher overall void space in the fiber collection board, lowering control of the fluid flow, decreasing the linear behavior and producing lower tolerances for the linear arrangements.

Fiber collection Board #3 has the largest amount of void space of any of the fiber collection boards (3927 mm^2 or 54% void space), as shown in Table 3. This accounts for the reasoning behind the irregular data. The three linear arrangements are still noticeable, but to a much lesser extent. The aperture spacing is so close; in fact it almost makes the 45^{o}, 90^{o} and

135^{o} linear arrangements obsolete. Their influence is still present but to a much lower tolerance than any of the other fiber collection boards. There is even an influence in the 10-20^{o} range showing that the closer aperture settings have created a new distinct linear arrangement within this pattern layout. The repeatability of the peak in the 10-20^{o} range proves that it was not a mere coincidence.

Fiber collection Board #5 utilized not only circular apertures, but each had a countersink cross section. This was derived from the influence of hydroentanglement jets in textile nonwoven production. In hydroentangling, countersink or "cone-down" cross section nozzle has proven to direct fluid in a more orderly manner and for a greater distance (known as having a greater "breakup length") when compared to a cylindrical cross section nozzle [78]. Essentially, the idea was that if this type of cross section can influence water jets in this manner, they could have the ability to control air jets to a greater extent than a cylindrical hole. Figure 51 shows the data resulting from fiber collection Board #5. The 90^{o} linear arrangement influence is evident; however the 135^{o} linear arrangement provided a very impressive distribution for both stages. The 45^{o} linear arrangement, on the other hand, is much more muted and has a wide distribution. In the first stage (dark blue), the 45^{o} linear arrangement had a distinct influence, but was not as repeatable through both stages. There is no explanation in this sampling why the fibers tend to be influenced with more concentration in the 135^{o} direction and with less tolerance in the 45^{o} direction.

Fiber collection Board #6 was designed with the largest aperture size of any of the fiber collection boards (4 mm diameter). The solid surface distance between each aperture is

equivalent fiber collection Boards #1, 2 and 5. This design criterion was set into place to see if a significantly larger aperture size would affect the orientation differently with spacing kept as a constant. The large aperture size in fiber collection Board #6 did pose the problem of fiber pull through more than any other fiber collection board. Fiber pull through is when the released fiber is pulled through an aperture into the suction box, this resulted in numerous lost fibers and more tedious sample collection. The results for fiber collection board #6 possess two very wide distributed peaks. The 45^{o} and 90^{o} linear arrangements almost appear to converge. The repeatability in the 90^{o} direction and the 135^{o} direction show that these two linear arrangements do influence the fiber behavior. However, due to the irregularity of the rest of the data in this set, it shows that there is a high amount of turbulence across the entire fiber collection board.

4.3 Oblong Aperture Results

In this portion of the experimentation, there were two fiber collection boards which utilized oblong aperture designs (fiber collection Boards #4 and #7). The oblong apertures had the same dimensioning (4.25 mm in length and 1.75 mm wide) and were set at the same angle within the pattern (135^{o}). This set aperture angle gave both of these fiber collection boards a very strong linear arrangement in the 135^{o} orientation. However, the differences in the two fiber collection boards came in the layout pattern itself.

Fiber collection Board #4 was designed with a 62^{o} pattern layout, resulting in what is known as a pattern offset, basically staggering the apertures. Even with the offset, the

aperture pattern still possesses a strong 90^{o} linear arrangement along with the built in 135^{o} linear arrangement due to the aperture settings as denoted in red in Figure 56.

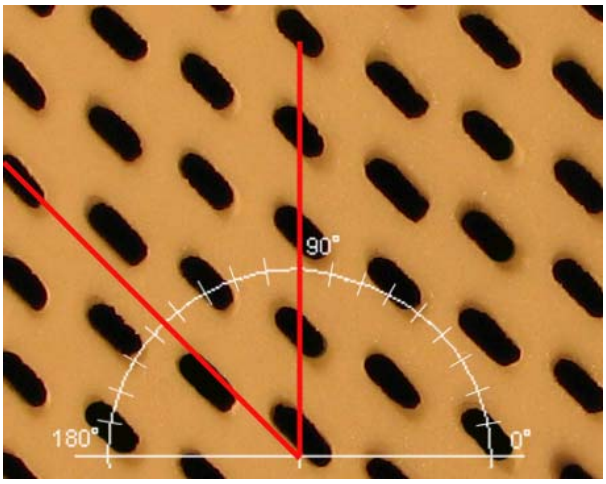

Figure 56. Fiber collection Board #4 linear arrangements.

The data collected from fiber collection Board #4 shows the strong influence in the 90^{o} orientation by a very high peak. The sharpness of this peak identifies a lower tolerance and higher control in the 90-100^{o} range when compared to the fiber collection boards with circular apertures with the same 90^{o} linear arrangements. This helps prove that the oblong aperture affects the precision tolerance of the fiber orientation.

The aperture setting angle of 135^{o} does show strong influence in by means of a distributed curve but retains a wide tolerance due to the lack of direct aperture alignment and staggered pattern in that direction. The curve in the 45^{o} direction was an unexpected result.

However, after reviewing the fiber collection board layout, it was evident that there is a subtle linear arrangement in the 45^{o} direction, which takes advantage of the wider dimension of the aperture. This could result in fiber orientations ranging from approximately 25^{o} - 40^{o} as visualized in Figure 57.

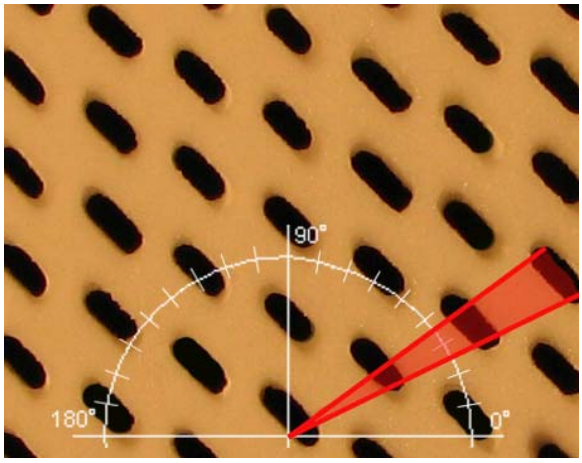

Figure 57. Wide linear arrangement found in fiber collection Board #4.

Fiber collection board #7 represents the use of the angled oblong apertures with an aligned pattern layout. The pattern layout was set at 45^{o}, creating a direct aperture alignment and producing a very highly dominate linear arrangement in the 135^{o} direction. The linear arrangements in fiber collection board #7 can be seen in Figure 58.

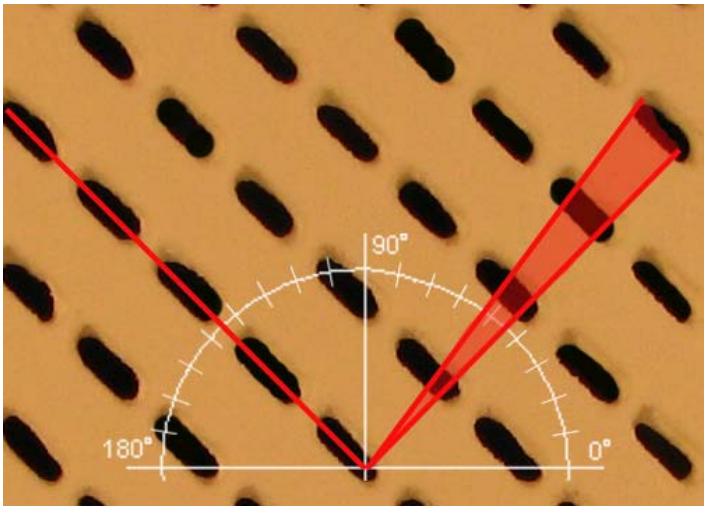

Figure 58. Linear arrangements in fiber collection Board #7.

The highest peak in Figure 53 from fiber collection board #7 represents the highest concentration of fiber orientation in the entire experiment. As seen in Figure 53, the sharp peak in the 130-140^{o} range is due to the combination of the aperture angle and pattern layout angle. This peak indicates that 20% of the fibers measured in on fiber collection Board #7 were found to settle between 130^{o} and 140^{o}. The peak in the 40-50^{o} range is due to the laminar arrangement using the wide dimension of the aperture in that direction as visualized in Figure 58. There is a very small curve in the 90^{o} direction, but due to the low repeatability in the data, it is not significant.

In order to concentrate on the peak in the 130-140^{o} range, the data from that 10^{o} range was placed into a new graph, individualizing the angles. Figure 54 shows the individualized angles from the peak. Between 130^{o} and 140^{o}, the angle at which the highest amount of fibers oriented was 135^{o}, the exact angle of the designed linear arrangement. The angle

individualization graph of Figure 54 confirms the high level of precision achievable by aligning oblong apertures.

CHAPTER 5: CONCLUSIONS

This research was intended to improve the understanding of fluid interactions with fibers in an air laying system. Ultimately, by understanding these interactions, controllable behaviors could be created. These behaviors could further the development of aligned fibers in nonwovens.

The analysis of discontinuous fiber behavior in an aerodynamically controlled process has been conducted through the detailed experimentation. A custom air laying apparatus was developed in order to test variables in order to determine controllable parameters. The variables of focus include the aperture shape, size and pattern on the fiber collection surfaces.

In order to test these variables, custom fiber collection boards were designed and fabricated. Each possessing specific aperture dimensions, spacing and patterning. These fiber collection boards were designed in order to test the influences of these aperture variables on the final fiber orientation.

The results of the experimentation established the influence of both aperture shape and pattern on the alignment fibers in a specific direction. By simply aligning circular apertures in the fiber collection boards, noticeable alignment was repeatedly achievable. A typical offset pattern produces linear arrangements in the patterns at the orientations of 45^{o}, 90^{o} and 135^{o}. The fiber collection boards possessing this offset pattern produced levels of distribution in these three ranges. However, depending on the aperture spacing and size, a certain level of tolerance and precision in these directions was obtainable. The larger aperture size produced lower fluid control, resulting in high levels of turbulence and low fiber

alignment precision. Fiber orientation measurements also became irregular when aperture spacing was reduced. Placing the apertures too close did not establish any linearity in fluid control, resulting in an even randomness.

Oblong apertures resulted in a high level of fiber orientation influence even when the pattern was offset. However, the greatest influence was produced when the pattern layout coincided in alignment with the oblong apertures, resulting in 20% alignment in a 10^{o} range.

5.1 Significance of Results

This proposed technique for fiber alignment has the potential to be integrated with current fiber air laying or spray up techniques in order to increase or optimize fiber orientation. Fiber orientation is of great importance when dealing with composite preforms. By obtaining higher precision in fiber alignment, nonwovens can be produced as high strength composite preforms. Instituting controllable parameters by which to create fiber alignment creates the ability to design nonwoven preforms with proposed directions of strength.

Another benefit of optimizing fiber placement is that it decreases the amount of fibers necessary in a reinforcement structure by using each at its highest potential. This not only lowers cost but weight of the structure. Introducing processes such as the one proposed may further the ability to lower the cost of composite materials. The automotive industry is an example of a cost driven market focusing on weight reduction materials which could benefit from composites utilizing this type of preform.

5.2 Limitations

While there are many benefits to this study, there were several notable limitations which could be useful to future researchers. Foremost, due to the deficit of research in this area, there were little to no standards to follow. This resulted in a considerable amount of time being dedicated to trial and error, ultimately limited the overall experimentation time.

Other limitations involve the resources used in the experimentation. For example, the design of the fiber collection boards was dependent on the limitations of the three dimensional printer. The three dimensional printer provided an 8" x 8" building area and the smallest aperture size was limited to 2 mm in diameter.

The use of only one type of fiber creates a limitation on the results. Fibers of different denier, bending rigidity, length or possessing different crimp could produce different results. However, these limitations create potential areas for future research.

5.3 Future Research

Nonwovens are attractive to the composites industry because of their versatility of properties and relatively low manufacturing costs when compared to other preforms. There are still many variables within this field of study for future research. Future research may include further investigation into aperture geometries and patterning. There is potential research into the means to optimize fiber accumulation and alignment on angled or vertical surfaces.

This study provided the foundation to further research the limits of the fiber collection board design. An example would be to investigate the feasibility of a single fiber

collection board producing several directions of fiber orientation with low tolerance. Furthering this study would increase the understanding of the limits of fiber orientation control. Increasing the knowledge of control could create areas of design, potentially using this technique to create aesthetic designs on the face of preform mats.

The type of fiber aligned nonwoven preforms described in this study could also have the ability to be combined with other types of fabrics to alter physical or mechanical properties. For example, to increase the bending rigidity of a nonwoven preform, a foam core or spacer fabric could be introduced between two layers of fiber aligned nonwovens. The fiber aligned nonwoven would provide the tensile strength and the core would provide bending strength. There are countless potential fiber and fabric combinations available for future research.

This study has provided a novel idea, data and ultimately a foundation of innovation for the advancement of material development.

CHAPTER 6: REFERENCES

[1] Pourdeyhimi, B., Maze, B., & Tafreshi, H. V. (2006). Simulation and Analysis of Unbonded Nonwoven Fibrous Structures. *Journal of Engineered Fibers and Fabrics*,*1*(2), 47-65.

[2] Mallick, P K. (2008). *Fiber-Reinforced Composites: Materials, Manufacturing and Design, 3rd Edition.* Boca Raton, FL: CRC Press.

[3] Krcma, Radko. *Manual of Nonwovens.* Manchester, England: The Textile Trade P, 1971. Print.

[4] Black, S. (2004). *Fiber Placement the Centerpiece of NCAM.* Retrieved Oct. 27, 2010, from Composites World, Cinncinati, OH. Web site: <http://www.compositesworld.com/articles/fiber-placement-the-centerpiece-of-ncam>.

[5] Harper, L.T., et al (2009). Fiber Alignment in Directed Carbon Fiber Preforms – A Feasibility Study. *Journal of Composite Materials,* 43(57), 57-74.

[6] Zino, K. (2010). *U.S. Automobile Industry Makes $500 Billion Dollar Contribution to the Economy.* Retrieved Oct. 27, 2010, from The Detroit Bureau, Detroit, MI. Web site: <http://www.thedetroitbureau.com/2010/04/u-s-automobile-industry-makes-500-billion-dollar-contribution-to-the-economy/>.

[7] Cramer, D. R., & Brylawski, M. M. (1996). ULTRALIGHT-HYBRID VEHICLE DESIGN: IMPLICATIONS FOR THE RECYCLING INDUSTRY. *Society of Plastics Engineers Recycling Division*, *3*, 1-9.

[8] Mascarin, Anthony E., Jeffrey R. Dieffenbach, Michael M. Brylawski, David R. Cramer, and Amory B. Lovins 1995: "Costing the Ultralite in Volume Production: Can Advanced Composite Bodies-in-White Be Affordable?," *Procs. 1995 Intl. Body Engineering Conf. & Exposition: Advanced Technologies & Processes* (Detroit, MI), **19**:56–69, 31October–2 November.

[9] Harper, L.T., et al.(2010). "Automated Charge Placement for Structural Molding Compounds (SMC)." *Society for the Advancement of Material and Process Engineering Journal* 46.5: 6-21.

[10] Rudd, C.D., et al. (1995). Design, Processing and Performance of Structural Preforms. *Materials and Manufacturing Processes*, 10(1), 89-102.

[11] Klein, W. (1987). *A Practical Guide to Opening and Carding, Volume 2.* Plymouth, UK: Latimer Trend & Co.

[12] Saco-Lowell Textile Machinery Division (1959). *Technical Data on Opening and Picking.* Easley, SC. Saco-Lowell Shops.

[13] Smith, P. A. (2000). Nonwoven Fabrics. In A. R. Horrocks & S. C. Anand (Eds.), *Handbook of Technical Textiles* (pp. 130-151). Cambridge, UK: Woodhead Publishing Ltd.

[14] Cordell, T., *et al*. (2000). The Programmable Powdered Preform Process for Aerospace—Affordable Performance Through Composites, *Sci. Adv. Mater. Process Eng. Ser.* **45**, pp. 254–265.

[15] Albrecht, W, Fuchs, H, & Kittelmann, W. (2003). *Nonwoven fabrics*. Weinheim, Germany: Wiley-VCH.

[16] Langdon, H. H. (1954). "Developments in Cotton Blending and Feeding." *Textile Research Journal* 24: 550-555. Print.

[17] Cook, L. (1993). *Nonwovens: theory, process, performance, and testing*. Atlanta, GA: Tappi Press.

[18] Nelson, David L. (1992). "Dry Lay Web Forming." *Principles of Nonwovens*. Ed. John E. Riedel. Cary, NC: Association of the Nonwoven Fabrics Industry: 549-566. Print.

[19] Bradean, R. *et al*. (2001)."Modelling of an Aerodynamic Technique of Forming Web Structures in Textile Industries: I. Turbulent Air Flow Past Filters." *Mathematical Engineering in Industry* 8.2: 137-160. Print.

[20] Ritter, M.E. *The Physical Environment: an Introduction to Physical Geography*. WebActive, 2006. Web. Retrieved: 1 Mar. 2010. <http://www.uwsp.edu/geo/faculty/ritter/geog101/textbook/title_page.html>.

[21] Massey, B S. (1968). *Mechanics of Fluid.* Toronto, CA: D. Van Nostrand Company.

[22] Benson, T. (2009). *Boundary Layer.* Retrieved Nov. 9, 2010, from National Aeronautics and Space Administration (NASA), Cleveland, OH. Web site: <http://www.grc.nasa.gov/WWW/K-12/airplane/boundlay.html>.

[23] Soltani, M., Ahmadi, G. (2000). Direct Numerical Simulation of Curly Fibers in Turbulent Channel Flow, *Aerosol Science and Technology, 33(5)*, 392-418.

[24] Marchioli, C., Fantoni, M., & Soldati, A. (2010). Orientation, distribution, and deposition of elongated, inertial fibers in turbulent channel flow, *Physics of Fluids, 22(3).*

[25] Jungbecker, P., Seide, G., & Gries, T. (2008), Kinematic Model for Yarn Movement in Turbulent Air Flows, *AUTEX Research Journal, 8(4), 94-100.*

[26] Zhang, H., Ahmadi, G., & Asgharian, B. (2007). Transport and Deposition of Angular Fibers in Turbulent Channel Flows. *Aerosol Science and Technology*, *41*(5), 529-548.

[27] Marheineke, N. (2006)."Fiber Dynamics in Turbulent Flows: General Modeling Framework." *Society for Industrial and Applied Mathematics* 66.5: 1703-1726. Print.

[28] Pourmohammadi, A., and Russell, S. J. (2000). "A Study of the Airflow and Fibre Dynamics in the Transport Chamber of a Sifting Air-Laying System. Part 1: Airflow Characteristics." *International Nonwovens Journal* 9.2: 76-83. Print.

[29] Pourmohammadi, A., and Russell, S J. (2000). "A Study of the Airflow and Fibre Dynamics in the Transport Chamber Of a Sifting Air-Laying System. Part 2: Fibre Dynamics." *International Nonwovens Journal* 9.3: 22-26. Print.

[30] Gallily, I., Eisner, A. (1978). On the Orderly Nature of the Motion of Nonspherical Aerosol Particles: I. Deposition from a Laminar Flow, *Journal of Colloid and Interface Science, 68(2),* 320-337.

[31] Marheineke, N. (2006). Modeling of Turbulence Effects on Fiber Motion. *Progress in Industrial Mathematics at ECMI 2004, 8(V),* 366-370.

[32] Gao, X. & Huang, H. *Dry-Laid Nonwovens.* Apparel Search Company, 25 Feb. 2003. Web. Retrieved: 1 Mar. 2010. <http://www.apparelsearch.com/Education/Research/Nonwoven/2001_Kermit_Duckett/education_research_nonwoven_dry-laid_nonwovens.htm>.

[33] Lin, F. (2001). "Configuration of PET Fiber Arrangement in Roller Drafting Air-Laid Webs." *Textile Research Journal* 71: 75-80. Print.

[34] Lee, F.B., and Jobes, O. “Apparatus for Continuously Making an Air-Laid Fibrous Web Having Patterned Basis Weight Distribution”, U.S. Patent No. 4388056, June 14, 1983.

[35] *Fly Dragon Wire Mesh Co. Ltd.* Web. Retreived: 1 Mar. 2011. <http://www.wiremeshdragon.cn/>

[36] Arnal, D. (1996). Control of Laminar-Turbulent Transition for Skin Friction Drag Reduction. In G. Meier & G. H. Schnerr (Eds.), *Control of Flow Instabilities and Unsteady Flows* (pp. 119-153). New York, NY: SpringerWien.

[37] Weeton, J. W. (1987). Engineers' guide to composite materials. American Society for Metals, Metals Park: Ohio.

[38] Kaw, A K. (1997). *Mechanics of Composite Materials.* Boca Raton, FL: CRC Press LLC.

[39] Batra, S. K. (1989). Fibers as Structural Elements in Nonwovens. In A. F. Turbak & T. L. Vigo (Eds.), *Nonwovens: An Advanced Tutorial* (pp. 9-22). Atlanta, GA: Tappi Press.

[40] Guell, D., & Benard, A. (1997). *Flow-induced alignment in composite materials.* Cambridge, UK: Woodhead Publishing Ltd..

[41] Composites 101: White Paper. Web. Retrieved: 1 Mar. 2011. <http://www.quartus.com/resources/whitepaper/composite/>.

[42] Kollar, L P, Springer, G S. (2003). *Mechanics of Composite Structures.* Cambridge, UK: Cambridge University Press.

[43] Hull, D. (1981). *An Introduction to Composite Materials.* Cambridge, UK: Cambridge University Press.

[44] Moutran, S. R. (2002). *Feasible Workspace for Robotic Fiber Placement.* MS Thesis. Virginia Polytechnic Institute and State University.

[45] Piggott, M R. (2002). *Load Bearing Fibre Composites.* New York, NY: Springer.

[46] Kim, Y. K. *et al*. (2009). *Engineered Reinforced Structures from Short Fibers*. National Textile Center Project: F08-MD01, National Textile Center Annual Report: October 2009.

[47] Hancox, N. L. (2000). An overview of the impact behavior of fibre-reinforced composites. In S. R. Reid & G. Zhou (Eds.), *Impact behavior of fibre-reinforced composite materials and structures* (pp. 1-29). Cambridge, England: Woodhead Publishing Ltd.

[48] Fu, S., & Lauke, B. (1996). Effects of Fiber Length and Fiber Orientation Distributions on the Tensile Strength of Short-Fiber-Reinforced Polymers. *Composites Science and Technology*, *56*(10), 1179-1190.

[49] Giurgiutiu, V., & Reifsnider, K. L. (1994). Development of Strength Theories for Random Fiber Composites. *Development of Strength Theories for Random Fiber Composites*, *16*(2), 103-114.

[50] Tsai, S.W. (1965). Strength Characteristics of Composite Materials. *NASA CR-224.*

[51] Hahn, T. H. (1975). On Approximation for Strength of Random Fiber Composites. *Journal of Composite Materials.* Vol. 9 pp. 316-326.

[51] Wang S.S., et al. (1984). Interlaminar Fracture of Random Short-Fiber SMC Composite. *Journal of Composite Materials.* Vol. 18 pp. 574-594.

[52] Blumentritt, B.F., Vu, B.T., and Cooper, S.T. (1975). The Mechanical Properties of Oriented Discontinuous Fiber-Reinforced Thermoplastics – Part I. Unidirectional Fiber Orientation. *Journal of Polymer Engineering & Science,* 14(9), pp. 633-640.

[54] Blumentritt, B.F., Vu, B.T., and Cooper, S.T. (1975). The Mechanical Properties of Oriented Discontinuous Fiber-Reinforced Thermoplastics – Part II. Random-in-Plane Fiber Orientation. *Journal of Polymer Engineering & Science,* 15(6), pp. 428-436.

[55] Brandt, M. R., and Reeve, S. R. (2001). "Directed Fiber Preform Case Studies." *Composites Fabricators Association: 2001 Convention and Trade Show*: 1-10. Web.

[56] Rosebro, J. (2006). *Does Ford Have a Better Idea about Sustainability?* Retrieved: Sep. 13, 2010, from Green Car Congress, Web site: <http://www.greencarcongress.com/2006/02/does_ford_have_.html>.

[57] Eyerman, J. R. (1952, February 25). Plastic Bodies for Autos. *Life*, *32*(8), 99-102.

[58] Kenney, R. (2008). *Energy Policy and Conservation Act of 1975, United States*. Retrieved Sep. 13, 2010, from The Encyclopedia of the Earth, Web site: <http://www.eoearth.org/article/Energy_Policy_and_Conservation_Act_of_1975,_United_States>.

[59] Sousanis, J. (2010). *Historical U.S. Car and Truck Sales, 1931-2009.* Retrieved: Sep. 13, 2010, from Wards Auto, Detroit, Mi. Web site: <http://wardsauto.com/keydata/>.

[60] Nieuwenhuis, P., Wells, P. E. (2003). *The Automotive Industry and the Environment.* Boca Raton, FL: Woodhead Publishing Ltd.

[61] Rahim, S. (2009, 19) White House proposes new, stricter national fuel efficiency standards. *New York Times*, 17.

[62] U.S. National Research Council (2002) *Effectiveness and Impact of Corporate Average Fuel Economy (CAFÉ) Standards*. Washington, D.C., National Academy Press.

[63] Tullo, A. "Driving Efficiency." *Chemical & Engineering News* 84.24 (2006): 12-18. Web. Retrieved: 25 Jan 2010.

[64] Ashby, M. F., & Johnson, K. (2002). *Materials and Design: The Art and Science of Material Selection in Product Design.* Burlington, MA: Butterworth-Heinemann.

[65] Poulton, M.L. (1997). *Fuel Efficient Car Technology.* Southampton, UK: Computational Mechanics Publications.

[66] Mallick, P K. (2010). *Materials, design and manufacturing for lightweight vehicles.* Boca Raton, FL: Woodhead Publishing Ltd.

[67] Evans, L. (2004). *How to Make a Car Lighter and Safer.* Science Serving Society, 2004 SAE International.

[68] Kanari, N., Pineau, J. L., & Shallari, S. (2003). End-of-Life Vehicle Recycling in the European Union. *Journal of the Minerals, Metals and Materials Society*, *55*(8), 15-19.

[69] Sullivan, J. (2007). Use of Plastics in Body Construction in Future Automobile Design and Production. In R. Stauber & L. Vollrath (Eds.), *Plastics in Automotive Engineering* (pp. 19-29). Cincinnati, OH: Hanser Gardner Publications.

[70] World Textile Publications Ltd (July 1999). Changing Landscape – Notable Developments in the Automotive Sector, Nonwovens Report International, No. 340, pp. 34–37.

[71] Farag, M. M. (2008). Quantitative Methods of Materials Substitution: Application to Automotive Components. *Materials and Design*, *29*(2), 374-380.

[72] SolidWorks® (Version SP 4.0) [Software]. (2010-2011). Concord, MA: Dassault Systemes SolidWorks® Corp.

[73] “ZPrinter® 450.” *ZCorporation.* N.p., 2007. Web. 20 Dec. 2010. <http://www.zcorp.com/en/Products/3D-Printers/ZPrinter-450/spage.aspx>.

[74] Ligget, B. (2010). “Scientists Use 3D Printer to Create First “Printed” Human Vein.” *Inhabitat.* N.p., 22 Mar. 2010. Web. Retrieved: 3 Mar. 2011. <http://inhabitat.com/scientists-use-3d-printer-to-create-first-printed-human-vein/>.

[74] Pourdeyhimi, B., & Ramanathan, R. (1996). Measuring Fiber Orientation in Nonwovens: Part I: Simulation. *Textile Research Journal,* 66(11), pp. 713-722.

[75] Pourdeyhimi, B., & Ramanathan, R. (1996). Measuring Fiber Orientation in Nonwovens: Part II: Direct Tracking. *Textile Research Journal,* 66(12), pp. 747-753.

[76] Pourdeyhimi, B. *et al.*(1999). Measuring Fiber Orientation in Nonwovens: Part V: Real Webs. *Textile Research Journal,* 69(3), pp. 185-192.

[77] Photoshop® (Version CS3) [Software]. (2007). San Jose, CA: Adobe.

[78] Begenier, A., Vahedi Tafreshi, H., & Pourdeyhimi, B. (2004). Effect of nozzle geometry on hydroentangling water jets: Experimental observations. Textile Research Journal, 74(2), pp. 178-184.

APPENDICES

Appendix A: Fiber Collection Board Screen Shots of Design Procedure [72; SolidWorks]

Fiber Collection Board #1:

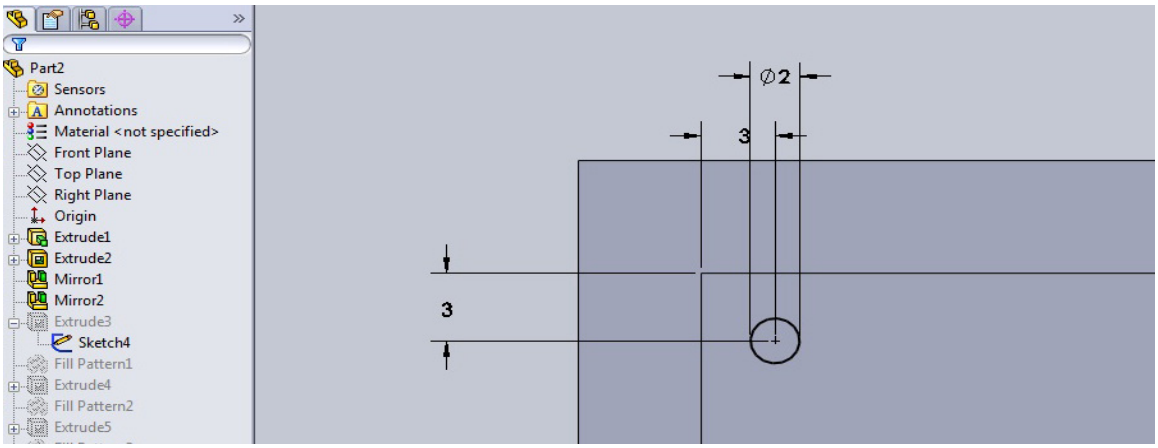

a) Two dimensional aperture dimensioning and spacing

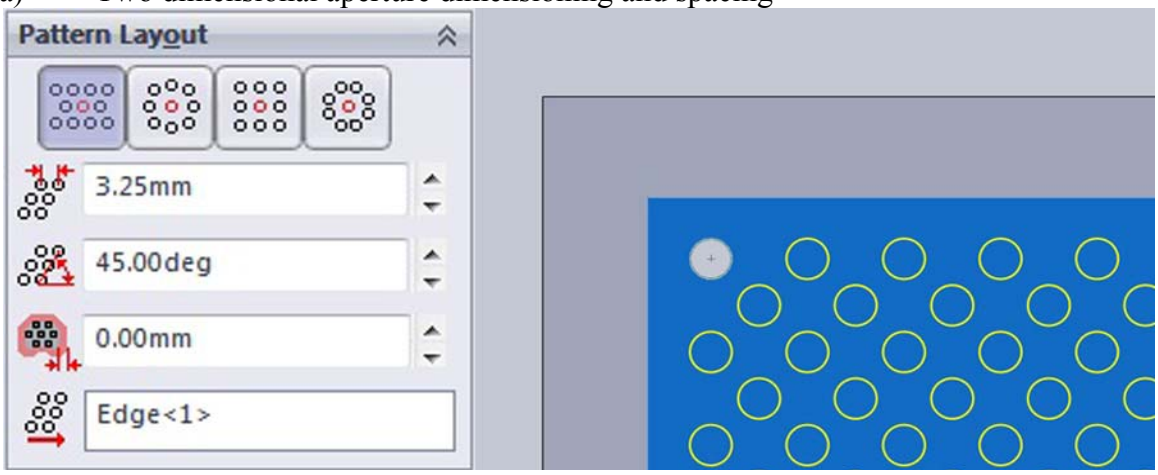

b) Pattern layout and spacing

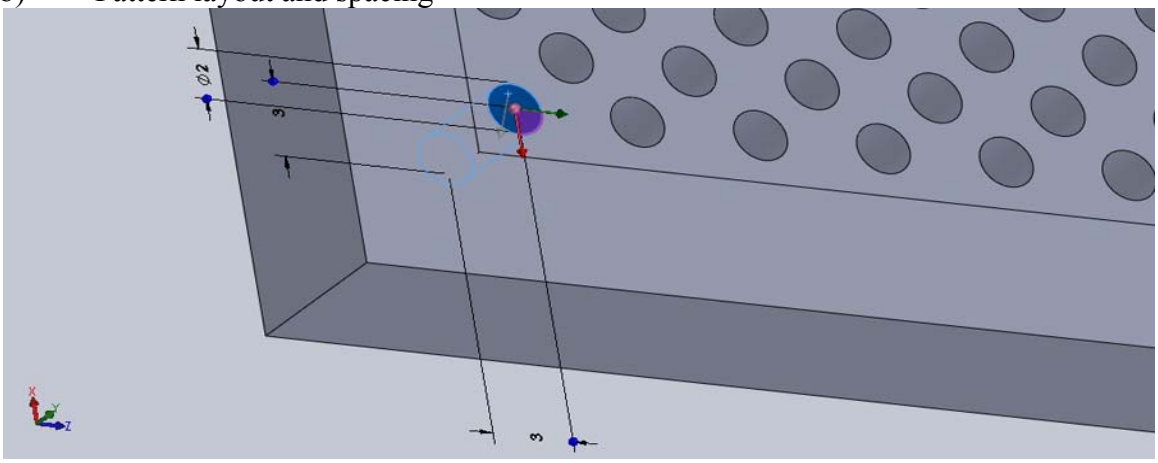

c) Aperture pattern extrusion

Fiber Collection Board #2:

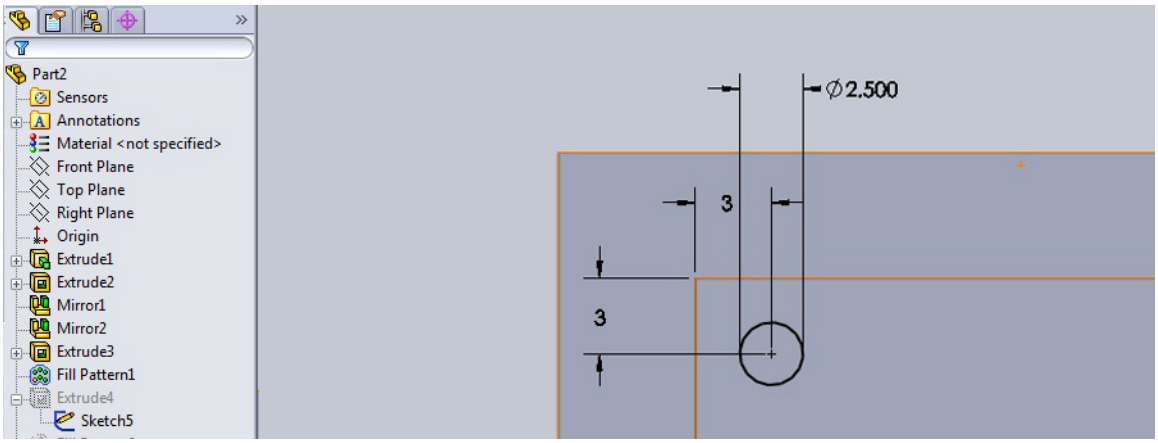

a) Two dimensional aperture dimensioning and spacing

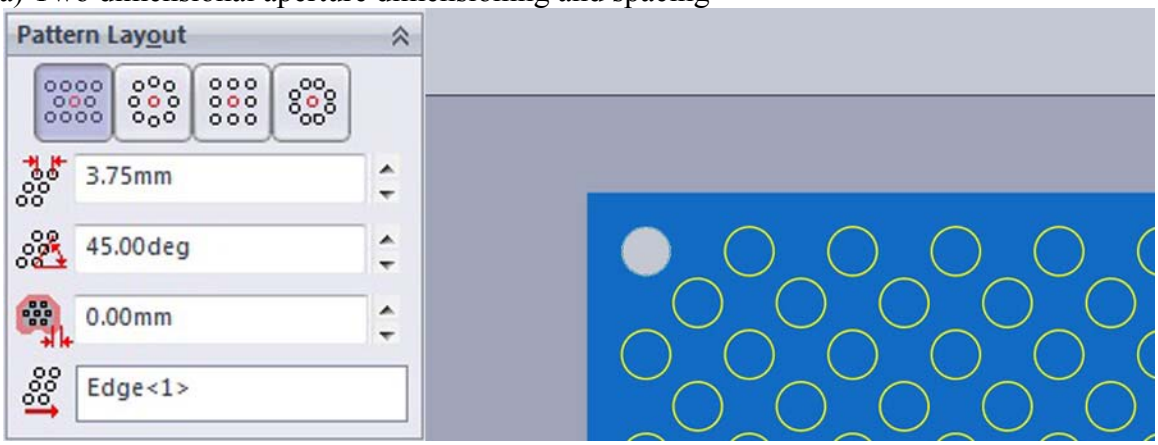

b) Pattern layout and spacing

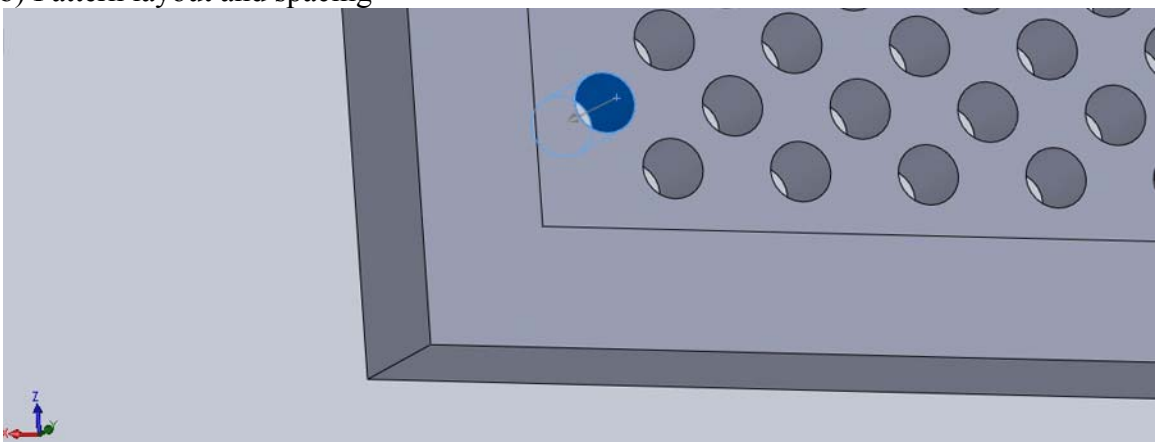

c) Aperture pattern extrusion

Fiber Collection Board #3:

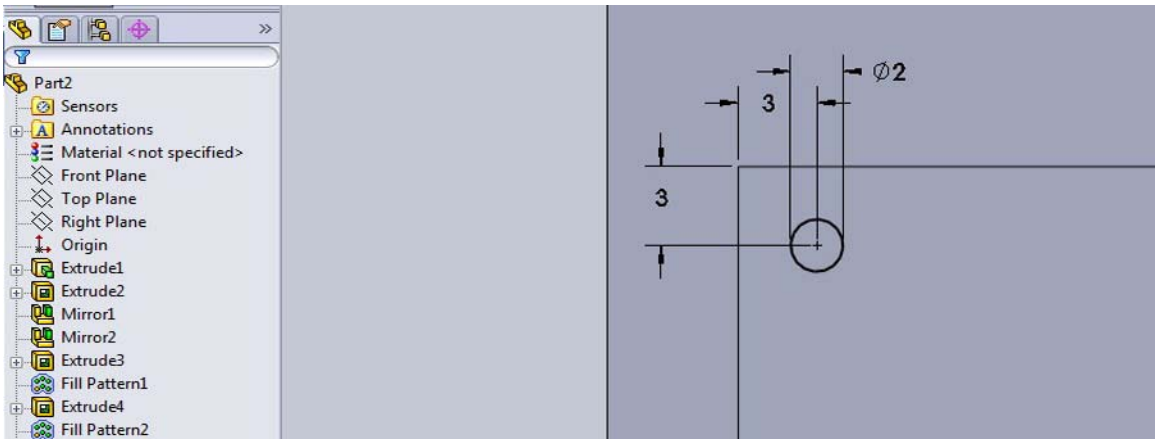

a) Two dimensional aperture dimensioning and spacing

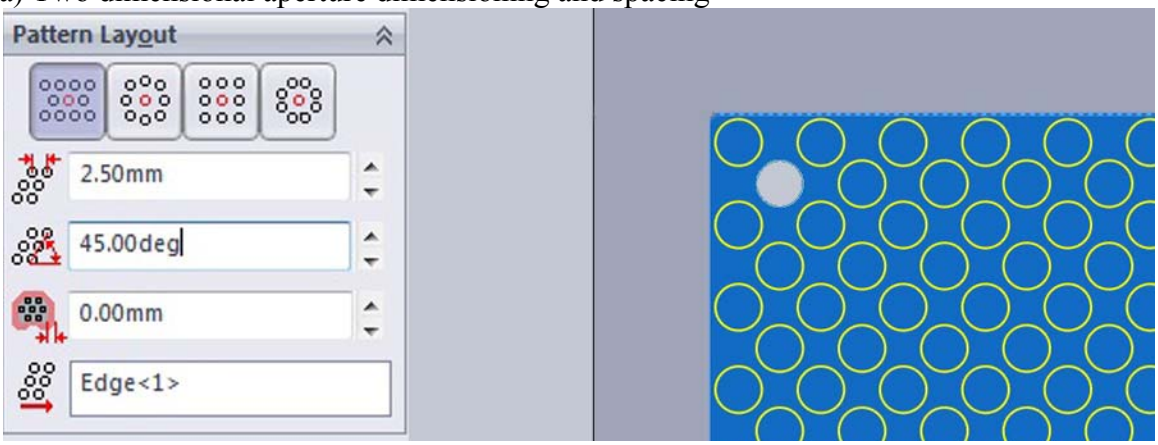

b) Pattern layout and spacing

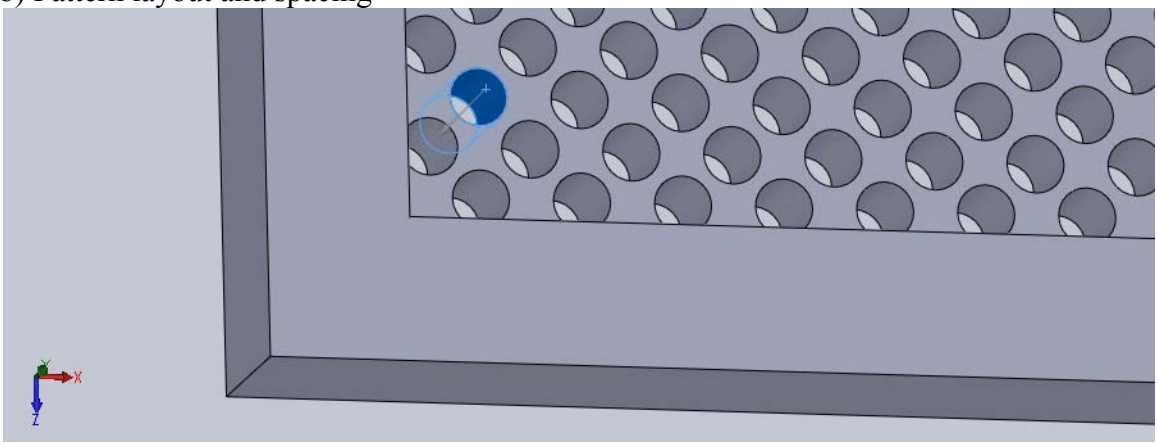

c) Aperture pattern extrusion

Fiber Collection Board #4:

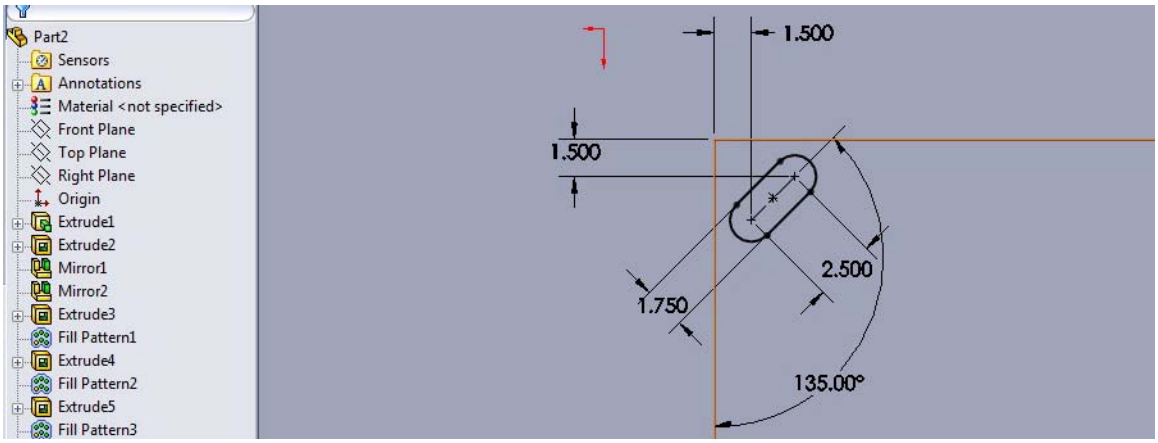

a) Two dimensional aperture dimensioning and spacing

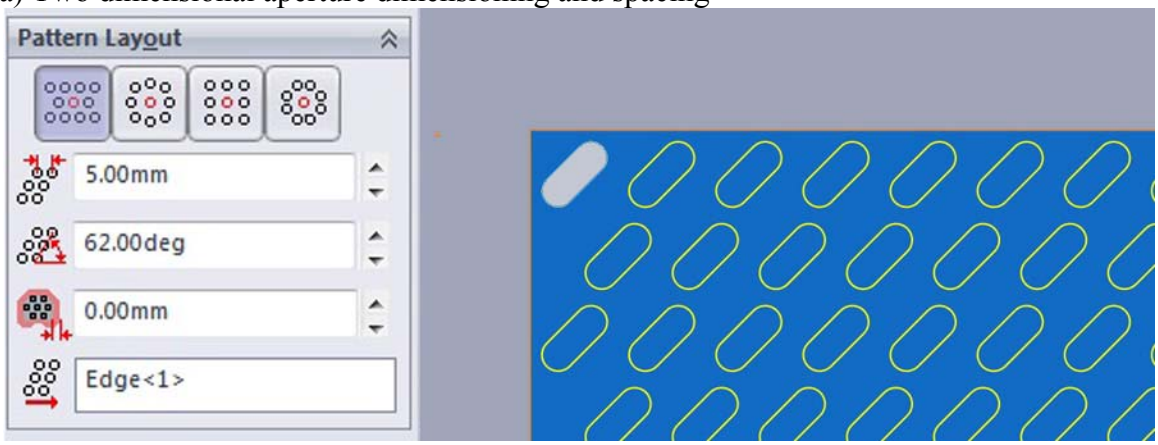

b) Pattern layout and spacing

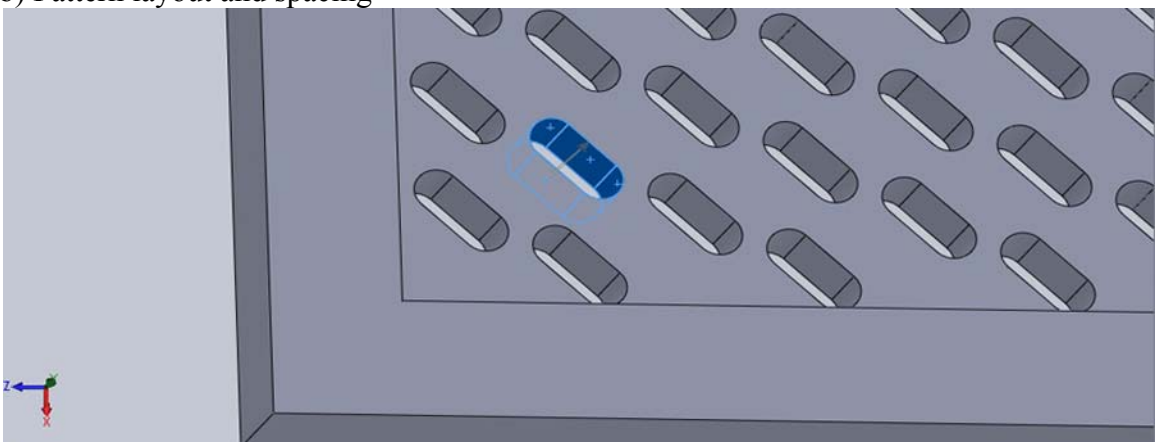

c) Aperture pattern extrusion

Fiber Collection Board #5:

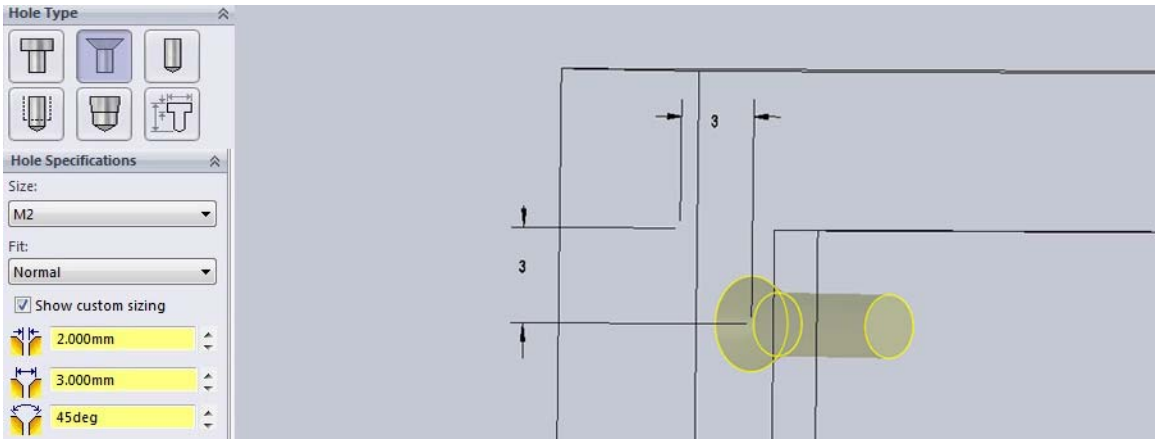

a) Aperture dimensioning and spacing

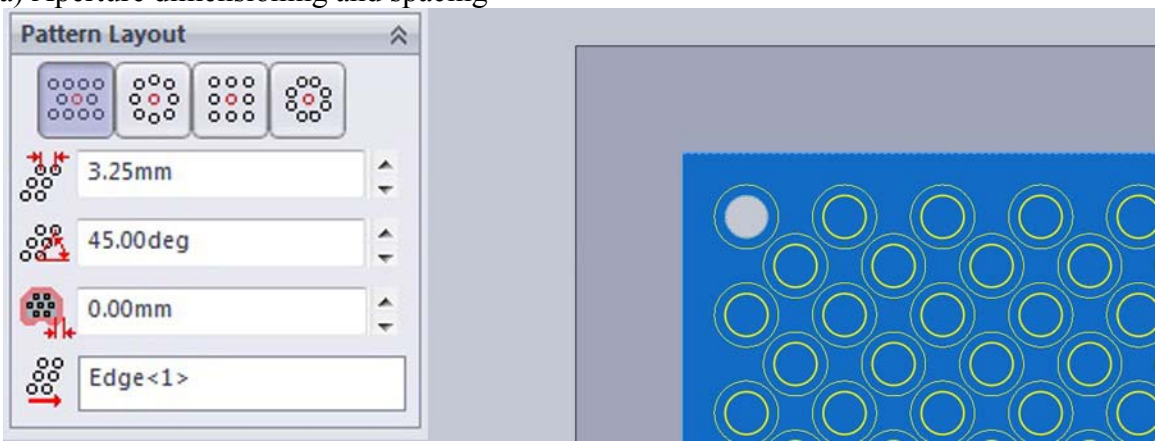

b) Pattern layout and spacing

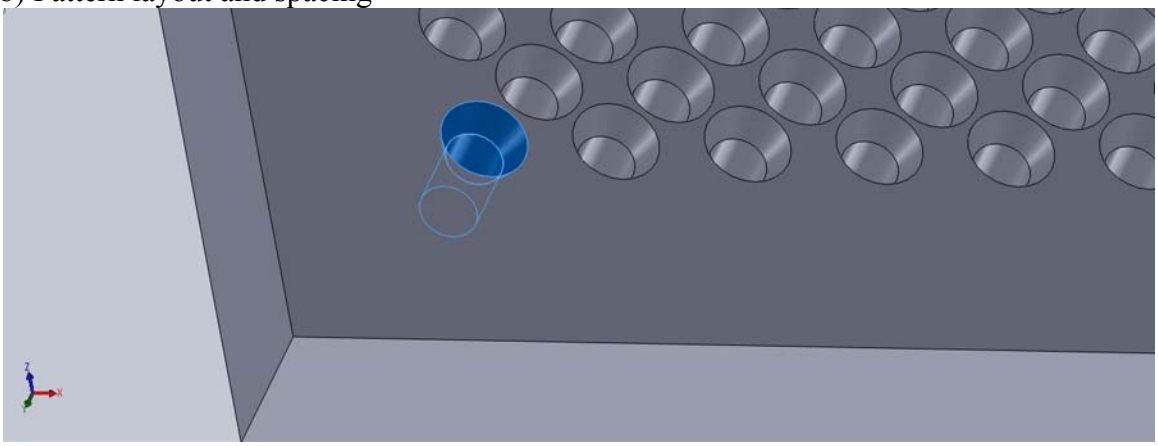

c) Aperture pattern extrusion

Fiber Collection Board #6:

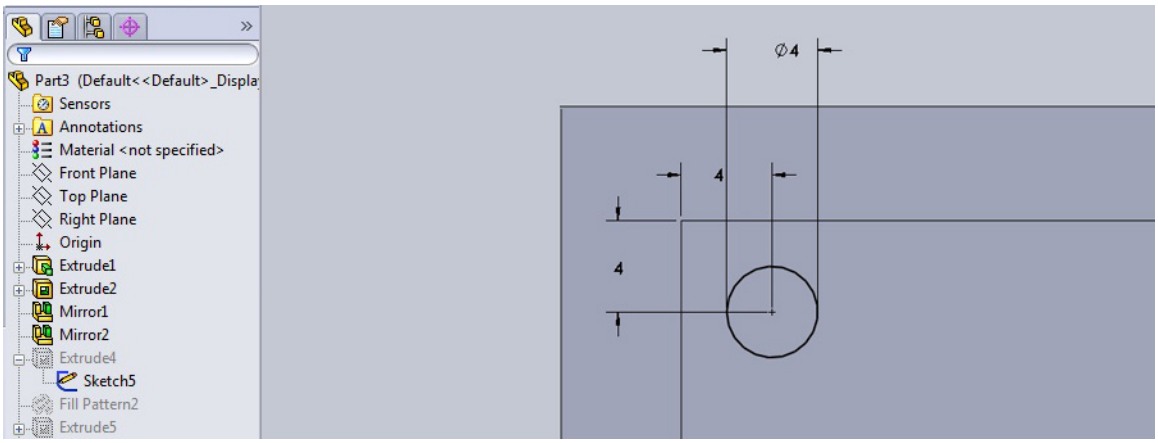

a) Two dimensional aperture dimensioning and spacing

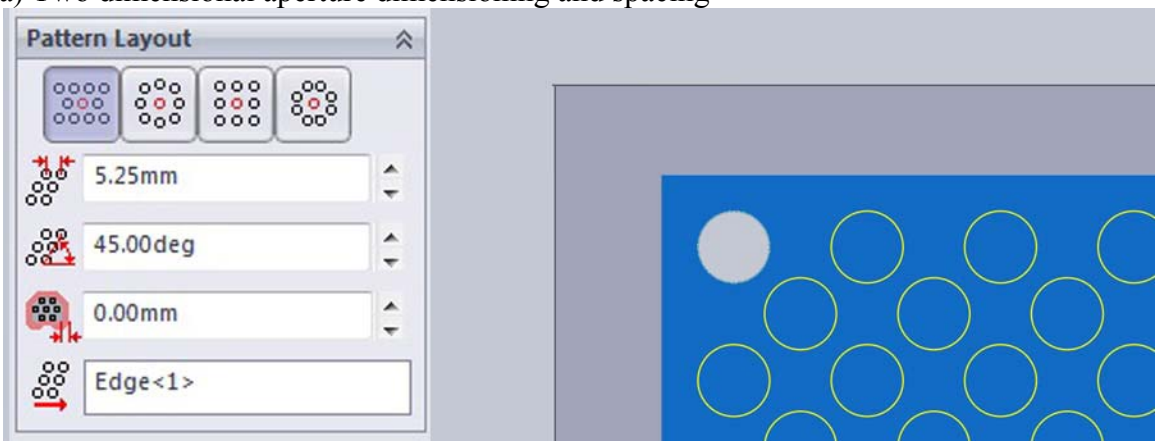

b) Pattern layout and spacing

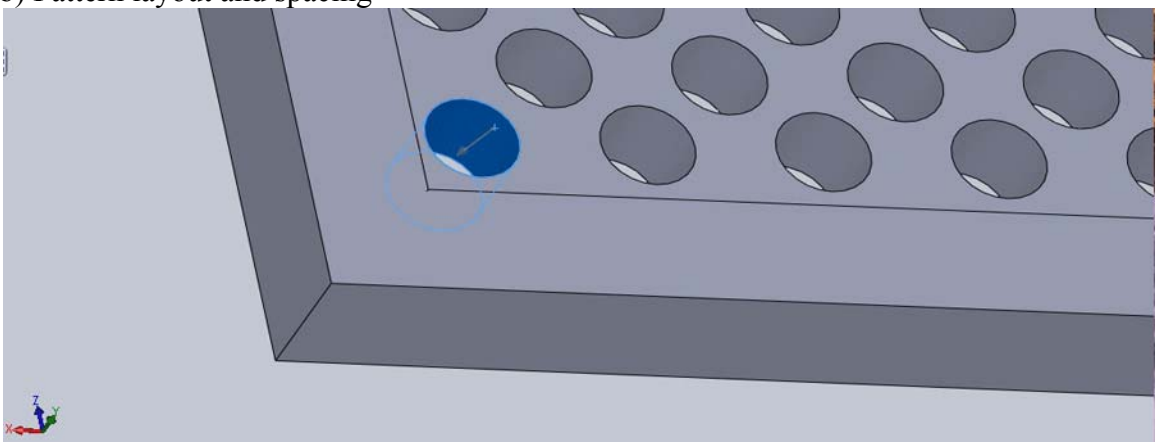

c) Aperture pattern extrusion

Fiber Collection Board #7:

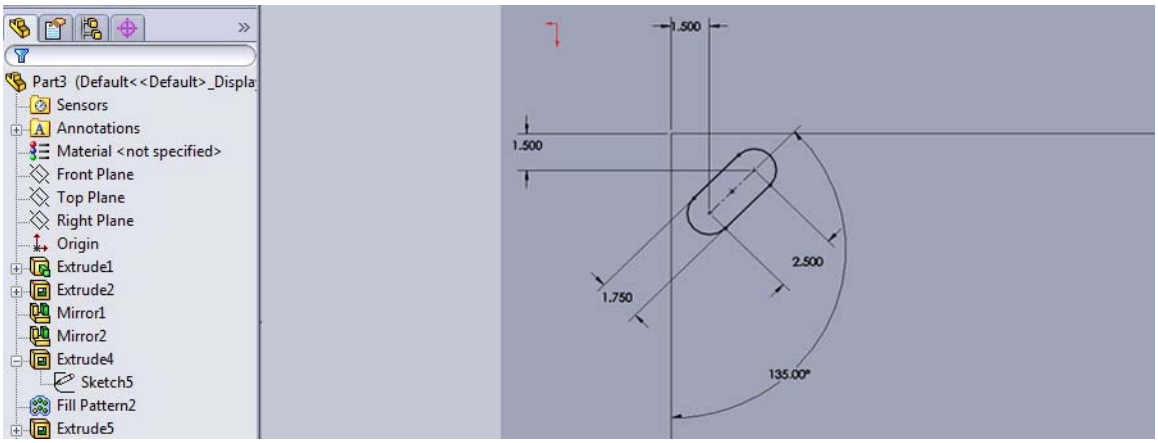

a) Two dimensional aperture dimensioning and spacing

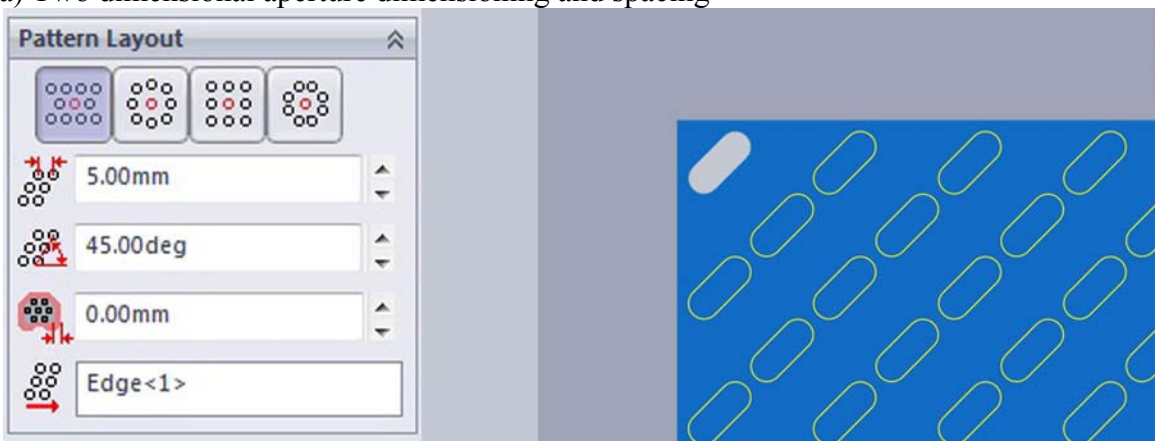

b) Pattern layout and spacing

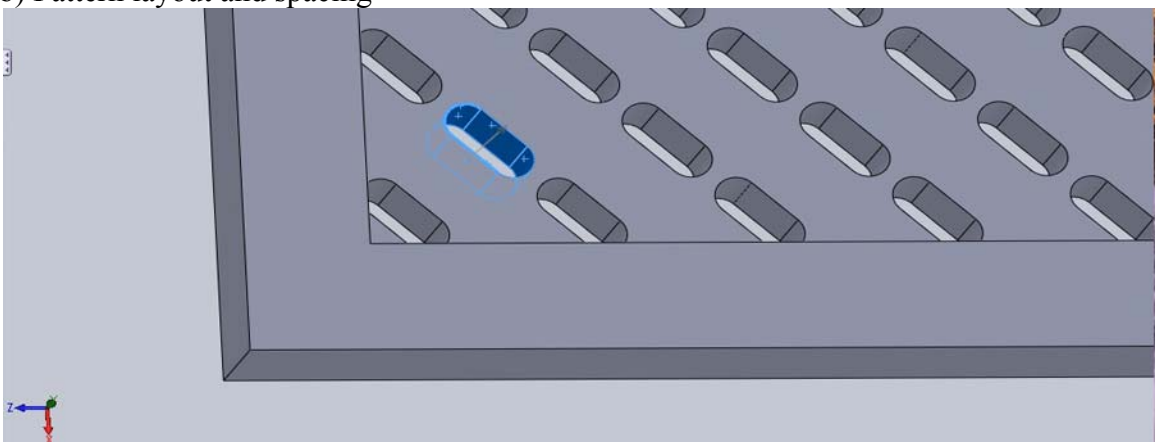

c) Aperture pattern extrusion

Appendix B: Fiber Collection Boards

Fiber Collection Board #1(not actual size):

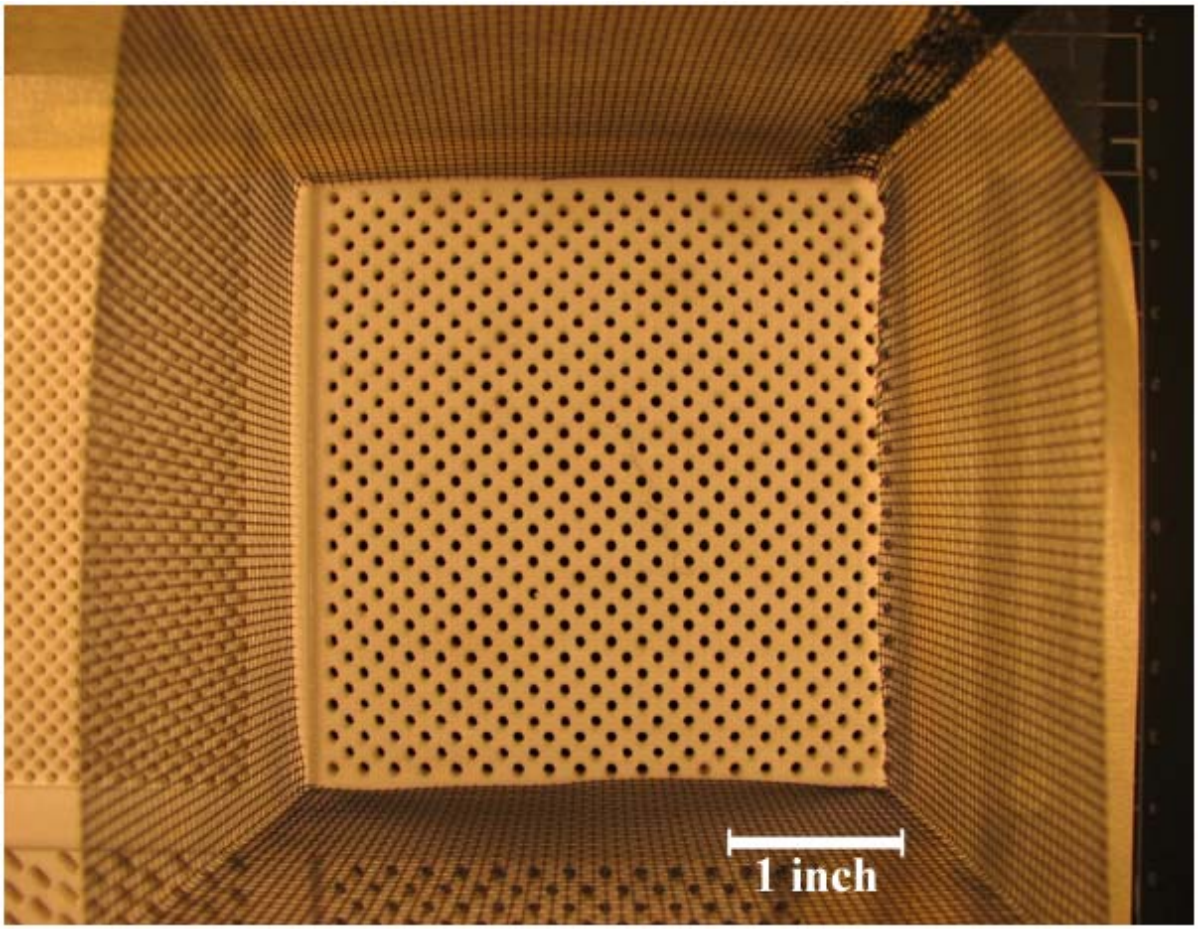

Fiber Collection Board #2 (not actual size)

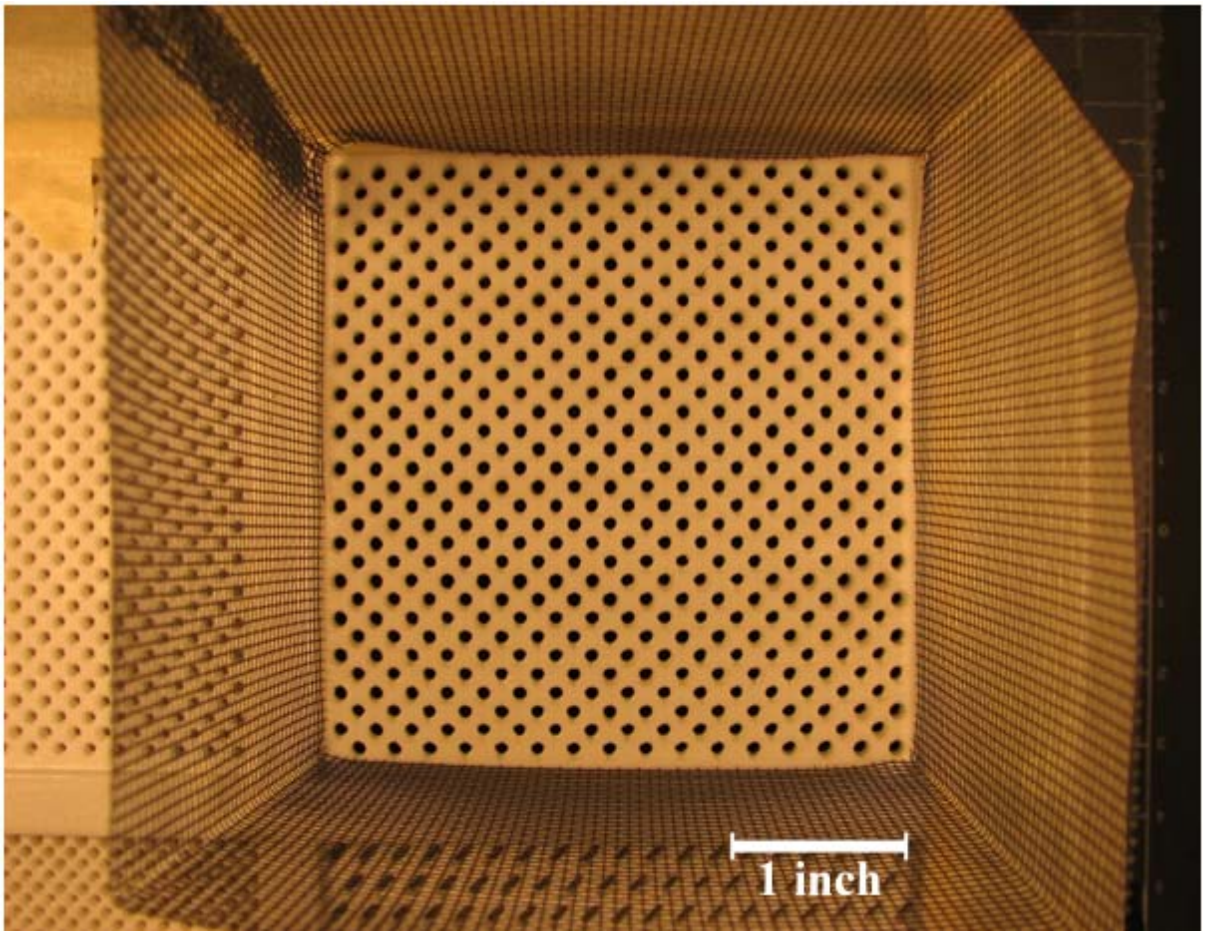

Fiber Collection Board #3 (not actual size):

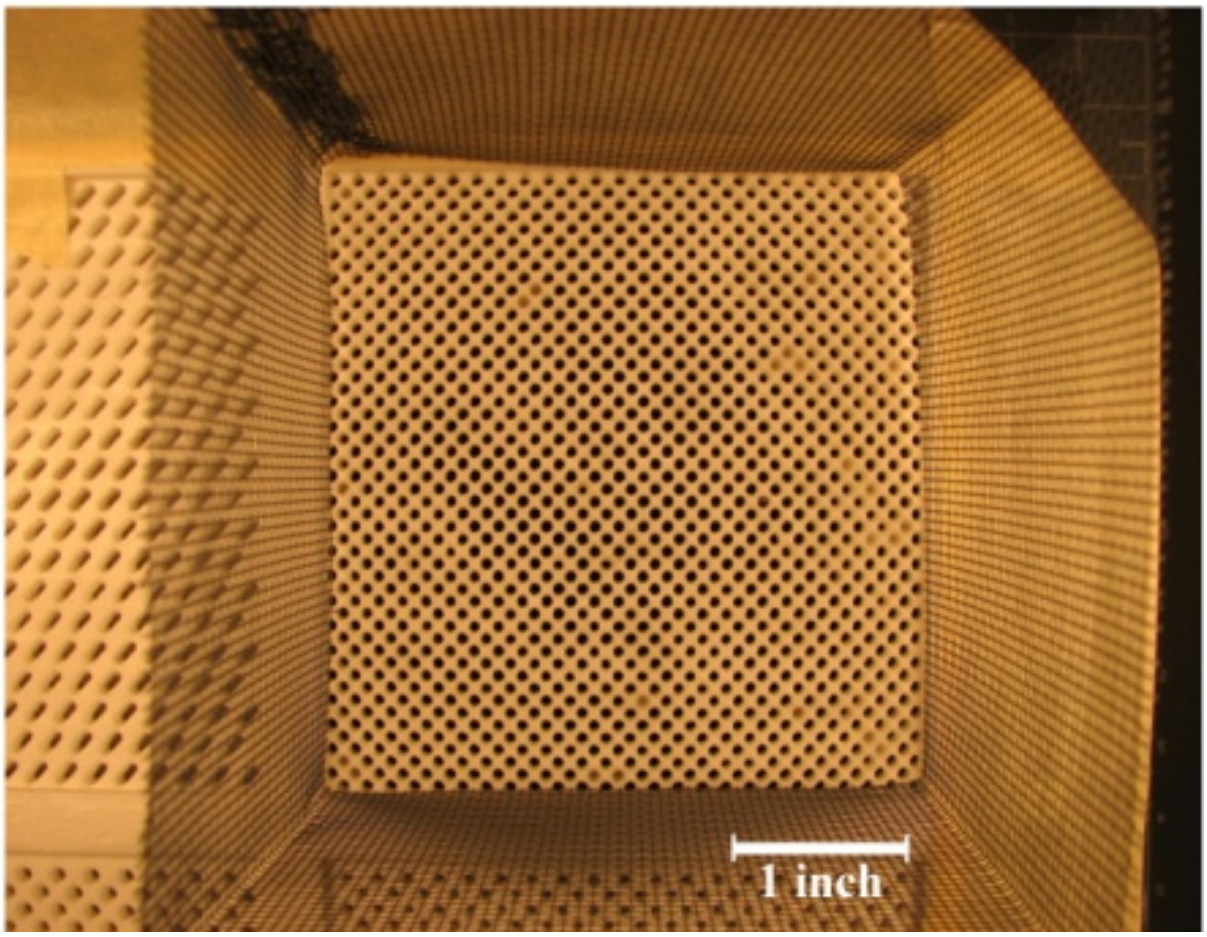

Fiber Collection Board #4 (not actual size):

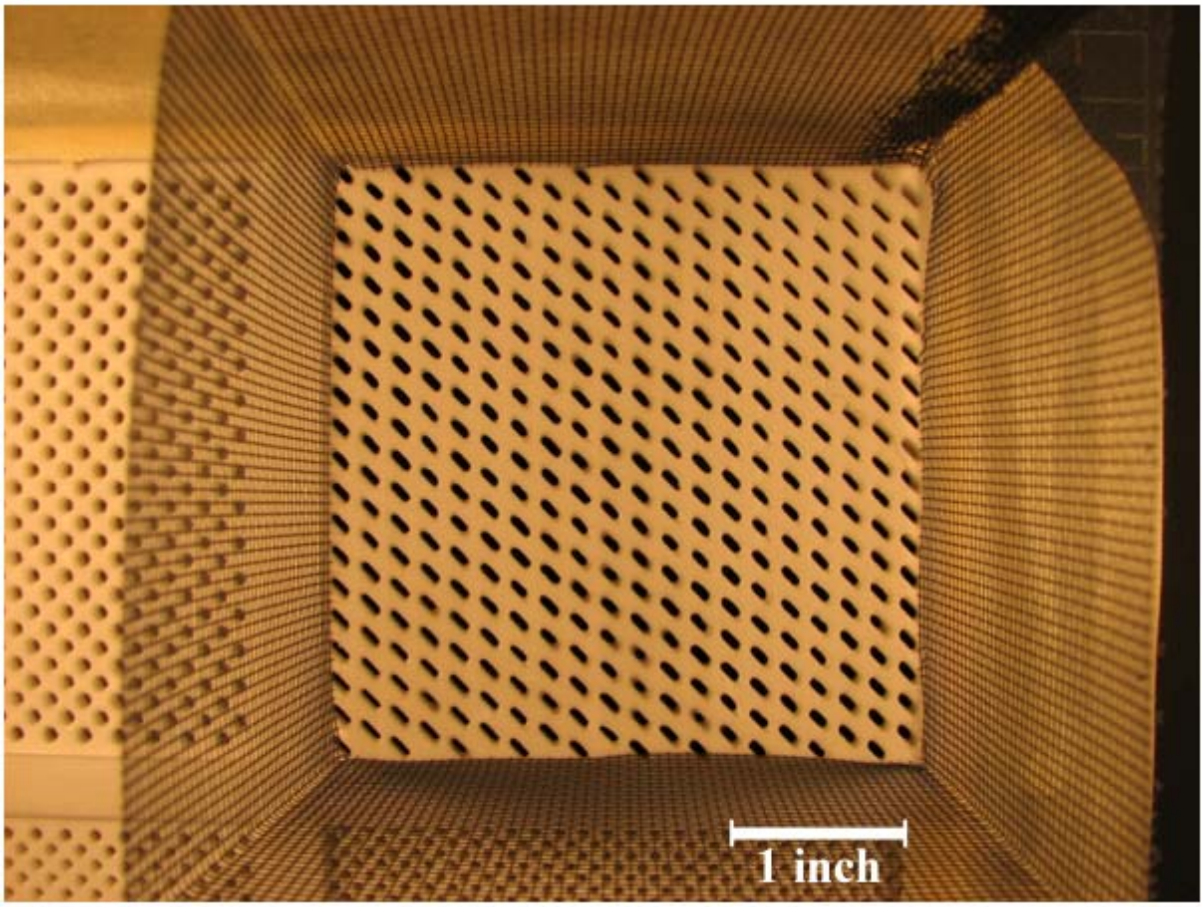

Fiber Collection Board #5 (not actual size):

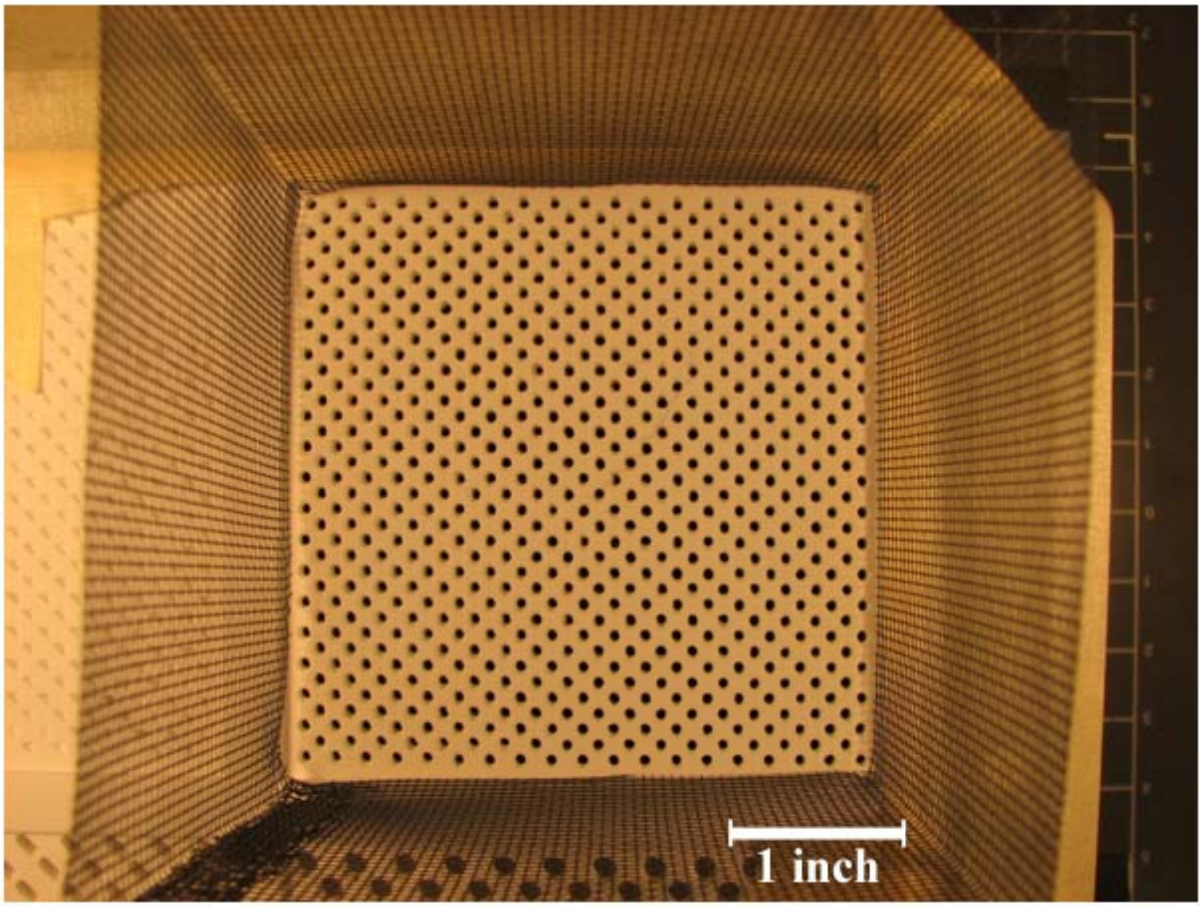

Fiber Collection Board #6 (not actual size):

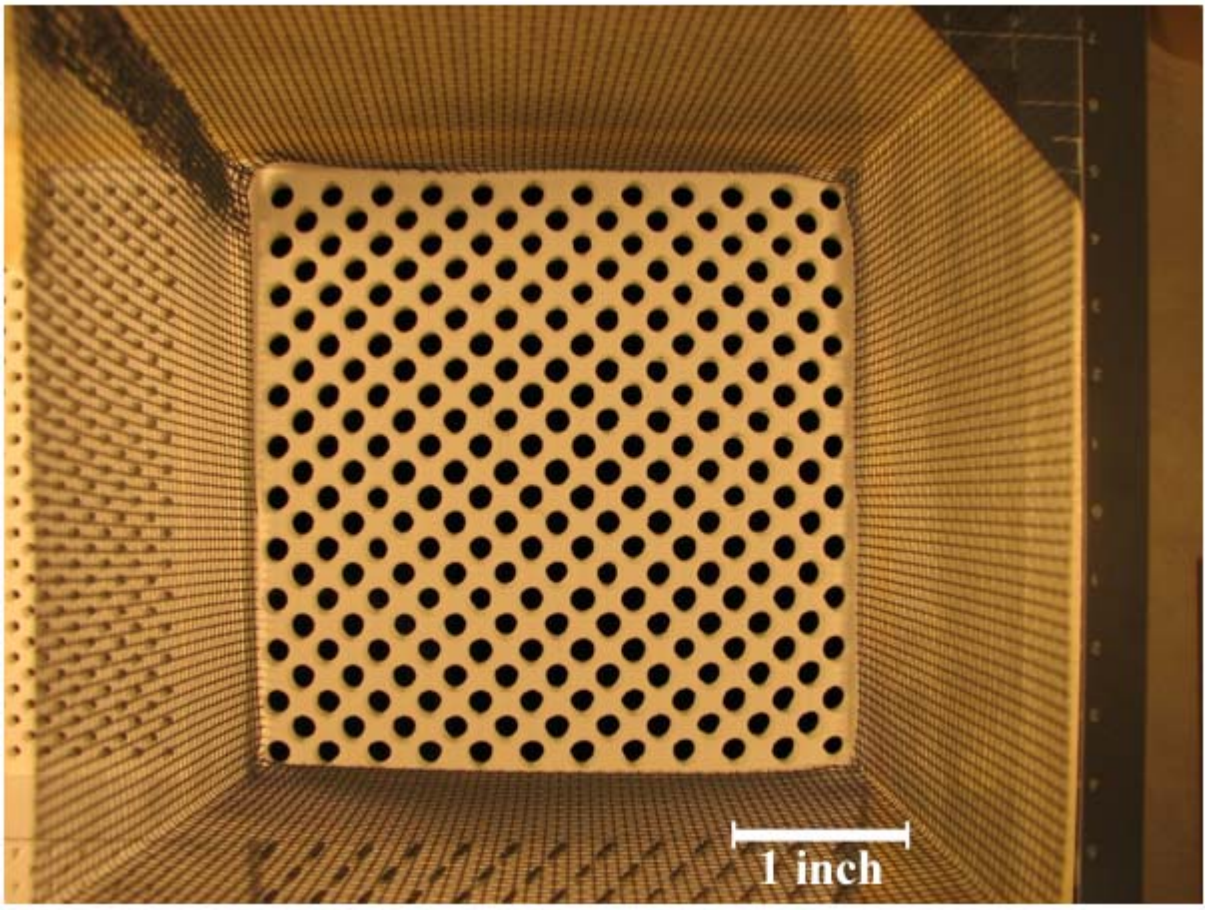

Fiber Collection Board #7 (not actual size):

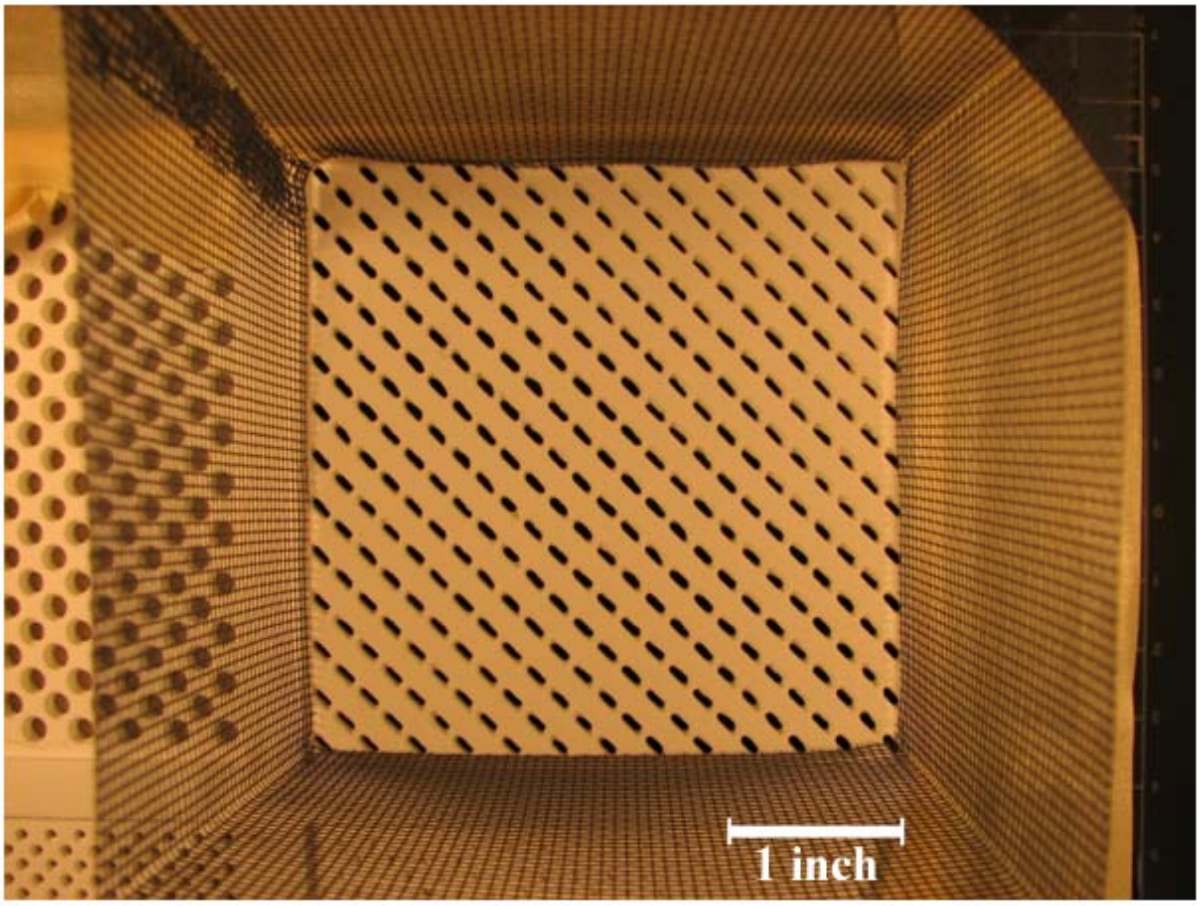

Appendix C: Fiber Orientation Measurement Data

Fiber Collection Board #1 Data

Sample #	Angle								
1	53	41	5	81	153	121	57	161	31
2	119	42	144	82	58	122	106	162	134
3	42	43	136	83	45	123	147	163	103
4	169	44	65	84	113	124	3	164	38
5	117	45	67	85	33	125	141	165	110
6	146	46	87	86	138	126	94	166	9
7	132	47	14	87	53	127	27	167	159
8	80	48	119	88	50	128	100	168	84
9	28	49	8	89	39	129	99	169	156
10	55	50	21	90	147	130	172	170	153
11	105	51	88	91	34	131	107	171	101
12	130	52	162	92	126	132	110	172	51
13	43	53	64	93	140	133	124	173	20
14	88	54	129	94	168	134	54	174	124
15	12	55	142	95	80	135	131	175	95
16	66	56	35	96	153	136	72	176	134
17	129	57	160	97	145	137	116	177	31
18	23	58	137	98	97	138	129	178	129
19	5	59	33	99	87	139	101	179	132
20	175	60	32	100	98	140	21	180	41
21	10	61	138	101	3	141	114	181	11
22	78	62	9	102	25	142	46	182	97
23	54	63	25	103	37	143	135	183	58
24	24	64	71	104	152	144	179	184	45
25	102	65	82	105	50	145	89	185	16
26	145	66	80	106	33	146	54	186	147
27	47	67	42	107	99	147	36	187	89
28	48	68	103	108	155	148	3	188	14
29	24	69	43	109	150	149	104	189	112
30	134	70	106	110	123	150	141	190	72
31	117	71	77	111	46	151	100	191	20
32	106	72	85	112	65	152	142	192	44
33	98	73	4	113	149	153	58	193	109
34	42	74	118	114	68	154	61	194	127
35	159	75	25	115	78	155	125	195	124
36	82	76	138	116	102	156	77	196	143
37	137	77	147	117	126	157	176	197	49
38	110	78	113	118	65	158	173	198	20
39	91	79	43	119	145	159	93	199	47
40	50	80	45	120	166	160	19	200	88

Average Orientation Angle: 87.07^{o}
Standard Deviation: 48.27^{o}

Fiber Collection Board #2 Data

Sample #	Angle								
1	44	41	14	81	71	121	54	161	102
2	134	42	34	82	158	122	98	162	3
3	75	43	78	83	15	123	30	163	148
4	135	44	111	84	28	124	149	164	53
5	118	45	159	85	59	125	165	165	15
6	142	46	14	86	132	126	45	166	147
7	116	47	166	87	136	127	134	167	177
8	177	48	53	88	113	128	144	168	8
9	40	49	16	89	138	129	69	169	42
10	71	50	7	90	55	130	152	170	123
11	47	51	84	91	100	131	180	171	10
12	145	52	93	92	96	132	58	172	38
13	88	53	49	93	145	133	73	173	28
14	138	54	15	94	81	134	102	174	137
15	1	55	141	95	129	135	32	175	179
16	54	56	103	96	5	136	63	176	24
17	136	57	128	97	123	137	56	177	38
18	117	58	174	98	165	138	20	178	40
19	45	59	94	99	17	139	172	179	77
20	48	60	2	100	153	140	34	180	142
21	29	61	127	101	156	141	151	181	84
22	41	62	99	102	144	142	136	182	70
23	12	63	50	103	131	143	160	183	6
24	92	64	155	104	70	144	9	184	120
25	164	65	59	105	88	145	23	185	58
26	71	66	52	106	147	146	165	186	91
27	44	67	119	107	93	147	58	187	68
28	143	68	122	108	144	148	119	188	33
29	124	69	131	109	91	149	37	189	25
30	141	70	152	110	64	150	145	190	140
31	44	71	26	111	66	151	89	191	101
32	55	72	44	112	117	152	136	192	21
33	171	73	11	113	31	153	91	193	143
34	46	74	174	114	79	154	10	194	64
35	128	75	135	115	128	155	70	195	38
36	88	76	107	116	77	156	78	196	28
37	123	77	41	117	102	157	96	197	146
38	65	78	129	118	131	158	10	198	3
39	171	79	59	119	57	159	142	199	55
40	89	80	20	120	129	160	157	200	118

Average Orientation Angle: 88.39^{o}
Standard Deviation: 51.09^{o}

Fiber Collection Board #3 Data

Sample #	**Angle**								
1	**102**	*41*	**3**	*81*	**12**	*121*	**86**	*161*	**91**
2	**122**	*42*	**37**	*82*	**107**	*122*	**65**	*162*	**75**
3	**86**	*43*	**123**	*83*	**150**	*123*	**13**	*163*	**150**
4	**7**	*44*	**49**	*84*	**21**	*124*	**15**	*164*	**89**
5	**155**	*45*	**103**	*85*	**104**	*125*	**7**	*165*	**24**
6	**162**	*46*	**45**	*86*	**174**	*126*	**139**	*166*	**34**
7	**128**	*47*	**28**	*87*	**64**	*127*	**65**	*167*	**37**
8	**83**	*48*	**114**	*88*	**136**	*128*	**65**	*168*	**135**
9	**137**	*49*	**144**	*89*	**4**	*129*	**96**	*169*	**151**
10	**17**	*50*	**135**	*90*	**144**	*130*	**161**	*170*	**17**
11	**151**	*51*	**111**	*91*	**83**	*131*	**51**	*171*	**37**
12	**135**	*52*	**127**	*92*	**87**	*132*	**57**	*172*	**161**
13	**130**	*53*	**20**	*93*	**32**	*133*	**13**	*173*	**69**
14	**4**	*54*	**17**	*94*	**167**	*134*	**11**	*174*	**91**
15	**154**	*55*	**54**	*95*	**86**	*135*	**38**	*175*	**110**
16	**69**	*56*	**36**	*96*	**16**	*136*	**152**	*176*	**54**
17	**35**	*57*	**50**	*97*	**55**	*137*	**178**	*177*	**162**
18	**119**	*58*	**109**	*98*	**67**	*138*	**112**	*178*	**109**
19	**176**	*59*	**43**	*99*	**41**	*139*	**38**	*179*	**93**
20	**166**	*60*	**12**	*100*	**61**	*140*	**176**	*180*	**36**
21	**61**	*61*	**153**	*101*	**108**	*141*	**50**	*181*	**44**
22	**137**	*62*	**140**	*102*	**152**	*142*	**2**	*182*	**40**
23	**18**	*63*	**78**	*103*	**81**	*143*	**102**	*183*	**114**
24	**55**	*64*	**139**	*104*	**81**	*144*	**92**	*184*	**113**
25	**83**	*65*	**126**	*105*	**101**	*145*	**9**	*185*	**34**
26	**98**	*66*	**112**	*106*	**154**	*146*	**18**	*186*	**41**
27	**21**	*67*	**167**	*107*	**33**	*147*	**57**	*187*	**46**
28	**3**	*68*	**61**	*108*	**101**	*148*	**142**	*188*	**78**
29	**77**	*69*	**4**	*109*	**60**	*149*	**143**	*189*	**92**
30	**13**	*70*	**13**	*110*	**143**	*150*	**26**	*190*	**174**
31	**72**	*71*	**82**	*111*	**135**	*151*	**95**	*191*	**165**
32	**85**	*72*	**165**	*112*	**39**	*152*	**99**	*192*	**119**
33	**88**	*73*	**171**	*113*	**51**	*153*	**54**	*193*	**76**
34	**151**	*74*	**22**	*114*	**159**	*154*	**83**	*194*	**47**
35	**40**	*75*	**147**	*115*	**169**	*155*	**45**	*195*	**70**
36	**88**	*76*	**58**	*116*	**164**	*156*	**11**	*196*	**61**
37	**54**	*77*	**96**	*117*	**106**	*157*	**41**	*197*	**132**
38	**134**	*78*	**12**	*118*	**144**	*158*	**50**	*198*	**77**
39	**64**	*79*	**162**	*119*	**66**	*159*	**42**	*199*	**114**
40	**106**	*80*	**101**	*120*	**134**	*160*	**57**	*200*	**43**

Average Orientation Angle: 84.54^{o}
Standard Deviation: 50.33^{o}

Fiber Collection Board #4 Data

Sample #	**Angle**									
1	**129**	*41*	**132**	*81*	**139**	*121*	**150**	*161*	**34**
2	**133**	*42*	**162**	*82*	**107**	*122*	**95**	*162*	**43**
3	**101**	*43*	**54**	*83*	**70**	*123*	**95**	*163*	**121**
4	**92**	*44*	**63**	*84*	**31**	*124*	**173**	*164*	**51**
5	**46**	*45*	**62**	*85*	**118**	*125*	**171**	*165*	**52**
6	**78**	*46*	**142**	*86*	**149**	*126*	**22**	*166*	**24**
7	**152**	*47*	**138**	*87*	**50**	*127*	**41**	*167*	**167**
8	**31**	*48*	**54**	*88*	**91**	*128*	**78**	*168*	**134**
9	**87**	*49*	**87**	*89*	**153**	*129*	**34**	*169*	**21**
10	**93**	*50*	**118**	*90*	**151**	*130*	**60**	*170*	**141**
11	**88**	*51*	**151**	*91*	**68**	*131*	**8**	*171*	**158**
12	**104**	*52*	**137**	*92*	**94**	*132*	**152**	*172*	**57**
13	**24**	*53*	**40**	*93*	**46**	*133*	**172**	*173*	**67**
14	**65**	*54*	**158**	*94*	**141**	*134*	**168**	*174*	**165**
15	**91**	*55*	**93**	*95*	**138**	*135*	**69**	*175*	**23**
16	**93**	*56*	**83**	*96*	**33**	*136*	**141**	*176*	**134**
17	**145**	*57*	**87**	*97*	**38**	*137*	**9**	*177*	**41**
18	**147**	*58*	**114**	*98*	**92**	*138*	**94**	*178*	**171**
19	**140**	*59*	**23**	*99*	**88**	*139*	**34**	*179*	**133**
20	**1**	*60*	**126**	*100*	**136**	*140*	**78**	*180*	**130**
21	**55**	*61*	**48**	*101*	**49**	*141*	**100**	*181*	**36**
22	**153**	*62*	**34**	*102*	**65**	*142*	**80**	*182*	**29**
23	**96**	*63*	**29**	*103*	**24**	*143*	**63**	*183*	**23**
24	**137**	*64*	**154**	*104*	**125**	*144*	**122**	*184*	**150**
25	**44**	*65*	**92**	*105*	**114**	*145*	**143**	*185*	**119**
26	**40**	*66*	**138**	*106*	**47**	*146*	**89**	*186*	**126**
27	**124**	*67*	**136**	*107*	**143**	*147*	**153**	*187*	**89**
28	**134**	*68*	**161**	*108*	**18**	*148*	**95**	*188*	**151**
29	**150**	*69*	**134**	*109*	**133**	*149*	**147**	*189*	**63**
30	**152**	*70*	**58**	*110*	**41**	*150*	**127**	*190*	**156**
31	**92**	*71*	**99**	*111*	**163**	*151*	**89**	*191*	**158**
32	**42**	*72*	**123**	*112*	**97**	*152*	**109**	*192*	**148**
33	**92**	*73*	**153**	*113*	**111**	*153*	**137**	*193*	**33**
34	**121**	*74*	**91**	*114*	**36**	*154*	**62**	*194*	**111**
35	**175**	*75*	**42**	*115*	**124**	*155*	**153**	*195*	**47**
36	**72**	*76*	**44**	*116*	**123**	*156*	**96**	*196*	**172**
37	**107**	*77*	**50**	*117*	**107**	*157*	**62**	*197*	**44**
38	**153**	*78*	**139**	*118*	**44**	*158*	**93**	*198*	**161**
39	**91**	*79*	**33**	*119*	**151**	*159*	**40**	*199*	**128**
40	**121**	*80*	**128**	*120*	**161**	*160*	**59**	*200*	**25**

Average Orientation Angle: 97.05^{o}
Standard Deviation: 46.56^{o}

Fiber Collection Board #5 Data

Sample #	Angle								
1	150	41	146	81	38	121	172	161	56
2	5	42	43	82	137	122	177	162	21
3	73	43	11	83	100	123	72	163	5
4	106	44	176	84	162	124	113	164	110
5	146	45	26	85	156	125	45	165	165
6	15	46	143	86	125	126	45	166	83
7	153	47	75	87	2	127	52	167	27
8	69	48	34	88	136	128	71	168	59
9	111	49	140	89	84	129	66	169	118
10	40	50	133	90	75	130	5	170	154
11	43	51	160	91	68	131	100	171	12
12	2	52	41	92	165	132	84	172	137
13	163	53	39	93	32	133	52	173	83
14	43	54	29	94	33	134	35	174	20
15	174	55	77	95	132	135	149	175	155
16	56	56	53	96	37	136	142	176	43
17	149	57	144	97	36	137	43	177	100
18	8	58	160	98	25	138	100	178	141
19	63	59	89	99	163	139	129	179	71
20	119	60	136	100	34	140	150	180	127
21	108	61	164	101	58	141	75	181	17
22	46	62	28	102	149	142	132	182	155
23	148	63	10	103	139	143	135	183	111
24	82	64	86	104	18	144	62	184	147
25	114	65	74	105	147	145	18	185	136
26	123	66	160	106	144	146	159	186	88
27	121	67	79	107	37	147	60	187	33
28	113	68	11	108	80	148	140	188	24
29	79	69	40	109	86	149	56	189	62
30	130	70	76	110	152	150	87	190	29
31	88	71	123	111	111	151	115	191	101
32	53	72	50	112	86	152	102	192	161
33	128	73	21	113	50	153	102	193	173
34	17	74	141	114	76	154	24	194	91
35	178	75	13	115	91	155	54	195	78
36	172	76	4	116	145	156	82	196	26
37	125	77	1	117	135	157	1	197	4
38	55	78	133	118	106	158	55	198	146
39	20	79	12	119	147	159	50	199	60
40	160	80	138	120	82	160	43	200	131

Average Orientation Angle: 87.8^{o}
Standard Deviation: 51.62^{o}

Fiber Collection Board #6 Data

Sample #	**Angle**									
1	**142**	*41*	**157**	*81*	**88**	*121*	**125**	*161*	**153**
2	**116**	*42*	**149**	*82*	**93**	*122*	**165**	*162*	**81**
3	**76**	*43*	**11**	*83*	**30**	*123*	**41**	*163*	**151**
4	**87**	*44*	**77**	*84*	**105**	*124*	**28**	*164*	**161**
5	**172**	*45*	**44**	*85*	**158**	*125*	**53**	*165*	**138**
6	**102**	*46*	**77**	*86*	**78**	*126*	**179**	*166*	**149**
7	**43**	*47*	**97**	*87*	**158**	*127*	**178**	*167*	**15**
8	**94**	*48*	**99**	*88*	**9**	*128*	**42**	*168*	**43**
9	**104**	*49*	**176**	*89*	**132**	*129*	**168**	*169*	**134**
10	**77**	*50*	**24**	*90*	**135**	*130*	**76**	*170*	**18**
11	**63**	*51*	**127**	*91*	**149**	*131*	**145**	*171*	**46**
12	**105**	*52*	**153**	*92*	**36**	*132*	**69**	*172*	**156**
13	**160**	*53*	**134**	*93*	**65**	*133*	**122**	*173*	**107**
14	**121**	*54*	**19**	*94*	**17**	*134*	**119**	*174*	**99**
15	**43**	*55*	**13**	*95*	**90**	*135*	**110**	*175*	**178**
16	**60**	*56*	**132**	*96*	**17**	*136*	**56**	*176*	**45**
17	**172**	*57*	**72**	*97*	**141**	*137*	**69**	*177*	**121**
18	**135**	*58*	**157**	*98*	**106**	*138*	**127**	*178*	**74**
19	**10**	*59*	**69**	*99*	**84**	*139*	**23**	*179*	**62**
20	**143**	*60*	**146**	*100*	**169**	*140*	**109**	*180*	**107**
21	**173**	*61*	**63**	*101*	**35**	*141*	**149**	*181*	**73**
22	**85**	*62*	**171**	*102*	**149**	*142*	**54**	*182*	**104**
23	**168**	*63*	**59**	*103*	**81**	*143*	**60**	*183*	**144**
24	**153**	*64*	**140**	*104*	**58**	*144*	**78**	*184*	**124**
25	**11**	*65*	**98**	*105*	**2**	*145*	**69**	*185*	**160**
26	**167**	*66*	**179**	*106*	**109**	*146*	**75**	*186*	**58**
27	**124**	*67*	**166**	*107*	**168**	*147*	**145**	*187*	**138**
28	**28**	*68*	**40**	*108*	**60**	*148*	**85**	*188*	**92**
29	**174**	*69*	**114**	*109*	**65**	*149*	**40**	*189*	**87**
30	**24**	*70*	**107**	*110*	**66**	*150*	**32**	*190*	**47**
31	**51**	*71*	**146**	*111*	**173**	*151*	**92**	*191*	**132**
32	**59**	*72*	**80**	*112*	**34**	*152*	**95**	*192*	**57**
33	**79**	*73*	**178**	*113*	**135**	*153*	**18**	*193*	**67**
34	**127**	*74*	**33**	*114*	**48**	*154*	**138**	*194*	**97**
35	**29**	*75*	**120**	*115*	**85**	*155*	**41**	*195*	**136**
36	**71**	*76*	**59**	*116*	**53**	*156*	**75**	*196*	**121**
37	**122**	*77*	**92**	*117*	**172**	*157*	**100**	*197*	**43**
38	**7**	*78*	**130**	*118*	**95**	*158*	**42**	*198*	**112**
39	**158**	*79*	**19**	*119*	**80**	*159*	**162**	*199*	**149**
40	**146**	*80*	**179**	*120*	**56**	*160*	**89**	*200*	**134**

Average Orientation Angle: 97.14^{o}
Standard Deviation: 49.11^{o}

Fiber Collection Board #7 Data

Sample #	**Angle**								
1	**149**	*41*	**20**	*81*	**55**	*121*	**135**	*161*	**173**
2	**117**	*42*	**43**	*82*	**177**	*122*	**111**	*162*	**42**
3	**171**	*43*	**134**	*83*	**95**	*123*	**132**	*163*	**175**
4	**46**	*44*	**125**	*84*	**66**	*124*	**135**	*164*	**76**
5	**5**	*45*	**155**	*85*	**130**	*125*	**97**	*165*	**135**
6	**118**	*46*	**91**	*86*	**120**	*126*	**89**	*166*	**162**
7	**128**	*47*	**50**	*87*	**146**	*127*	**120**	*167*	**47**
8	**69**	*48*	**104**	*88*	**55**	*128*	**99**	*168*	**135**
9	**134**	*49*	**41**	*89*	**5**	*129*	**135**	*169*	**135**
10	**12**	*50*	**144**	*90*	**89**	*130*	**75**	*170*	**15**
11	**117**	*51*	**110**	*91*	**55**	*131*	**135**	*171*	**136**
12	**133**	*52*	**145**	*92*	**147**	*132*	**79**	*172*	**89**
13	**86**	*53*	**4**	*93*	**136**	*133*	**152**	*173*	**76**
14	**68**	*54*	**117**	*94*	**94**	*134*	**135**	*174*	**162**
15	**136**	*55*	**145**	*95*	**148**	*135*	**106**	*175*	**159**
16	**134**	*56*	**122**	*96*	**26**	*136*	**64**	*176*	**136**
17	**77**	*57*	**67**	*97*	**87**	*137*	**47**	*177*	**34**
18	**137**	*58*	**32**	*98*	**20**	*138*	**103**	*178*	**47**
19	**36**	*59*	**170**	*99*	**76**	*139*	**135**	*179*	**92**
20	**48**	*60*	**110**	*100*	**136**	*140*	**78**	*180*	**41**
21	**137**	*61*	**53**	*101*	**180**	*141*	**85**	*181*	**33**
22	**118**	*62*	**5**	*102*	**178**	*142*	**180**	*182*	**50**
23	**173**	*63*	**42**	*103*	**149**	*143*	**96**	*183*	**90**
24	**135**	*64*	**138**	*104*	**135**	*144*	**135**	*184*	**135**
25	**136**	*65*	**142**	*105*	**137**	*145*	**64**	*185*	**85**
26	**101**	*66*	**52**	*106*	**80**	*146*	**4**	*186*	**134**
27	**131**	*67*	**50**	*107*	**46**	*147*	**73**	*187*	**89**
28	**20**	*68*	**144**	*108*	**87**	*148*	**105**	*188*	**1**
29	**165**	*69*	**42**	*109*	**63**	*149*	**26**	*189*	**136**
30	**14**	*70*	**95**	*110*	**52**	*150*	**178**	*190*	**78**
31	**6**	*71*	**7**	*111*	**29**	*151*	**135**	*191*	**141**
32	**148**	*72*	**130**	*112*	**136**	*152*	**20**	*192*	**75**
33	**52**	*73*	**137**	*113*	**124**	*153*	**92**	*193*	**22**
34	**49**	*74*	**22**	*114*	**36**	*154*	**43**	*194*	**135**
35	**45**	*75*	**136**	*115*	**123**	*155*	**66**	*195*	**38**
36	**169**	*76*	**110**	*116*	**58**	*156*	**43**	*196*	**47**
37	**57**	*77*	**38**	*117*	**136**	*157*	**135**	*197*	**135**
38	**30**	*78*	**30**	*118*	**15**	*158*	**71**	*198*	**121**
39	**95**	*79*	**31**	*119*	**86**	*159*	**71**	*199*	**144**
40	**11**	*80*	**136**	*120*	**88**	*160*	**64**	*200*	**164**

Average Orientation Angle: 93.76^{o}
Standard Deviation: 48.66^{o}